**Année : 2007** **N° d'ordre : 4150**

# Université des Sciences et Technologies de Lille

## École Doctorale ″Sciences Pour l'Ingénieur″

### Laboratoire de Mécanique de Lille (UMR 8107)

## Thèse pour le grade de docteur en Génie Civil

**Présentée et soutenue publiquement par**

**Yousef PARISH**

**Le 17 Décembre 2007**

# Analyse numérique du comportement sismique des barrages en terre : Influence de la plasticité et de la pression d'eau

**Président :**

**OUAHSINE Abdellatif** Professeur Univ. de Technologie de Compiègne

**Rapporteurs :**

**M. HJIAJ Mohammed** Professeur INSA de Rennes

**M. CHEN Sheng-Hong** Professeur Wuhan University China

**Directeur de la thèse :**

**SHAHROUR Isam,** Professeur, Université Lille1 / Polytech'Lille

**Co- Directeur :**

**SADEK Marwan,** Maître de Conférences – Université Lille1 / Polytech'Lille

**Année : 2007** **N° d'ordre : 4150**

# University of Science and Technology of Lille

## Doctoral School of Engineering Science

### Laboratory of Mechanics of Lille (UMR 8107)

**Thesis for the degree of Doctorate in Civil Engineering**

**by**

**Yousef PARISH**

**17 December 2007**

# Numerical analysis of the seismic behavior of earth dams: Influence of plasticity and pore water pressure

**President :**

**OUAHSINE Abdellatif** Professor Univ. of Technology of Compiègne

**Reviewers :**

**M. HJIAJ Mohammed** Professor INSA de Rennes

**M. CHEN Sheng-Hong** Professor Wuhan University, China

**Supervisor :**

**SHAHROUR Isam,** Professor, University Lille1 / Polytech'Lille

**Co-supervisor :**

**SADEK Marwan,** Associate professor – University Lille1 / Polytech'Lille

## AKNOWLEDGMENTS

At first, I would like to express my deepest gratitude to my advisor, Professor Isam SHAHROUR and Dr. Marvan Sadek for their continuous advice, guidance, support, supervision, and encouragement throughout my doctoral study and research at University of Science and Technology of Lille. Their ideas and comments helped me to achieve the results that can be seen in the thesis.

I would also like to thank my committee members, Professor Mohammed HJIAJ, Professor Sheng-Hong CHEN and Professor Abdellatif OUAHSINE for their kind review of this document and their valuable remarks.

Thanks to Professor Jean Pierre HENRY, Dr. Mohammad HAJI SOUTOODEH, Dr. Hamid VARASTEPOUR and Dr. Esmail KHOSHRAVAN AZAR, for their involvement in my education at University of Science and Technology of Lille.

I also want to thank all the people at the Labroatory of Machanic of Lille (LML) and department of Civil Engineering at École polytechnique universitaire de Lille for creating a warm and friendly atmosphere. I especially appreciate.

I am grateful for the help and friendship of all my fellow graduate students friends and specially (without any order): Ahmad ASNAASHARI, Ali Mohammad Ajorloo, Hussein Ghoreishi, Loay khalil and Bassem Ali.

Special thanks are extended to Dr. Afzaliyan A., Dr. Golipour E., Pishnamazi M., Dr. Banan K., Mortazavi M., Zeraatparvar A., Rashtchizadeh A. for their assistance, guidance and encouragement in pursuing this area of research.

This thesis was supported by the Ministry of Energy – IRAN, the Institute for Energy and Hydro Technology (IEHT) and Azarbaijan Higher Training and Research campus in Tabriz. I would like to acknowledge their generous support.

Finally, I am grateful to my family especially my father and mother for their support and encouragements over the years despite their incredible hard time. I want to owe a great debt to my wife for sacrificing many things and giving moral support throughout the study period and to my girl, for his love and smile.

# Résumé


La thèse traite d'un sujet important et complexe de géotechnique et de génie parasismique. Ce sujet porte sur l'analyse de l'influence de la plasticité et de la pression d'eau sur la réponse séismique des barrages en terre. Les analyses sont effectuées en utilisant le logiciel FLAC 3D. Le travail comporte trois chapitres:

Le premier chapitre présente une analyse bibliographique sur les recherches menées sur des barrages de la terre. Il présente d'abord une analyse des observations réalisées lors des de tremblements de terre. Ensuite, il donne une synthèse des différentes méthodes d'analyse séismique des barrages de la terre, tels que méthodes simplifiées, les méthodes à base expérimental, la méthode linéaire équivalente et les méthodes non linéaires.

Le deuxième chapitre présente une analyse numérique du comportement séismique des barrages en terre. L'analyse est conduite pour la phase solide. Elle correspond à la réponse de barrage avant le remplissage de l'eau. L'analyse est d'abord conduite pour un cas simple qui concerne la réponse élastique du barrage. Cette analyse fournit des indications sur la réponse du barrage, principalement l'amplification dynamique. Elle est également utile pour comprendre l'influence de la plasticité sur la réponse de barrage. La deuxième partie du chapitre concerne une analyse plus réaliste du barrage, où le comportement élastoplastique du sol est considéré. Cette analyse est conduite en utilisant le critère non associé de Mohr-Coulomb. Pour les analyses élastiques et plastiques, une étude paramétrique est réalisée sur l'influence de principaux paramètres tels que les propriétés mécaniques du sol, la géométrie du barrage et la fréquence du chargement.

Le troisième chapitre présente une analyse numérique de l'influence de l'interaction eau-squelette sur la réponse sismique des barrages en terre. L'analyse est conduite d'abord sous condition non drainée, qui correspond à une analyse simplifiée de la réponse du barrage. Cette analyse ne fournit pas la variation de la pression d'eau ; elle constitue une première étape de l'analyse de la réponse séismique du barrage en contraintes totales. Par la suite une analyse couplée est conduite en contraintes effectives en utilisant le critère non associé de Mohr-Coulomb. Cette analyse fournit la variation de la pression d'eau. Elle permet d'étudier l'influence de la phase de l'eau sur la réponse de barrage à un chargement sismique réel. Cette 'analyse est d'abord conduite pour un cas de référence, qui est suivi d'une comparaison des analyses drainée et non drainée.


**Mots-clés :** Barrage en terre, FLAC, sismique, plasticité, non drainée, couplage, fluide-squelette, pression d'eau, enregistrement sismique

# Abstract

The thesis deals with an important and complex issue in geotechnical and earthquake engineering, which concerns the influence of both plasticity and pore water pressure on the influence of the seismic response to real earthquake records. Analyses are carried using the software FLAC3D. The work includes three parts:

The first chapter presents a literature review of research on earth dams. It presents observation during earthquake loading, the different methods of seismic analysis of earth dams, such as the simplified methods, the empirical methods, the equivalent-linear analyses and the non linear methods.

The second chapter presents a numerical analysis of the seismic behaviour of earth dams. Analysis is conducted for the solid phase. It corresponds to the response of the dam before water filling. Analysis is first conducted for a simple case which concerns the elastic response of the dam. This analysis provides some indications about the response of the dam, mainly the dynamic amplification. It is also useful to understand the influence of plasticity on the dam response. The second part of the chapter concerns a more realistic analysis of the dam, where the elastoplastic behaviour of the earth material is considered. This analysis is conducted using the simple and popular non associated Mohr-Coulomb criterion. For both the elastic and plastic analyses, a parametric study is conducted for the investigation of the influence of major parameters such as the mechanical properties of the earth material, the geometry of the dam and the frequency of the input loading.

The third chapter presents a numerical analysis of the influence of the water-skeleton interaction on the response of earth dams to seismic loading. Analysis is conducted first under undrained condition, which corresponds to a simplified analysis of the response of the dam. This analysis does not provide the variation of the pore water pressure; it constitutes a first stage of the analysis of the seismic response of the dam in total stresses. Then, full coupled analysis is conducted in effective stresses using the non associated Mohr-Coulomb criterion. This analysis provides the variation of the pore water pressure. It allows investigating the influence of the water phase on the dam response to real earthquake input motion. This analysis will is first conducted for a reference case, which is followed by a comparison of the undrained response of the dam to its full-coupled response.


**Key words:** Earth dam, F LAC, seismic, plasticity, undrained, coupling, fluid-skeleton, pore pressure, seismic recording.

# TABLE OF CONTENTS



## CHAPTER I:

### Bibliographical Analysis

# CHAPTER II:

## Seismic Response of the Earth Dams: Influence of plasticity



# CHAPTER III:

## Seismic Response of the Earth Dams:

## Influence of the water-skeleton interaction





 

# LIST OF TABLES

# LIST OF FIGURES

# General Introduction

According to the International Commission on Large Dams, the majority of the old dams were designed using methods and seismic criteria, which are considered now as obsolete. In many cases, it is not known if an old dam is in accordance with the current seismic safety guidelines of the International Commission on Large Dams (ICOLD 1989). Indeed, according to these guidelines, large dams must withstand the maximum credible earthquake (MCE). This is the strongest ground motion that could occur, which has a return period of several thousand years.

During the last decades, significant progress in the assessment of dynamic analysis of dams has been achieved. The trend goes towards higher intensities of the earthquake ground motion at dam sites, which is usually characterized by the peak ground acceleration (PGA). Most dams were designed against earthquakes using the pseudo-static approach and a PGA of 0.1 g. An MCE with a magnitude of larger than 6 can generate (locally) a PGA of more than 0.5 g, which is five times larger than the design value. Because of this large discrepancy between the design acceleration and the PGA values to be expected during the MCE, it is often not possible to make a reliable statement about the earthquake safety of an existing dam. The main conclusion that can be made is that the earthquake safety of most existing dams is unknown. In addition, design of new earth dams must take into consideration new and major issues such as the nonlinear behaviour of earth material, the fluid-skeleton interaction, the soil liquefaction, the fluid-structure interaction. It should also consider the response of dams to real earthquake using seismic records.

The prediction of the response of an earth dam during an earthquake constitutes a major challenge. Factors such as dam characteristics, site conditions, and earthquake loading specifications highly affect the dynamic responses of the dams. The non-linear behaviour of the soil materials, extensively influence the dam responses.

Progress in the area of geotechnical computation offers interesting facilities for the analysis of the dam response in considering complex issues such as the soil plasticity, the evolution of the pore pressure the dam construction procedure and real earthquake records. They allow following during the earthquake the evolution of the soil movement, the stress and strain distribution and the pore pressure excess. They allow permit the determination of the distribution of plasticity and to check the dam stability. Numerical analysis allows also conducting parametric analysis for the investigation of the influence of main parameters and to check strategies for the dam design and construction.

The aim of this work is to analyse the seismic response of dams using numerical methods, which can consider the nonlinear behaviour of the soil material, the pore pressure evolution, the construction of the dam, the foundation-dam interaction. Analysis will focus on the influence of plasticity and on the fluid-skeleton interaction. Real earthquake records are used in this study. The work is presented in three chapters.

The first chapter presents a literature review of research on earth dams. It presents observation during earthquake loading, the different methods of seismic analysis of earth dams, such as the simplified methods, the empirical methods, the equivalent-linear response analyses and the non linear methods.

The second chapter presents a numerical analysis of the seismic behaviour of earth dams. Analysis is conducted for the solid phase. It corresponds to the response of the dam before water filling. Analysis is first conducted for a simple case which concerns the elastic response of the dam. This analysis provides some indications about the response of the dam, mainly the dynamic amplification. It is also useful to understand the influence of plasticity on the dam response. The second part of the chapter concerns a more realistic analysis of the dam, where the elastoplastic behaviour of the earth material is considered. This analysis is conducted using the simple and popular non associated Mohr-Coulomb criterion. For both the elastic and plastic analyses, a parametric study is conducted for the investigation of the influence of major parameters such as the mechanical properties of the earth material, the geometry of the dam and the frequency of the input loading. This chapter is composed of three parts. The first one presents briefly the numerical model used in the analysis, the second part presents results of the elastic analyses, while the last one presents a discussion of elastoplastic response of the dam.

The third chapter presents a numerical analysis of the influence of the water-skeleton interaction on the response of earth dams to seismic loading. Analysis is conducted first under undrained condition, which corresponds to a simplified analysis of the response of the dam. This analysis does not provide the variation of the pore water pressure; it constitutes a first stage of the analysis of the seismic response of the dam in total stresses. Then, full coupled analysis is conducted in effective stresses using the non associated Mohr-Coulomb criterion. This analysis provides the variation of the pore water pressure. It allows investigating the influence of the water phase on the dam response to real earthquake input motion. This analysis will is first conducted for a reference case, which is followed by a comparison of the undrained response of the dam to its full-coupled response.



 

# CHAPTER I

## Bibliographical Analysis

# Chapter I:

## Bibliographical Analysis

## 1.1 Introduction

Many dams are built across rivers that follow fault traces. While such faults are not necessarily active, the potential for differential movement across the dam foundation must be taken into account. Dam should operate with no risk to the public in case of an earthquake. Indeed, dams and reservoirs located near urbanized areas represent a potential risk to the downstream population and property in the event of uncontrolled release of the reservoir water due to earthquake damage. That's why, the stability of dam embankments is of great concern to geotechnical engineers.

The most common method used in engineering practice to assess the seismic stability of earth fill dam consists on a pseudostatic approach where the earthquake effect on a potential soil mass is represented by means of equivalent static horizontal force equal to the soil mass multiplied by a seismic coefficient. This approach is based on several simplified assumptions neglecting the soil deformability, which could lead to misestimating therefore the earthquake effects on dams. Indeed, the problem of seismic response and behavior of dams and their foundations, when formulated in general terms, is complex.

Since the 1971 San Fernando earthquake in California (Ming and Li 2003), major progress has been achieved in the understanding of earthquake action on dams. The dynamic response of soil-structures has received significant attention. The progress was mainly due to the development of numerical methods for the dynamic analysis. Also, considerable advancement has been made in the definition of the seismic input motion, which is one of the main uncertainties in the seismic design and seismic safety evaluation of dams.

However, it is still not possible to reliably predict the behaviour of dams during strong ground shaking due to the difficulty in modeling joint opening and the crack formation in the dam body, the nonlinear behaviour of the foundation, the insufficient information on the spatial variation of the ground motion in arch dams and other factors.

It should always keep in mind that even the best analytical methods do not provide precise insight in the seismic design of dams. Depending on the type and size of the dam, its seismic exposure, and other factors such as regulatory requirements, numerical analysis may be conducted using simplified or complex procedures.

In this thesis, we propose numerical modeling using the finite difference method to analyze the seismic performance of embankments dams under artificial and real seismic input motion. The analysis concerns a real case study "the Alaviyan dam" situated in the northwest of Iran.

This chapter presents a bibliographic review that summarizes the state of the art on the seismic performance of earthfill dams, their vulnerability, their safety evaluation and different methods used in the stability assessment of dams under seismic loading.

## 1.2 Earthfill dam with central clay core

Central cores of puddled clay were used in the traditional British dam in the nineteenth century. It had an upstream slope of 1 in 3 and a downstream slope of 1 in 2.5. The puddled clay core was usually taken down in trench to form a below-ground waterstop.

An earth dams contains materials of different kinds in different parts. Figure 1.1 illustrates different component of a typical earthfill dam. It is composed of a central impervious core which is flanked by zones of more pervious material. The upstream shell provides stability against rapid drawdowns of reservoir while the downstream shell acts as a drain to control the line of seepage and provides stability to the dam during its construction and operation. The maximum width of the impervious core is governed by stability and seepage criteria and also by the availability of the material. An earth dam with a sufficiently thick impervious core of strong material with pervious outer shells can have relatively steeper embankment slopes limited only by the foundation and embankment characteristics. However, a thin core dam is usually more economical and more easily constructed because of lesser amount of fine-grained soil to be handled. Core widths of 30 to 50% of the water head are usually adequate for any type of soil and any dam height while core widths of 15 to 20% of water head are thin and considered satisfactory, if adequately designed and constructed filter layers are provided. Core widths of less then 10% of water head should not be used as far as possible (G.L.Asawa, 2005).

Earth dams are constructed of a variety of the available materials in different quantities and locations within the fill (.Sharam et al. 2007):

1. **Impervious zone:** Within the earthfill the distribution of materials is to be such that permeability and coarseness increases towards the outer slope. That's why clay soils are used in impervious zone which provides the water barrier. The material must be sufficiently impervious but also must not consolidate or soften excessively on saturation by water from the reservoir. To satisfy the design criteria of impervious-ness, low consolidation and resistance to softening, the maximum possible density is desirable. From the point of view of stress and deformation conditions in the core zone, more favorable conditions can be obtained from the core by giving it some inclination towards the upper side.

2. **Filter zone:** It is impracticable to stop all seepage through the dam. As such an inverted filter is provided abutting both the upstream and downstream slopes of the core to collect seepage emerging out of the core and thereby keeping the downstream casing relatively dry. Filter is constructed of selected free draining sand and gravel to prevent the displacement of fine soil particles which constitute the core. Provision of downstream filter is important for lowering the phreatic line and to prevent the movement of fine materials.

3. **Permeable zone:** Pervious zones provide an outer shell of high strength to impart stability and protect the impervious core, secure favorable hydraulic conditions of drainage, and act as filters between materials of greatly differing grain sizes. Within the pervious zone, individual loads are directed so that the material is graded in coarseness towards the outer slopes. The inner pervious zone provides stability against sudden drawdowm and supports and protects the impervious zone, while the outer pervious zone acts as a drain to control the line of seepage.

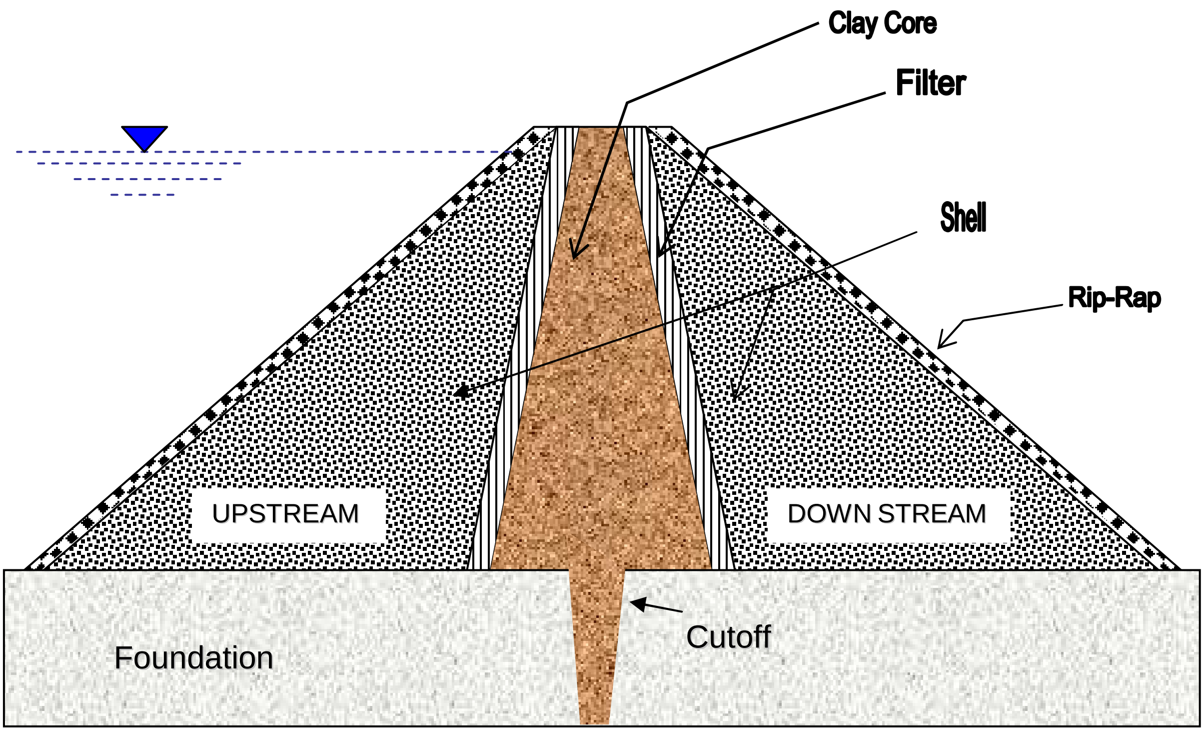


**Figure 1.1:** Typical section of an earthfill dam

## 1.3 Seismic performance of existing embankment Dams

The first failure of a dam due to earthquake reported in the literature is Augusta Dam, GA, during the 1886 Charleston, SC earthquake. Worldwide, fewer than 30 dams have failed completely during earthquakes (USCOLD, 2000). These were primarily tailings or hydraulic fill dams, or relatively small embankments of questionable design. Few large embankment dams have been severely damaged.

As reported by Chen et al. (2003), during the San Francisco earthquake (1906, Magnitude 8.3, estimated), about 30 medium-sized earthfill dams within 50 km of the fault rupture trace (15 of these were less than 5 km away) were affected. Most survived the shaking with only minor damage. More recently, during the 1999 Kocaeli earthquake in Turkey (M 7.4), Gokce Dam, a 200-ft-high earth core rockfill dam and Kirazdere Dam, a 356-ft-high earthfill embankment with clay core, sand and gravel filters, and rockfill shells were located within the area of strong damage. The only observed effect at Gokce Dam was a longitudinal crack along the upstream side of the crest, about 0.33 in. wide. Kirazdere Dam is located within 2 to 3 km of the epicenter and in close proximity to the causative fault, the North Anatolian Fault. There was about 7 ft of right-lateral movement within about 1 mi of the dam. A few longitudinal cracks, each about 0.1 in. wide, occurred on the crest gravel road. Overall, both dams performed satisfactorily and demonstrated the high seismic resistance of rockfill dams.

This satisfactory performance demonstrated the ability of clayey dams to withstand extreme seismic loading, despite the questionable methods of compaction used for these historic facilities.

Performance data and detailed references regarding the approximately 400 dams that have been subjected to significant earthquake shaking are provided by USCOLD (1984, 1992b, 2000). The seismic performance of embankment dams has been closely related to the nature and state of compaction of the fill material. Well-compacted modern dams can withstand substantial earthquake shaking with no detrimental effects. In particular, earth dams built of compacted clayey materials on competent foundations and rockfill dams have demonstrated excellent stability under extreme earthquake loading. In contrast, old embankments built of poorly compacted sands and silts or founded on loose alluvium, hydraulic fill dams, and tailings dams represent nearly all the known cases of failures.

Beside the formation of transverse and longitudinal cracks, Seismic damage induced in embankment dams is mainly related to the following two aspects:

- Sliding failure with large induced settlement during and after an earthquake and the stability of slopes.
- Build-up of excess pore water pressure in embankment and foundation materials (soil liquefaction).

The following paragraphs summarize the most notable case histories where dams have suffered from one of the two main types of failures: significant induced settlement and soil liquefaction.

### 1.3.1 Case histories with significant induced settlement

During the 1985 Mexico earthquake (M 8.1), Two large dams, La Villita (197 ft high) and El Infiernillo (485 ft high) were affected. Although neither experienced significant damage, these dams were shaken from 1975 to 1985 by a string of closely spaced seismic events, five of magnitudes greater than 7.1. Cumulative earthquake-induced settlements of La Villita Dam, an earth-rockfill embankment with a wide, central clayey core, approach 2 ft and have increased in the latest events, perhaps due to progressive weakening of some of the materials. The deformations of El Infiernillo Dam, an earth-core rockfill dam, have remained small and consistent from one event to the next.

A wide region around the San Francisco Bay was affected during the 1989 Loma Prieta earthquake (M 7.1). About 100 embankment dams of various sizes were within 100 km of the epicentre. Austrian Dam, a 200-ft-high earth dam about 12 km from the epicenter, suffered substantial transverse abutment cracking and settled nearly 3 ft. The reservoir was half full at the time of the earthquake. Overall damage to the dam was extensive, considering the short duration of shaking. Austrian and other dams affected by the Loma Prieta earthquake must be capable of withstanding earthquakes considerably more demanding in intensity and duration of shaking than experienced in 1989.

Five large earth and rockfill dams were located between 1.5 and 12.5 miles from the fault rupture trace during the 1990 Philippines earthquake (M 7.7). Ground motion was estimated at these sites at between 0.35 and 0.70 g. None of the dams failed but they all experienced settlement, deformations, and cracking. One of the dams, Diayo Dam, 197 ft high, experienced a major slump along the total length (660 ft) of its upstream slope. The scarp of that slump was about 1 ft high on the downslope side.

More recently, the 1994 Northridge earthquake – (M6.7) The hypocenter was centered about 32 km west-northwest of the San Fernando Valley. This earthquake was the second significant event to affect the San Fernando Valley in less than 25 years. More than 100 dams were located within 75 km of its epicenter, including most of those shaken in 1971. Eleven earth and rockfill dams experienced cracking and slope movements but none threatened life and property. The 82-ft-high Upper Van Norman Dam (operated since 1971 with an empty reservoir) experienced transverse cracks near its abutments and along the downstream slope. These cracks were up to 60 ft long and 3 in. wide. Maximum crest settlement was about 2.4 ft, with over 6 in. of horizontal upstream movement.

### 1.3.2 Case histories that have experienced soil Liquefaction

Liquefaction is a major problem for tailings dams and small earth dams constructed of or founded on relatively loose cohesionless materials, and used for irrigation and water supply schemes that have not been designed against earthquakes.

The 1925 Santa Barbara earthquake (M 6.3) earthquake caused catastrophic slope sliding failure of the 25-ft-high Sheffield Dam in Santa Barbara, CA. This was the first recognition that shaking of embankments with low relative density materials may cause liquefaction failures.

Engineers' concerns regarding the vulnerability of dams constructed of poorly compacted, saturated fine sands and silts were confirmed in 1971 after the San Fernando Earthquake (M 6.5). The Lower Van Norman Dam, a 140-ft-high hydraulic fill dam, experienced widespread liquefaction and major slope failures. Flooding of the downstream area with its 70,000 residents was barely avoided, due to an unusually low reservoir level. The 80-ft-high Upper Van Norman Dam was also severely damaged. This experience triggered numerous reassessments of other dams and led to the development of modern numerical methods of dynamic analysis of dams.

The 2001 Bhuj (India) earthquake (M 7.7) resulted in widespread soil effects and liquefaction in low-lying estuaries and young alluvial deposits. Strong ground motion lasted more than 85 sec, and lower-level shaking several min. Numerous embankment dams were damaged in the epicentral area, including seven medium-sized (40 to 120 ft high) earth dams. Fourteen smaller dams were also damaged, some extensively. The reservoirs were very low at the time of the earthquake but liquefaction of the foundation caused moderate to severe failure of the upstream and, locally, the downstream slopes of the dams.

## 1.4 Lessons concluded from past earthquakes

The behavior of earth and rock-fill dams when subjected to earthquake shaking depends strongly on the design of internal drainage features and the method of construction used. A comprehensive review of past experience with numerous embankment dams shaken by six earthquakes produced the following conclusions (Seed et al 1978, Seed 1979):

**a.** Hydraulic fill dams have been found to be vulnerable to failures under unfavourable conditions, in particular shaking produced by strong earthquakes. The near failure of the Lower Van Norman Dam during the 1971 San Fernando earthquake is the most famous case history in that it triggered the development of modern methods for the dynamic analysis of embankment dams (USCOLD 1992).

**b.** Virtually any well-built compacted embankment dam can withstand moderate earthquake shaking, with peak accelerations of 0.2g and more, with no detrimental effects.

**c.** Dams constructed of clay soil on clay or rock foundations have withstood extremely strong shaking, ranging from 0.35 to 0.8g, from a magnitude 8.25 earthquake with no apparent damage. This conclusion is based on the results of the performance of 33 embankment dams that were shaken during the 1906 San Francisco earthquake. These dams range in height from 15 to 140 feet, and are located within 37 miles (60km) of the San Andreas Fault. Almost one-half (16) were located within 5 miles (8km) of the causative fault. Explorations performed in the 1980's and observations of piezometers indicate that puddled cores in some of the higher dams may have kept the downstream slopes from being saturated. Performance of embankment dams in 43 earthquakes subsequent to the Seed publication (Seed et al 1978) has also been good, except when liquefaction or unusual circumstances have been involved.

**d.** Two rockfill dams have withstood moderately strong shaking with no significant damage. If the rockfill dam is kept dry by means of an impervious facing, they should be able to withstand extremely strong shaking with only small deformations. The strongest shaking to which a concrete face rockfill (CFR) dam has been subjected to is around 0.2g. In areas of moderate seismic shaking, CFR dams have been built with slopes of the order of 1H:1.3V. Analysis of the dams under these conditions show the dam should have an acceptable level of seismic performance. When the design earthquake is as high as Magnitude 7.5 and capable of producing a peak ground acceleration of 0.5g, the desirable slope is on the order of 1H:1.65V (Seed et al 1985). However site-specific analysis should always be performed for critical structures.

**e.** The performance of modern compacted embankment dams was further demonstrated in 1994 when the Los Angeles Reservoir, a modern reservoir constructed in 1979 comprising two rolled fill embankments, was severely shaken by the Northridge Earthquake, a magnitude ML of 6.8 with its epicenter approximately 7 miles south of the site (Davis and Sakado 1994). The Los Angeles Dam (LAD), on the south side of the reservoir, is 155 feet high. The North Dike (ND), on the northern side of the reservoir, is 117 feet high. Both dams are founded on Saugus Formation bedrock, are zoned with shell material on the upstream and downstream slopes, and contain a chimney drain at the center section. The LAD also has a clay zone upstream of the chimney drain. The degree of compaction of fill, clay zone, and blended sand and gravel was specified to be compacted to 93 percent modified Proctor (ASTM D1557 2002) and was carefully controlled during construction. Peak horizontal acceleration values of up to 0.43g were measured on the right abutment and 0.56g on the crest of the LAD. A survey of the reservoir following the earthquake showed 3-1/2 in. of crest settlement and lateral downstream movement of over 1 in. on the crest of LAD. The ND showed no more than 1-1/4 in. of crest settlement and lateral downstream movement of less than 1/3 in. on the crest. The reservoir was within nearly 80 percent of its capacity, as defined by the high water elevation, at the time of the earthquake.

**f.** A few recent case histories have provided opportunities to verify analysis procedures for estimating earthquake-induced deformations. In each of these cases, instrumental measurements have been made of accelerations and displacements during and after strong ground shaking, allowing comparison with numerical model predictions of the same quantities.

Elgamal et al. (1990) describe the dynamic response and permanent deformations recorded at La Villita Dam in Mexico consequent to five earthquakes, most recently the September 19, 1985 Michoacan Earthquake. Yielding was confirmed to have occurred within the embankment by asymmetry of acceleration records recorded at various points on the dam, i.e., some of the peaks in the acceleration history were truncated as material slipped in the vicinity of the accelerograph. The authors used simplified displacement estimation techniques involving a “sliding rock” analogy (Newmark 1965) to successfully predict stick-slip type deformations and to evaluate the accumulation of displacement over several earthquake events.

Matahina Dam, New Zealand was shaken and deformed by the 1987 Edgecumbe Earthquake (M6.7)and the dynamic response and displacements were recorded by extensive instrumentation (Finn et al 1994). A nonlinear finite element computer code, TARA-3 (Finn et al 1986), was employed to simulate the performance of the Matahina Dam, using engineering properties carefully determined by laboratory and field-testing. Deformations were generally small (less than 0.5m), but the results of this study boosted the confidence of geotechnical engineers to analytically estimate earthquake behavior of embankment dams for stronger events.

To summarize, experience has shown that well-compacted, impervious rolled-fill dams are resistant to earthquake forces, provided they are constructed on rock or overburden foundations resistant to liquefaction. The same is true of well-drained, compacted rockfill dams or dumped rockfill dams with impervious cores, although some surface deformation can be expected on steep slopes. Rockfill dams with membrane facing (e.g., concrete) have performed well under strong shaking; however, permanent displacement or cracking of the facing can be expected which may require remediation following the seismic event. Low-density embankments built of low plasticity granular soils, especially hydraulic or semihydraulic fills, are highly susceptible to earthquake damage due to the potential for liquefaction. Existing dams that have been constructed on foundations of low density cohesionless materials formed in continuous layers also may be subject to excessive deformations during the seismic event due to liquefaction.

## 1.5 Analysis of Embankment Dams

Basically, the seismic safety and performance of embankment dams is directly related to permanent deformations experienced during and after an earthquake, the stability of slopes during and after the earthquake, dynamic slope movements, and build-up of excess pore water pressures in embankment and foundation materials which may induce soil liquefaction. Therefore, the dynamic response of a dam during strong ground shaking is governed by the deformational characteristics of the different soil materials.

The problem of seismic response and behavior of dams and their foundations, when formulated in general terms, is extremely complex. Depending on the type and size of the dam, its seismic exposure, and other factors such as regulatory requirements, numerical analysis may be conducted using simplified or complex procedures.

The seismic safety of embankment dams is governed by whether loss of strength might occur within the dam or its foundation, and whether nonrecoverable deformations remain within acceptable limits. Large deformations reduce freeboard and often cause longitudinal or transverse cracking

The past 25 years have resulted in significant progress in methods and tools to evaluate the seismic performance of embankment dams. The simplest of these methods relies on empirical correlations and simplified procedures derived from observed or calculated seismic response data, and requires few input parameters. Field penetration data can be interpreted to assess the potential for liquefaction. Detailed analysis techniques include EQL (decoupled) solutions, and NL finite element and finite difference coupled or decoupled formulations. Information on applicable computer programs for dam engineering has been compiled in a USCOLD publication (1992a) and Bureau (1997) presented a review of various applicable procedures and some examples of their application. In the sequel, we will present the essential methods used in dam calculation. These methods range from simplified procedure to three-dimensional numerical approaches in attempt to analyse the interactive response of the dam body, the reservoir water, and the dam foundation, using sophisticate constitutive modeling for different parts of the dam.

### 1.5.1 Simplified Analysis Procedures

Simplified procedures are used for small dams analysis or to assess the need for detailed studies of large dams. Two common procedures are described in the following. Other simplified approaches for estimating dam deformations can be found in the literature (e.g., Jansen, 1987; Romo and Resendiz, 1981). If liquefaction is of concern to the dam or its foundation, the simplified procedure of Seed and Idriss (1970b) can be implemented for dams with flat slopes. A better approach is to assess the liquefaction potential from corrected field penetration data (Seed et al., 1983; Seed, 1983).

#### 1.5.1.1 Newmark's Method

Newmark (1965) computed earthquake-induced displacements in embankments by assuming that movements occur when inertia forces on a rigid block of soils above a fixed potential failure surface exceed its sliding resistance. He assumed that the slope deformed only during those portions of the earthquake when the out-of-slope earthquake forces cause the pseudostatic factor of safety to drop below 1.0.

For planar sliding surfaces, he related the maximum displacement to the peak acceleration (A) and velocity (V) of the input motion and the yield acceleration (N, or Ky). The yield acceleration is the horizontal load coefficient (in g) that results in a factor of safety of exactly 1.0 for the sliding block. The method can be applied to any soil mass and planar, circular, or noncircular failure surfaces by double-integrating the increments of an applied acceleration time history above the yield acceleration, for a downslope direction of movement. The sliding soil mass is defined by the slip surface with the lowest Ky in conventional static slope stability analyses. Figure 1.2 presents the corresponding horizontal velocity and slope displacement that occur in response to the darkened portions of the two acceleration pulses.

Computer programs such as STABL (Siegel, 1975) or UTEXAS3 (Wright, 1992) can be used to obtain Ky. The input acceleration time history is the specified ground motion, in the case of small dams, or is obtained by dynamic analysis at a suitable central location along the assumed slip surface, in the case of large dams. The main limitations of the method is that it assumes a well-defined sliding block that must be predefined and does not account for any progressive loss of soil strength during earthquake shaking. However, Ky may be adjusted as a function of time to consider strength degradation.A derivative of Newmark's method consists of estimating crest settlement by vectorially combining the displacements of the upstream and downstream slopes (Vrymoed, 1996).

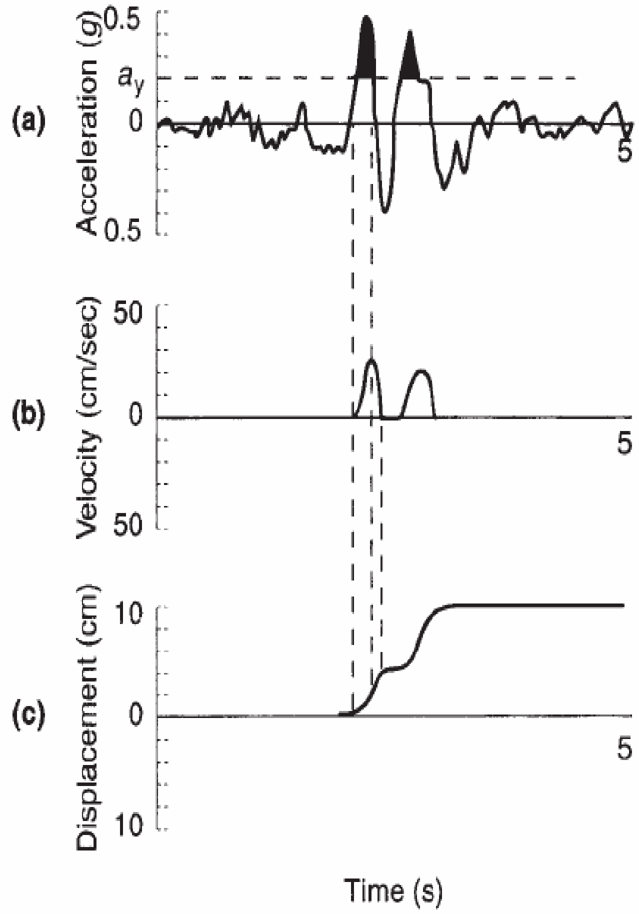


**Figure 1.2:** Diagram illustrating the Newmark method. (a) Acceleration versus time; (b) velocity versus time for the darkened portions of the acceleration pulses; (c) the corresponding downslope displacement versus time in response to the velocity pulses (After Wilson and Keefer 1985)

### 1.5.1.2 Makdisi–Seed's Procedure

A dam responds as a flexible body, and accelerations vary as a function of depth within the embankment. To take this into account, Makdisi and Seed (1977) estimated the peak crest acceleration ($\ddot{u}_{max}$) from a specified response spectrum and a square-root-of-the-sum-of-the-squares (SRSS) combination of the spectral accelerations of the first three modes of dam vibration. By interpreting the results of EQL finite element analyses of several dams, they related the average peak acceleration ratio of the sliding mass ($K_{max}$) and $\ddot{u}_{max}$ to the depth of the assumed failure surface. Then, for several magnitudes, they expressed the normalized peak displacement of the soil mass, $\ddot{u}_{max}/K_{max}gT_0$, as a function of $K_y/K_{max}$ as described in figure 1.3.

In their investigation, Makdisi and Seed used the examples of clayey dams of medium height (75 to 150 ft). Hence, their procedure applies best to similar dams. For dams higher than 200 ft, it may be prudent to increase calculated displacements proportionately to the dam height. Due to the assumptions of no loss of strength during shaking and EQL properties, the procedure is questionable for severe ground shaking (0.50 g or greater) and only applies to dams built of materials experiencing little or no loss of strength during shaking (such as densely compacted sands or cohesive clays).

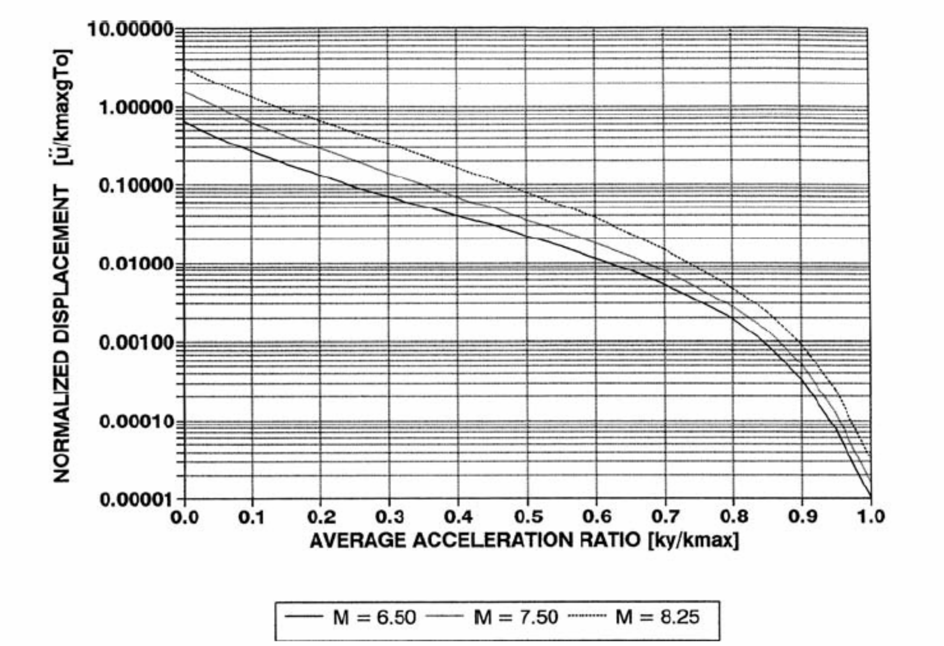


**Figure 1.3:** Simplified estimation of normalized displacements by Makdisi-Seed's procedure (Makdisi, F. and Seed, H.B. 1977. EERC Report no. UCB/EERC–77/19, Earthquake Engineering Research Center, University of California, Berkeley)

### 1.5.2 Empirical Methods

Empirical methods are based on the observed or computed performance of existing dams and correlate crest settlement with peak ground motion parameters.

#### 1.5.2.1 Bureau's Method (1985, 1987)

Observed performance of concrete face and earth core rockfill dams was used to develop an empirical relationship between the earthquake severity and the relative crest settlement for this type of dam. The dam is assumed founded on bedrock or hard soils, although several of the dams used in developing the correlation were on alluvial foundations. The original correlation was developed for compacted rockfill, a material that does not develop significant loss of strength during shaking. In 1987, the authors tested the correlation with friction angles lower than encountered in rockfill, using the results of physical model tests on dry sand embankments (Roth et al., 1986). Figure 1.4 gives the relative crest settlement function of earthquake severity Index. The extended correlations can be used for dams built of densely compacted granular materials, using the applicable friction angle.

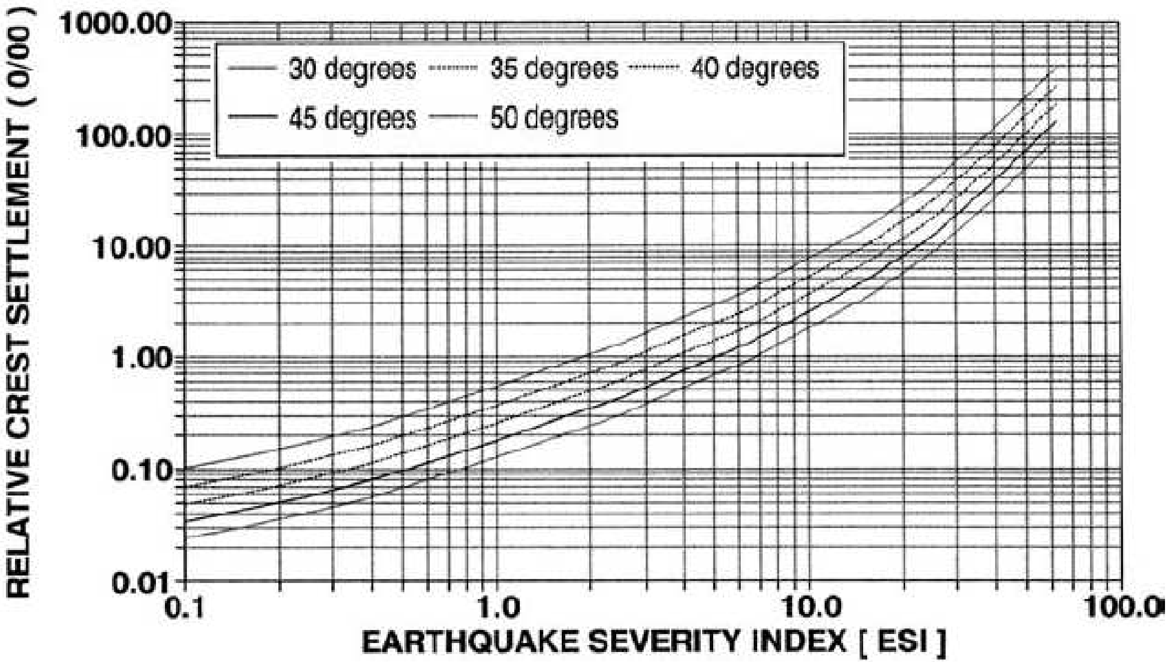


**Figure 1.4:** Crest settlement estimates for rockfill dams and sand embankments based on Earthquake Severity Index (ESI) (Roth, W.H., Scott, R.F., and Cundall, P.A. 1986. 3rd U.S. National Conference on Earthquake Engineering, August 24–28, Charleston, SC, vol. I, Earthquake Engineering Research Institute, Oakland, CA, pp 506–516)

#### 1.5.2.2 Swaisgood's Method (1995, 1998)

Swaisgood estimated seismic crest settlements by statistical treatment of data collected from the seismic performance review of about 60 existing dams. In 1995, he related the crest settlement (CS), expressed in percent of combined dam and alluvium thickness, to a seismic energy factor (SEF) and three constants based on type of dam construction ($K_{typ}$), dam height ($K_{dh}$), and alluvial thickness ($K_{at}$). Similar to the ESI, the SEF depends on the magnitude and peak ground acceleration of the causative earthquake. In 1998, Swaisgood streamlined his approach and expressed the crest settlement as the product of the SEF and a resonance factor (RF) differentiating between rockfill, earthfill, or hydraulic fill dams. As is the case with other simplified procedures, Swaisgood's method is questionable when applied to loose embankments.

### 1.5.3 Equivalent-Linear Response Analyses

Equivalent-linear (EQL) analyses typically use two-dimensional numerical models of the maximum dam section. Static analysis is first required to establish the initial state of stress. Finite element analyses used to define the initial state of static stresses often rely on hyperbolic soil models (Duncan et al., 1984) and variations of the initial tangent static modulus $E_i$ with the confining pressure, as originally suggested by Janbu (1963):

$$E_i = K.P_a.(\sigma/P_a)^n \qquad \text{(Eq.1.1)}$$

in which K is a constant, $\sigma$ the minor principal stress, $P_a$ the atmospheric pressure, and n an exponent defining the rate of variation of $E_i$ with $\sigma$.

Strain-dependent equivalent dynamic shear moduli and damping ratios as first introduced by Seed and Idriss (1970a) (Figure 1.5), are essential to EQL analyses.

Gradual embankment construction and progressive reservoir filling can be simulated. Then dynamic response can be computed. EQL response is sometimes obtained for representative soil columns within the dam section using SHAKE91 (Idriss and Sun, 1992). Most frequently, two-dimensional finite element programs are used, such as FLUSH (Lysmer et al., 1975), SuperFLUSH (Civil Systems, Inc., 1980), DYNDSP (Von Thun and Harris, 1981) or QUAD4M (Hudson, Idriss, and Beikae, 1994). SuperFLUSH and QUAD4M include simulation of a compliant base, which improves the solution. QUAD4M allows indirect calculation of dam deformations based on the concept of sliding wedges and seismic coefficients. If three-dimensional effects are expected, two-dimensional models can be stiffened so that the fundamental period of the modeled section matches that of the threedimensional dam, or three-dimensional analysis is performed with TLUSH (Mejia and Seed, 1983). Following the response analysis, induced stresses can be compared with stresses causing liquefaction (Seed, 1983), or computed acceleration histories used in Newmark's Method to obtain displacement estimates. Attempts to convert EQL strains into non recoverable deformations have been made using the concepts of stiffness softening or strain potential (Serff et al., 1976). Such concepts required significant judgment in their application, and are now rarely implemented.

The reliability of EQL analyses decreases when the specified ground motion becomes very demanding. After such analyses, it is desirable to perform conventional stability analyses of the upstream and downstream slopes of the dam, using computer programs such as STABL or UTEXAS3 and assigning post liquefaction residual strength properties to the affected zones of the embankment.

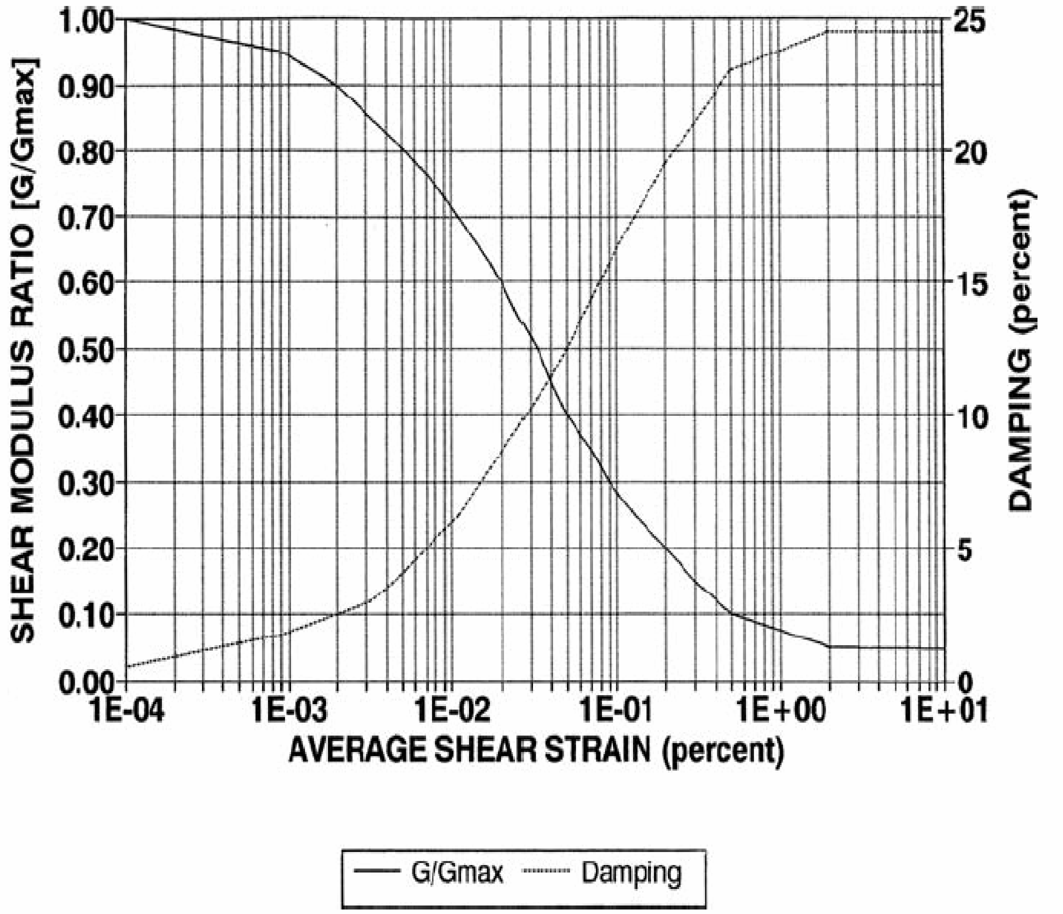


**Figure 1.5** Typical strain-dependent average shear modulus and damping factors (Seed, H.B. and Idriss, I.M. 1970a. Report no. EERC/70–10, December, Earthquake Engineering Research Center, University of California, Berkeley)

### 1.5.4 Nonlinear Analysis

Recent methods developed for dam earthquake analysis include nonlinear (NL) finite element or finite difference analysis. These methods apply when loss of strength, large deformations, or liquefaction are a concern for the embankment or its foundation. A significant advantage of NL analysis is that the same numerical model can be used for both static and dynamic conditions. Post-earthquake stability can also be evaluated by pursuing the analysis through a period of quiet time after the end of the excitation and verifying whether the dam maintains a stable configuration.

NL analyses include elasto-plastic (EPNL) and direct nonlinear (DNL) solutions. Dynamic pore pressures are semicoupled or fully coupled with deformations and volume changes. EPNL (two-dimensional) computer programs include DYNAFLOW (Prevost, 1981; Elgamal et al., 1984), DYNARD (Moriwaki et al., 1988) and FLAC (Itasca Consulting Group, 1992). A three-dimensional version of FLAC (FLAC 3D) was released in 1995. DNL (two-dimensional) programs include TARA-3 and TARA-3L (Finn and Yogendrakumar, 1989) and GEFDYN (Coyne and Bellier/ECP/EDF-REAL, 1991). The Bureau of Reclamation (USBR) has also used ADINA/BM (Bathe, 1978) with hyperbolic and cap models and an endochronic pore pressure generator based on computed strains (Harris, 1986).

The previously mentioned programs use various constitutive models. TARA-3 and TARA-3L use total or effective stresses, hysteretic cyclic shear behavior, and undrained strength parameters. Response depends on the mean effective normal stress and hyperbolic stress-strain curves, with the tangent shear and bulk moduli being continuously updated during the calculations. Excess pore pressures are coupled with the strain response through the Martin–Finn–Seed model (1975). Permanent deformations accumulate due to gravity action and consolidation of the softened soils. If liquefaction is triggered, the specified residual strength replaces the undrained shear strength.

GEFDYN relies on the Hujeux–Aubry constitutive model (Aubry et al., 1982). This model attempts to reproduce fully coupled fluid-soil behavior based on elasto-plastic strain softening/hardening and the concept of critical state, where soils continue to deform at constant stress and void ratio. GEFDYN requires common soil parameters (effective friction angle and cohesion; stress-dependent moduli and Poisson's ratio) and critical state, dilatancy, deviatoric, and isotropic parameters (Martin and Niznik, 1993).

FLAC and FLAC3D are explicit, finite difference programs. Constitutive equations are solved incrementally (Cundall, 1976), thus allowing large strains, material anisotropies, sliding interfaces, and other nonlinearities. For dam analysis, the Mohr–Coulomb constitutive model has been shown to be particularly applicable (Roth et al., 1986). Other models are built in the program or can be coded through a macro programming language. At every calculation step, incremental strains are computed in each elementary zone and resulting stress increments derived from the applicable constitutive relationship. Zone stresses and gridpoint displacements are updated, and new incremental strains are computed. Massand stiffness-dependent Rayleigh damping is used at low strain. At higher strains, damping occurs primarily through hysteretic looping. A semicoupled empirical procedure (Roth et al., 1991; Dawson et al., 2001), based on the concept of cumulative damage, has been used in FLAC to generate excess pore pressures at each calculation step. Figure 1.6 shows the two-dimensional finite element model of a large embankment dam, the time history of the computed settlement at the crest center, and shear stress and excess pore pressures histories obtained for a typical model grid zone.

In another NL approach using Cundall's equations, Beikae (1996) extended Newmark's method to calculate three-dimensional seismic displacements in an embankment. The procedure uses a Lagrangian formulation, coded in the computer program BLOCK3D. It simulates gravity, hydrostatic, and seismic forces on elementary soil blocks with fixed masses representing the geometry of the embankment. Soil blocks can move, expand, compress, and distort in space relative to each other. The equations of motions are solved explicitly at the gravity center of each elementary block. A significant limitation is that BLOCK3D applies to materials not susceptible to developing excess pore pressures.

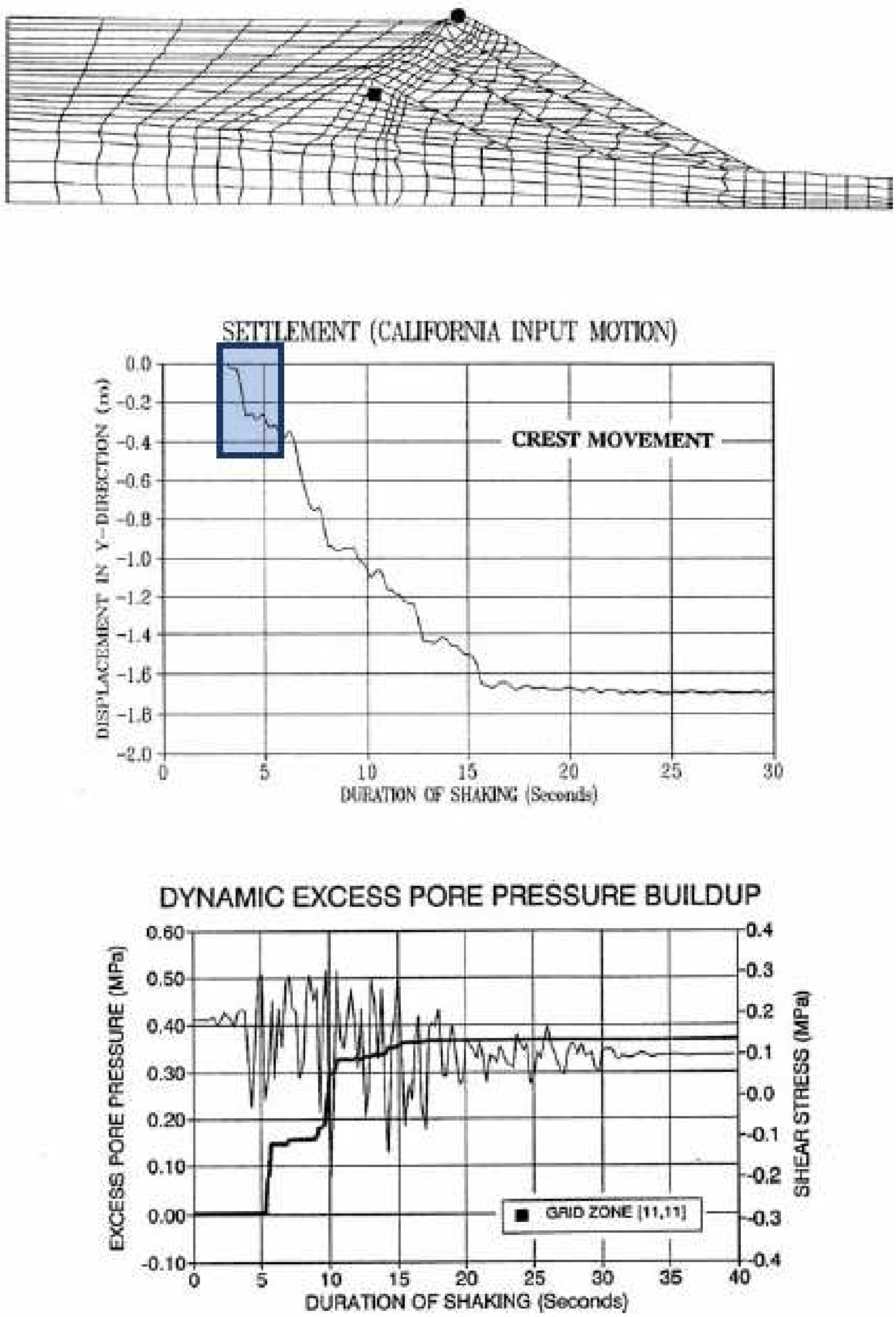


**Figure 1.6** Example of results provided by a typical Nonlinear two-dimensional finite difference model of an embankment dam (Roth, W.H., Bureau, G., and Brodt, G. 1991. Proc. 17th International Congress on Large Dams, Vienna, June, pp 1199–1223),( Dawson, E.M., Roth, W.H., Nesarajah, S., Bureau, G., and Davis, C.A. 2001. Proc. 2nd International FLAC Symposium, October, Lyon-Ecully, France, Itasca Consulting Group, Minneapolis, MN)

## 1.6 Unsaturated Soils

Classical soil mechanics has emphasized specific types of soils (e.g., saturated sands, silts, and clays and dry sands). Textbooks cover the theories related to these types of soils in a completely dry or a completely saturated condition. Recently, it has been shown that attention must be given to soils that do not fall into these common categories. Many of these soils can be classified as unsaturated soils. Engineering related to unsaturated soils has typically remained empirical due to the complexity of their behavior. An unsaturated soil consists of more than two phases and therefore the natural laws governing its behavior are changed. Central to the behavior of an unsaturated soil is the relationship between water and air as the soil desaturates. This relationship is described by the Soil-Water Characteristic Curve (SWCC).

For prediction of the shear strength of an unsaturated soil, two approaches had been proposed by Bishop (1959—effective stress approach) and Fredlund et al.(1978—independent stress variables approach). Many researchers have demonstrated both theoretical and empirical formulations to estimate unsaturated shear strength, e.g. the verification of the nonlinear change in cohesion of an unsaturated soil (Escario and Sáez 1986; Gan et al. 1988); an analytical model based on a soil–water retention curve (Fredlund et al.1995; Vanapalli et al. 1996); an empirical formulation based on Bishop's concept (Öberg and Sällfors 1997; Khalili and Khabbaz 1998); the prediction of soil cohesion using hyperbolic equation (Miao et al. 2002;Lee et al. 2003).

The effective stress variable proposed by Terzaghi (1936) has been used with Mohr-Coulomb criterion for predicting the shear strength of saturated soils. The shear strength equation for saturated soils is expressed as a linear function of effective stress and is given as follows:

$$\tau = c' + (\sigma_n - u_w) \tan \Phi' \qquad \text{(Eq.1.2)}$$

where:

$\tau$ is the shear strength;

$c'$ is the effective cohesion;

$\Phi'$ is the effective angle of internal friction;

$\sigma_n$ is the total normal stress on the plane of failure;

$(\sigma_n - u_w)$ is the effective normal stress of the plane of failure ;and

$u_w$ is the pore water pressure.

Many practical problems involve assessing the shear strength of unsaturated soils. According to Bishop(1959), the generalized Mohr-Coulomb failure criteria is:

$$\tau = c' + (\sigma_n - u_a) \tan \Phi' + (\chi\,(u_a - u_w)) \tan \Phi' \qquad \text{(Eq.1.3)}$$

$u_a$ is the pore-air pressure;

$\chi$ is the coefficient that depends on $S_r$ and void ratio (e), whose determination presents major difficulties.

Fredlund and Morgenstern (1978) showed that the shear strength of unsaturated soils can be described dy any two of three stress state variables, namely $(\sigma\text{-}u_a)$, $(\sigma\text{-}u_w)$,and $(u_a\text{-}u_w)$.They proposed the following equation for the shear strength of unsaturated soils:

$$\tau = c' + (\sigma_n - u_a) \tan \Phi' + (u_a - u_w) \tan \Phi^b \qquad \text{(Eq.1.4)}$$

$(\sigma_n - u_a)$ and $(u_a - u_w)$ stand for the normal stress and the suction, respectively.
φb is the friction angle associated with the suction; generally it is not a constant, but decreases as the tension increases.

Lamborn (1986) proposed a shear strength equation for unsaturated soils by extending a micromechanics model based on principles of irreversible thermodynamics to the energy versus volume relationship in a multiphase material (i.e., solids, fluids ,and voids). The equation is as follows:

$$\tau = c' + (\sigma - u_a) \tan \Phi' + (u_a - u_w)\, \theta_w \tan \Phi' \qquad \text{(Eq.1.5)}$$

$\theta_w$ is the volumetric water content, which is defined as the ratio of the volume of water to the total volume of the soil. The volumetric water content decreases as suction increases, and it is a nonlinear function of suction.

Some attempts have also been made to predict the shear strength of an unsaturated soil using empirical procedures. Abramento and Carvalho (1989) used a curve fitting technique for representing their experimental data. They used an exponential function that retains the form of the shear strength equation proposed by Fredlund et al., treating tan $\Phi^b$ as a variable with respect to the matric suction. Vanapalli et al. (1996) developed an empirical and analytical model to predict nonlinear shear strength in terms of soil suction. The formulation makes use of a soil water characteristic curve, saturated shear strength parameters, and an empirical parameter, κ. Öberg and Sällfors (1997) roughly replaced the χ-parameter that Bishop introduced, by Sr degree of saturation). Khalili (1998) introduced a unique relationship between the effective stress parameter, χ and the ratio of suction over the air entry value, and proposed a method to estimate the unsaturated shear strength using this parameter with cohesion, friction angle and confining pressure. Rassam and Williams (1999) proposed a function that describes the shear strength of unsaturated soils in terms of suction and normal stress, based on three-dimensional nonlinear regression analysis results. It incorporates the effect of normal stress on the contribution of suction to shear strength.

The existing methods need additional tests for unsaturated soils such as unsaturated shear strength tests or SWCC tests, in order to predict the nonlinear characteristics of the shear strength of the unsaturated soil. However, since these tests for unsaturated soils are very difficult, time-consuming and costly to conduct, it is practically difficult to apply for predicting the shear strength by them, even though the shear strength of the unsaturated soils could be represented by the most of these methods.

Miao et al. 2002; Lee et al. 2003 suggested an empirical equation for the prediction of unsaturated shear strength as a function of volumetric water content. In this formulation, shear strength $\tau$ was expressed as:

$$\tau = \sigma' \tan \Phi' + C\, e^{-\mu\theta} \qquad \text{(Eq.1.6)}$$

Where $\sigma'$ is net normal stress, $\Phi'$ is effective angle of shearing resistance, C is maximum cohesion, $\mu$ is a susceptibility coefficient and $\theta$ is volumetric water content of soil. The variables can be obtained by a basic shear test and a subsequent regression analysis.
An advantage of this formulation is that all the parameters required are available without any elaborate soil testing.

## 1.7 Program Validation

An important step in the use of NL analysis is to perform calibration tests and verifications. TARA-3 was validated with centrifuge testing (Finn, 1991) and using the example of Matahina Dam, New Zealand (Finn et al., 1992). GEFDYN has been tested using the observed performance of El Infiernillo Dam (see the proceedings of the International Benchmarks Workshops on Numerical Analysis of Dams, Bergamo, Italy, 1992, Paris, 1994, and Denver, CO, 1999 (ICOLD, 1992, 1994, 1999)). Verifications of FLAC for dam analysis purposes include prediction of centrifuge liquefaction testing results (Inel et al., 1993) and comparison between observed and back-calculated performances of South Haiwee Dam (Dames and Moore, 1991), Los Leones Dam (Bureau et al., 1994), Los Angeles Dam (Bureau et al., 1996), and Upper San Fernando Dam (Dawson et al., 2001).

## 1.8 Conclusion

Design of earth dams in seismic areas requires analysis of their response to typical input motions in order to ensure their safety and stability. Such issue is particularly complex, because it needs the resolution of a soil-structure interaction taking into account the non linear behaviour of the soil material, the fluid-structure interaction, the fluid-skeleton interaction and the interaction of the dam with the soil foundation.

Recent developments in the area of numerical modelling allow theatrically dealing with these complex issues. Indeed, recent development allowed the formulation of advanced constitutive relations which can correctly describe the soil behaviour under complex paths included cyclic loading. These relations were implemented in numerical code which can deal with 3D configuration and take into account coupled phenomena such as the soil-water interaction. They can also deal with seismic loading. Their use in practice encounters major difficulties, which are mainly related to the determination of constitutive parameters and to the input motion. Consequently, engineers use simplified methods for the seismic design of dams or simplified constitutive relation for the soil material.

This work will focus on two topics of the seismic response of dams. The first one concerns the influence of plasticity on this response. Indeed, since we deal with unconfined material, the seismic loading generally induces plasticity in the dam. This plasticity can influence the all over response of the dam, because of its influence on damping and on the dominant frequencies of the dam. We propose in the first part of the thesis to deal with issue using the simple and popular Mohr-Coulomb criterion.

The second issue concerns the water-skeleton interaction. Indeed, due to the low permeability of the core and the rapid variation of the input motion, the seismic loading induces a variation in the pore pressure, which in the case of an increase can reduce the soil resistance and consequently leads to instability. This issue is analysed first using an undrained analysis which allows the determination of total stresses induced by the seismic loading. Then we use a full coupled analysis for the determination of the pore pressure variation and ti study the influence of this variation on the dam's response.

# CHAPTER II

## Seismic Response of the Earth Dams:

## Influence of plasticity

# CHAPTER II:

## Seismic Response of the Earth Dams: Influence of plasticity

### 2.1 Introduction

This chapter presents a numerical analysis of the seismic behaviour of earth dams. Analysis is conducted for the solid phase. It corresponds to the response of the dam before water filling. Analysis is first conducted for a simple case which concerns the elastic response of the dam. This analysis could provide some indication about the response of the dam, mainly the dynamic amplification. It will be also useful to understand the influence of plasticity on the dam response. The second part of the chapter concerns a more realistic analysis of the dam, where the elastoplastic behaviour of the earth material is considered. This analysis is conducted using the simple and popular non associated Mohr-Coulomb criterion. For both the elastic and plastic analyses, a parametric study is conducted for the investigation of the influence of major parameters such as the mechanical properties of the earth material, the geometry of the dam and the frequency of the input loading.

This chapter is composed of three parts. The first one presents briefly the numerical model used in the analysis, the second part presents results of the elastic analyses, while the last one presents a discussion of elastoplastic response of the dam.

## 2.2 Numerical model

Numerical analyses are conducted using the FLAC program. This program is based on a continuum finite difference discretization using the Langrangian approach. Every derivative in the set of governing equations is replaced directly by an algebraic expression written in terms of the field variables (e.g. stress or displacement) at discrete point in space (ITASCA, 2005). For dynamic analysis, it uses an explicit finite difference scheme to solve the full equation of motion using lumped grid point masses derived from the real density surrounding zone. The calculation sequence first invokes the equations of motion to derive new velocities and displacements from stresses and forces. Then, strain rates are derived from velocities, and new stresses from strain rates. Every cycle around the loop correspond to one time step. Each box in updates all of its grid variables from known values that remain fixed over the time step being executed.

Numerical distortion of the propagating wave can occur in dynamic analyses. Both the frequency content of the input motion and the wave-speed characteristics of the system will affect the numerical accuracy of wave transmission. Kuhlemeyer and Lysmer (1973) showed that for an accurate representation of the wave transmission through the soil model, the spatial element size, $\Delta l$ , must be smaller than approximately one-tenth to one-eighth of the wavelength associated with the highest frequency component of the input wave i.e.,

$$\Delta l \leq \lambda / 10 \qquad \text{(Eq.2.1)}$$

Where, $\lambda$ is the wave length associated with the highest frequency component that contains appreciable energy. Expressing $\lambda$ in the form of the shear wave velocity ($V_s$) and the highest frequency introduced to the system $f_{max}$, equation 2.1 can be written as:

$$\Delta l \leq V_S / (10 .f_{max}) \qquad \text{(Eq.2.2)}$$

This requirement may necessitate a very fine spatial mesh and a corresponding small time step. The consequence is that reasonable analyses may be time and memory consuming. In such cases, it may be possible to adjust the input by recognizing that most of the power for the input history is contained in lower frequency components. By filtering the history and removing high frequency components, a coarser mesh may be used without significantly affecting the results. Rayleigh damping is used in the analyses to compensate the energy dissipation through the medium. According to literature (FLAC manual, Paolucci, 2002; Lokmer et al., 2002), the damping for the geological materials lies between 2 % and 5%, and hence 5% Rayleigh damping is used in the following analyses.

## 2.3 Elastic analysis

This section presents analysis of a reference example, which will be followed by a parametric study.

### 2.3.1 Reference example

The reference example concerns an earth dam with a clay core constructed on a homogeneous soil layer (Figure 2.1). This example is a simplified representation of typical earth dam geometry. Geotechnical properties of the dam are summarized in table 2.1. They are chosen close to references cases. The foundation is assumed to be stiff with a Young's Modulus E = 1000 MPa. The Young's modulus of the core is equal to 40 MPa, while that of the shell is equal to 60 MPa. The frequencies of the foundation-dam system were determined by the Fourier analysis of the free response of the dam (Figure 2.2). It shows a fundamental frequency $f_1$ = 0.7 Hz; the second frequency is close to $f_2$ = 1.4 Hz.

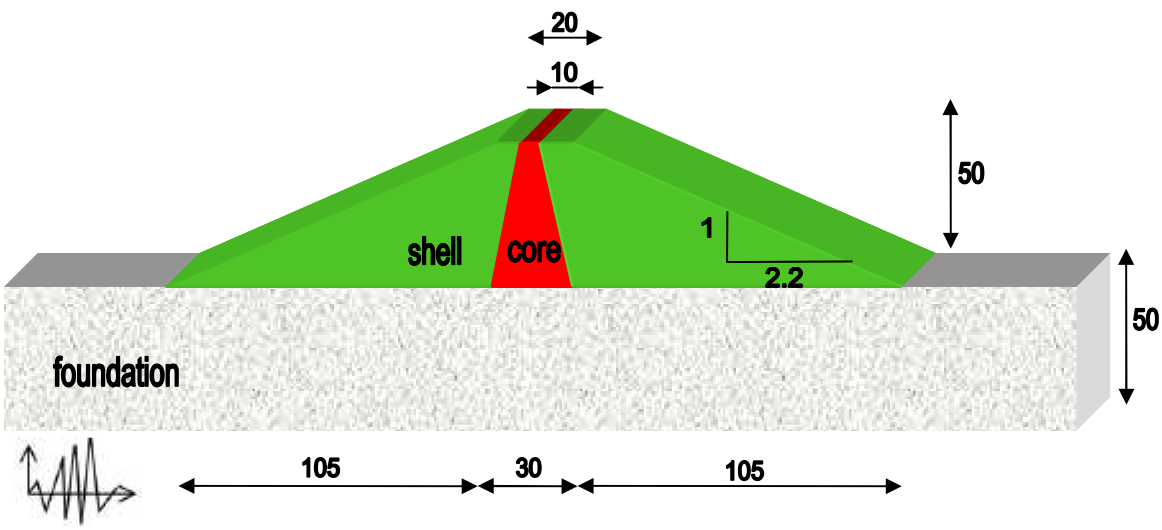


**Figure 2.1:** Reference example: Geometry of the dam

| Parameter | Units | Core | Shell | Foundation |
|---|---|---|---|---|
| Dry density (ρ) | (kg/m$^3$) | 1800 | 2000 | 2200 |
| Young's modulus (E) | (MPa) | 40 | 60 | 1000 |
| Poisson's ratio (ν) | - | 0.3 | 0.3 | 0.25 |
| Elastic shear modulus (G) | (MPa) | 15 | 23 | 400 |
| Bulk modulus (K) | (MPa) | 33 | 50 | 666 |

**Table 2.1:** Reference example: properties of the dam material

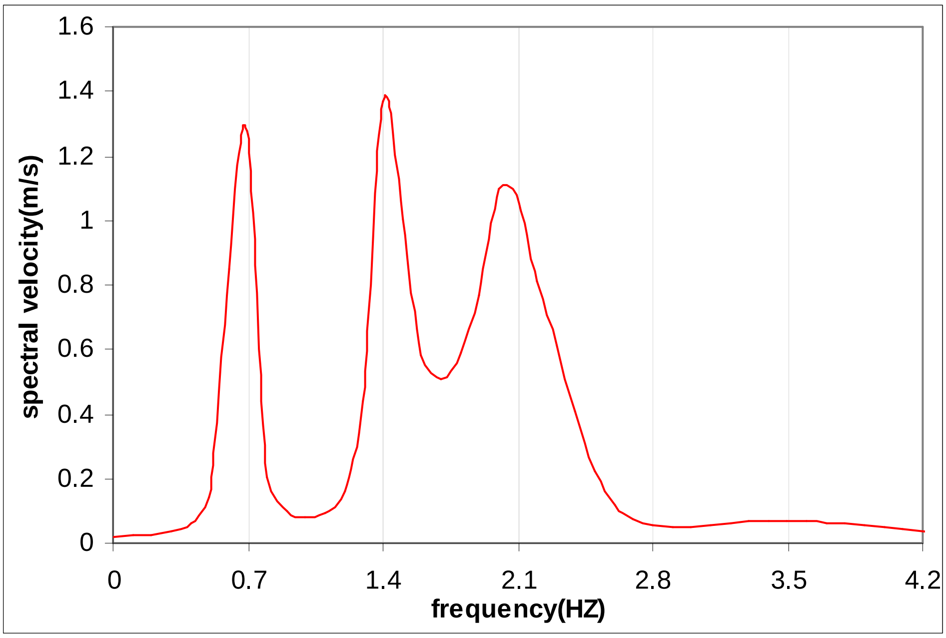


**Figure 2.2:** Reference example: Spectral response of the free motion

### 2.3.1.1 Response to harmonic loading

Analysis is conducted first to a sinusoidal loading, which is applied at the base of the foundation layer as a velocity excitation. The loading frequency is equal to 0.8 Hz, which is close to the fundamental frequency of the dam-foundation system ($f_1$ = 0.7 Hz). The loading amplitude is equal to $V_a$ = 1 m/s, while the load duration is equal to 10 sec.

The response of the dam at the maximum excitation is presented in figure 2.3. It shows an important lateral deformation in the dam. Figure 2.4 shows the velocity amplification in the axis of the dam. It can be observed that the deformation mode corresponds to the fundamental mode of the dam. Negligible amplification is observed in the foundation, while the amplification increases with the distance from the foundation; it attains 5 at the dam crest. Figure 2.5 shows the variation of the lateral amplification in the horizontal direction for two sections: the middle height of the dam and the crest. In the first section, we observe an increase in the amplification when going from the lateral surface of dam towards the dam axis: The amplification at extremities of the dam is equal to 1.5, while it attains 3 at the dam axis. At the crest, we observe a uniform distribution of the amplification.

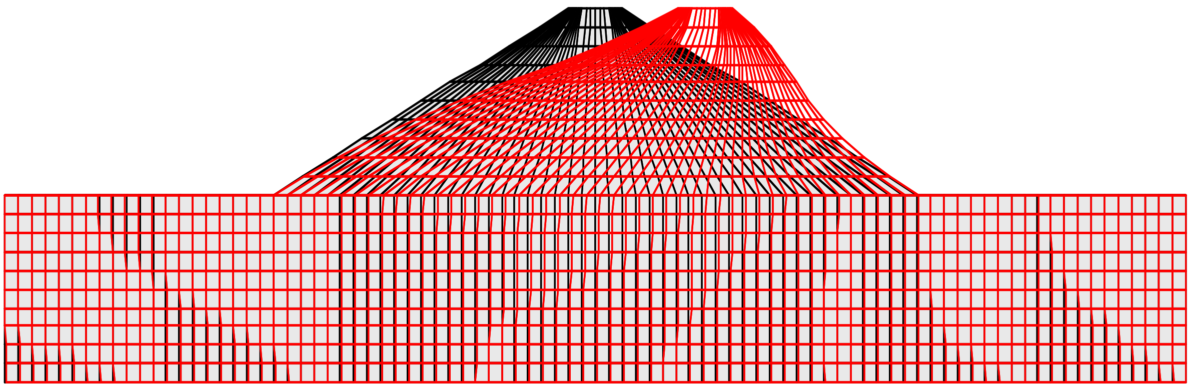

**Figure 2.3:** Reference example: Dam deformation at the maximum of excitation ($U_{max}$ = 1.649 m at the dam crest)

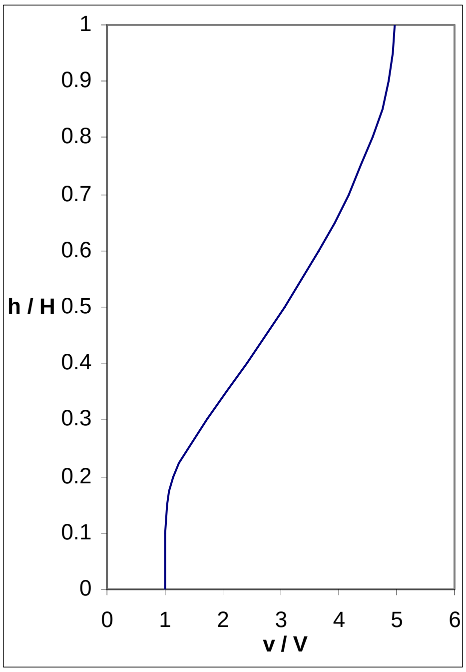


**Figure 2.4:** Reference example: Velocity amplification in the dam axis (harmonic loading)

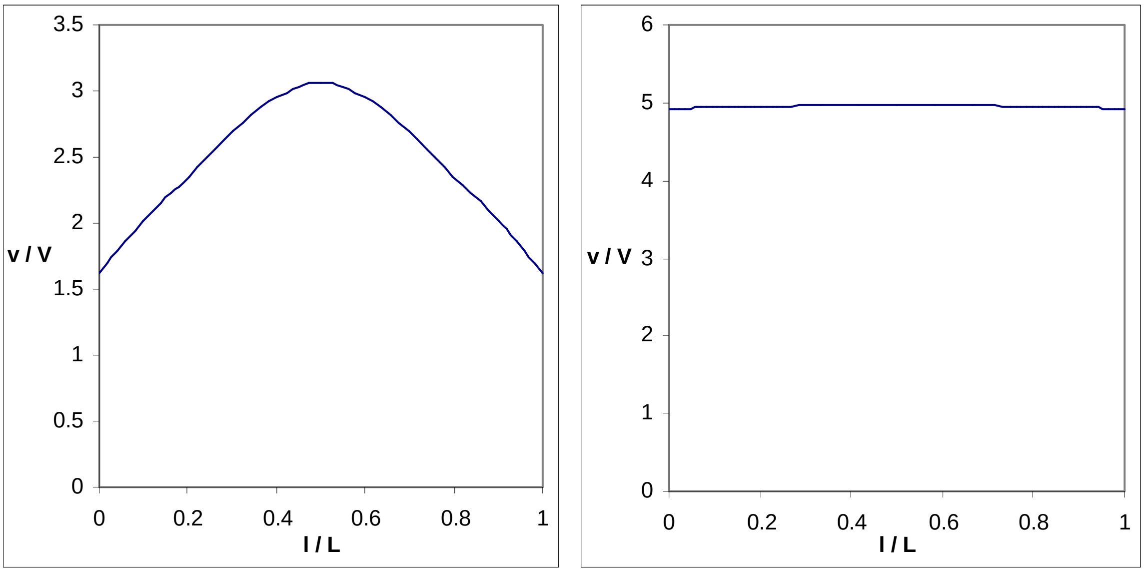


**(Middle height)** **(Dam crest)**

**Figure 2.5:** Variation of the velocity amplification in the horizontal direction

### 2.3.1.2 Response to a real earthquake record

In order to study the dam response to real earthquake loading, analysis was conducted with the 1999 Kocaeli earthquake record. The estimated peak velocity of this record is approximately equal to 0.40 m/sec (peak acceleration 0.247g), and its duration is approximately equal 30 sec. The record for base acceleration, velocity, and displacement of the input motion are shown in Figure 2.6. The frequency of the major peak is equal to 0.9 Hz.

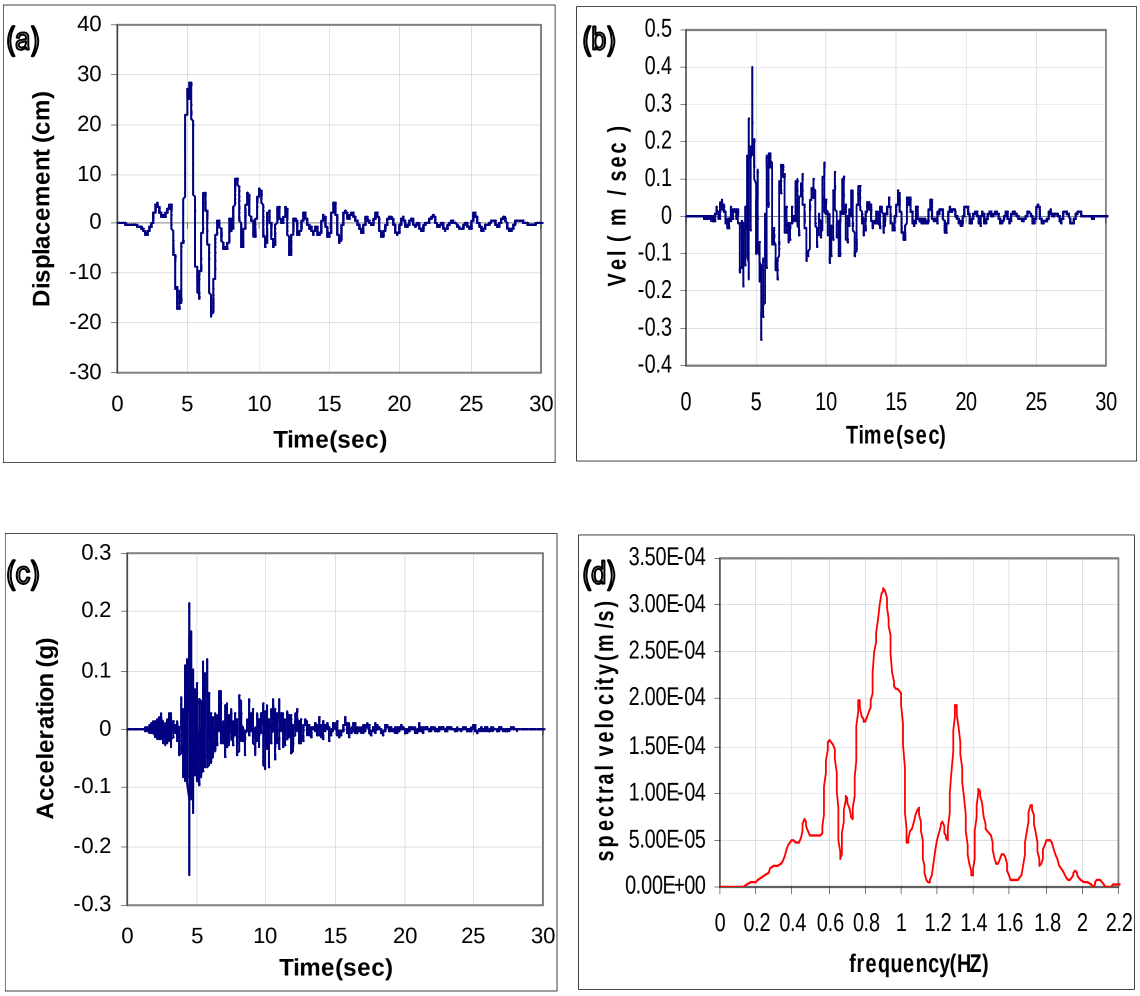


**Figure 2.6:** Kocaeli earthquake record (1999):

a) Displacement, b) Velocity, c) Acceleration, d) Spectra

The response of the dam at the maximum excitation is presented in figure 2.7. It shows an increase in the lateral deformation with the distance from the dam foundation. The variation of the lateral deformation in the horizontal direction seems to be low.

Figure 2.8 shows the velocity amplification in the axis of the dam. It can be observed that the amplification increases with the distance from the foundation; it attains 3.45 at the top of the dam. Figure 2.9 shows the variation of the lateral amplification in the horizontal direction at the middle height of the dam and the crest. In the first section, we observe a variation in the dynamic amplification between 2 and 2.5. At the crest, we observe a uniform distribution of the amplification (close to 3.45).

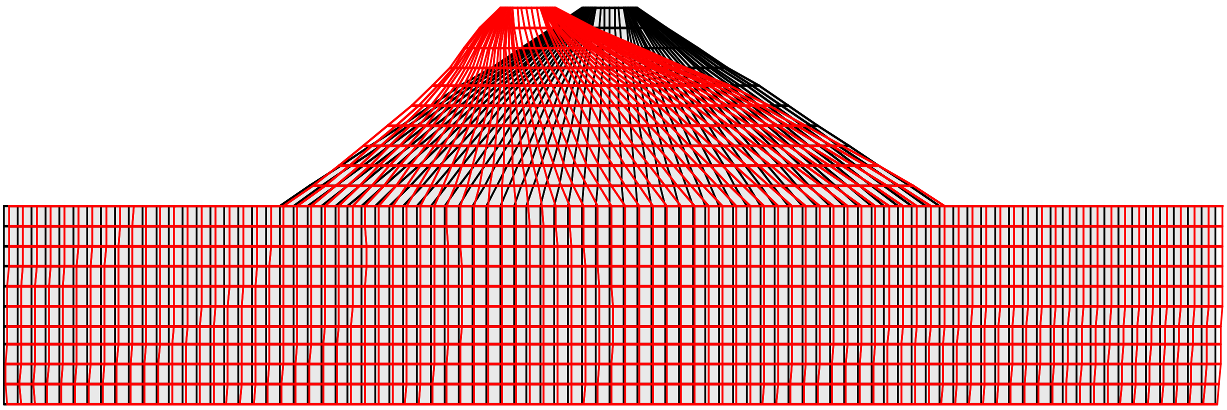

**Figure 2.7:** Dam deformation at the maximum of excitation (Kocaeli earthquake record) ($U_{max}$ = 0.30 m at the dam crest)

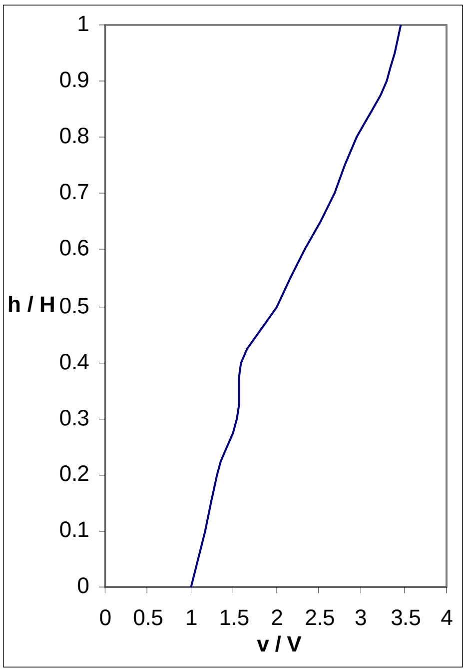


**Figure 2.8:** Velocity amplification in the dam axis (Kocaeli earthquake record)

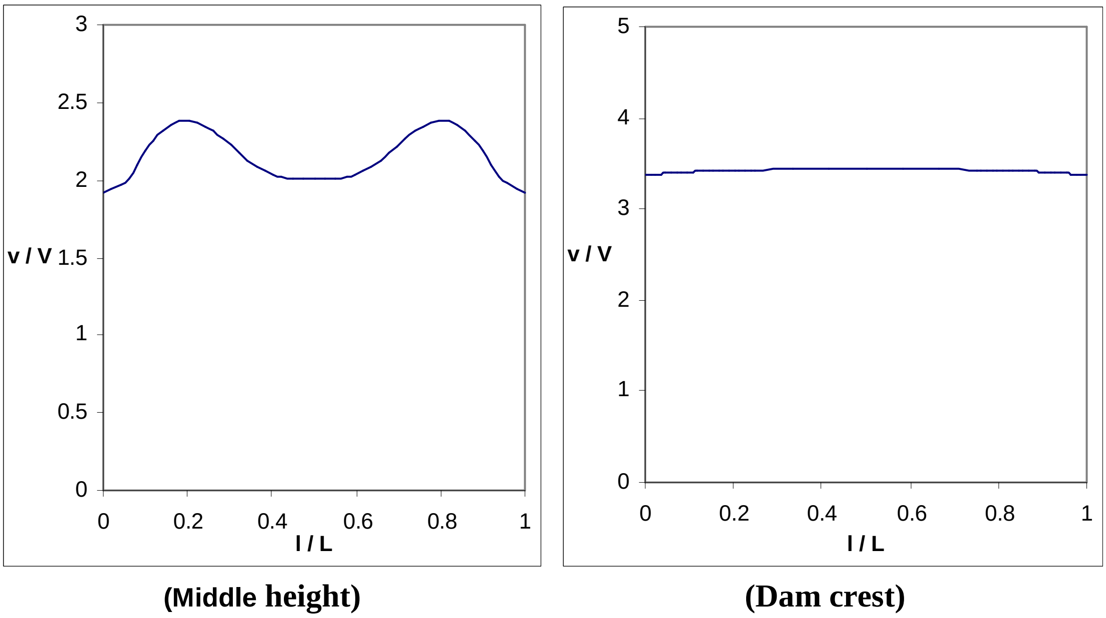


**Figure 2.9:** Variation of the amplification in the horizontal direction

## 2.3.2 Parametric analysis - elastic response

The seismic response of the dam is affected by the mechanical properties of the earth material, the geometry of the dam and the frequency of the input motion. In the following we present a study of the influence of the following parameters:

- Earth material density
- Soil stiffness

### 2.3.2.1 Earth material Density

Analyses were conducted for the dam subjected to the Kocaeli earthquake record for three densities of the core (1800, 2000 and 2200 kg/m$^3$) and three densities of the shell (1600, 1800 and 2000 kg/m$^3$). Figure 2.10 shows the influence of the variation of the core density on the seismic amplification in the dam. It can be observed that this variation does not affect the dam response. This result is expected, because the mass of the core presents a small part of the mass of the dam. The influence of the variation of the shell density on the seismic amplification of the dam is illustrated in figure 2.11. It can be observed that the decrease in the shell density leads to an increase in the dynamic amplification. This result is also expected, because the decrease in the mass of the dam leads to an increase of its fundamental frequency (0.7 Hz for the reference case $\rho$ = 1800), towards the frequency of the major peak of the loading (0.8 Hz).

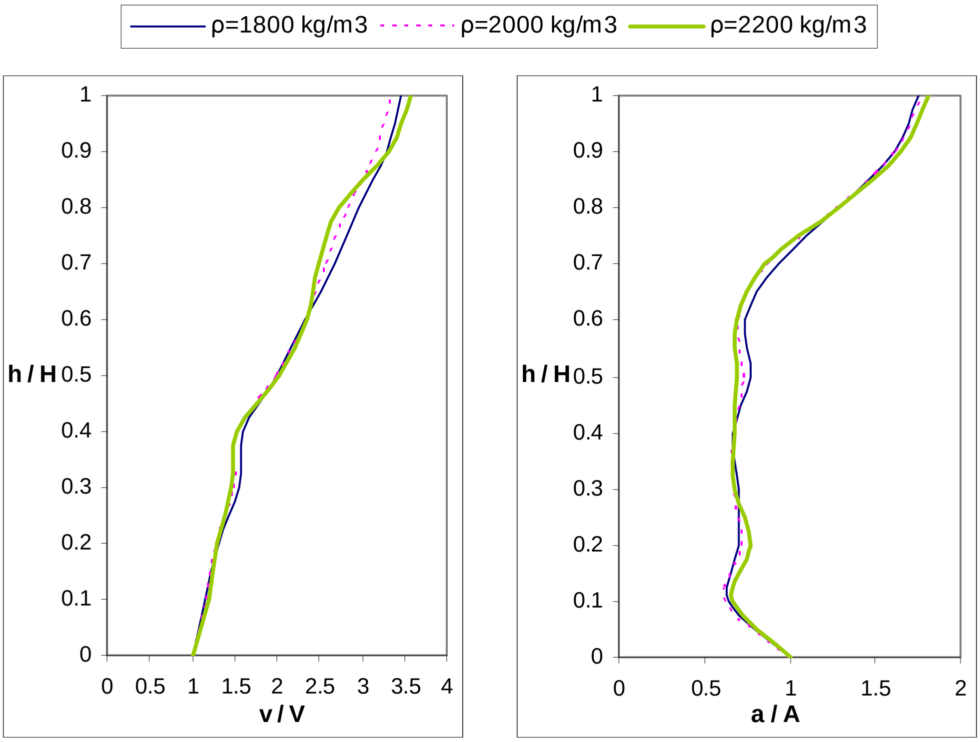


**(Velocity)** **(Acceleration)**

**Figure 2.10:** Influence of the core density on the seismic response of the dam (Kocaeli earthquake record)

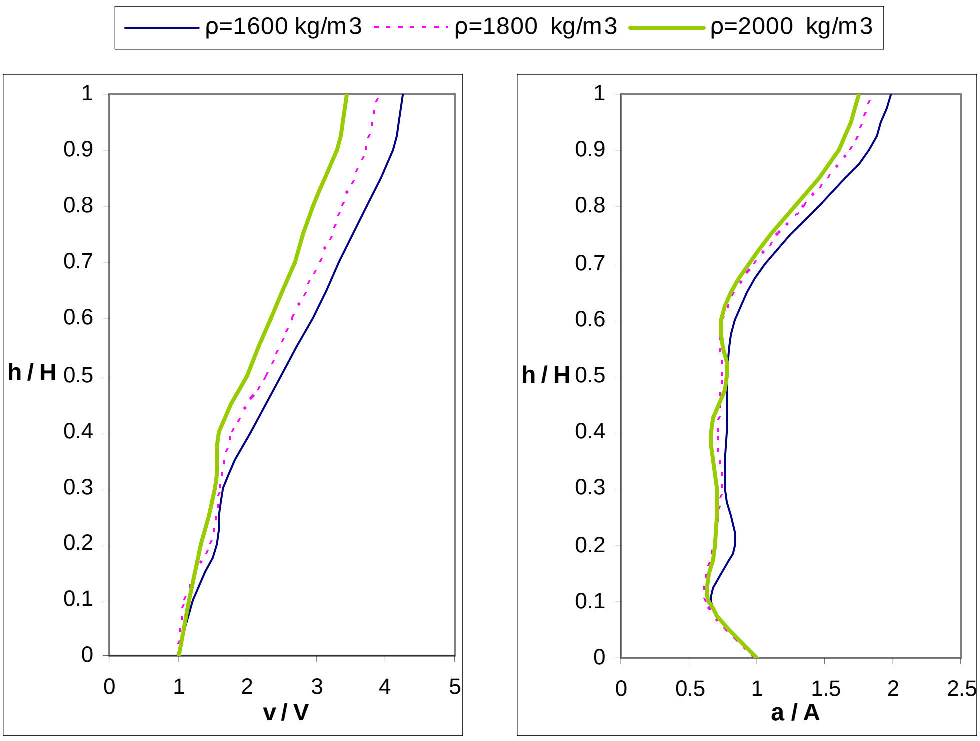


**(Velocity)** **(Acceleration)**

**Figure 2.11:** Influence of the shell density on the seismic response of the dam (Kocaeli earthquake record)

### 2.3.2.2 Earth material stiffness

Analyses were also conducted for the Kocaeli earthquake record for:

- Three values of the Young's modulus of the core: E = 40, 60 and 80 MPa; G = (15, 23 and 31 MPa).
- Three values of the Young's modulus of the shell: E = 30, 40 and 60 MPa; G = (11, 15 and 23 MPa).
- Three values of the Young's modulus of the foundation: E = 500, 750 and 1000 MPa; G = (200, 300 and 400 MPa).

Figure 2.12 shows the influence of the variation of the shear modulus of the core on the seismic amplification of the dam. It can be observed that this variation leads to a moderate increase in the dynamic amplification. This increase results from the increase of the fundamental frequency of the dams towards the dominate frequency of the loading. The influence of the variation of the shearing modulus of the shell on the seismic amplification in the dam is illustrated in figure 2.13. It can be observed that the increase in the shell shearing modulus leads to a significant increase in the dynamic amplification. This result is also expected, because the increase in the shell shearing modulus leads to an increase in its fundamental frequency towards the frequency of the major peak of the input motion.

The influence of the variation of the shear modulus of the foundation on the dynamic amplification is depicted in figure 2.14. It can be observed that an important variation of this parameter (100%) slightly affects the seismic response of the dam.

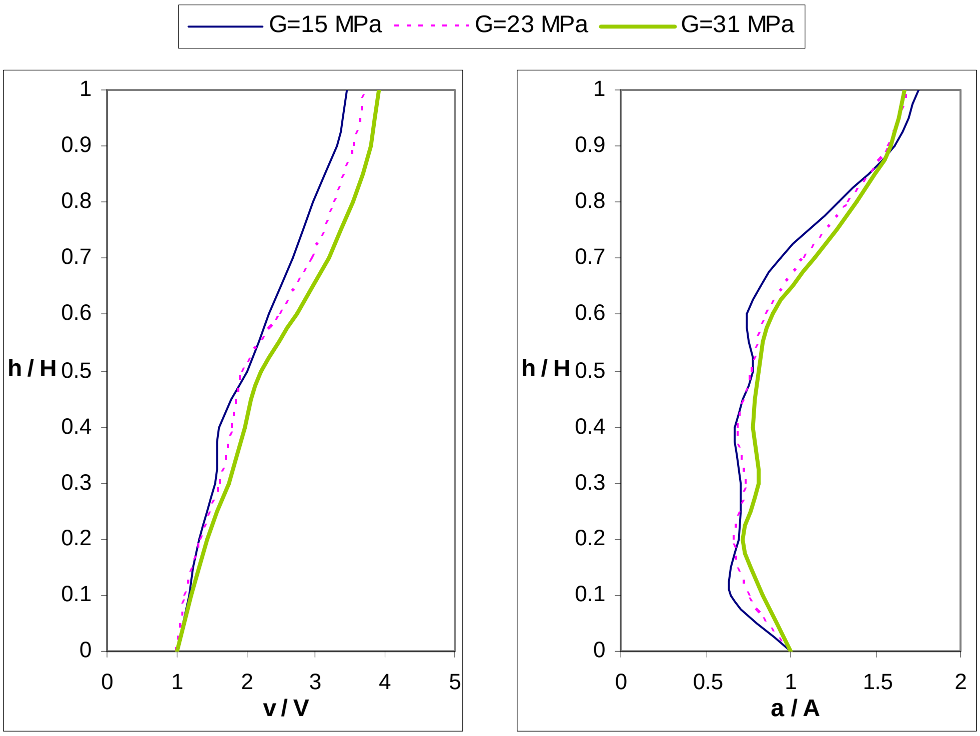


**(Velocity)** **(Acceleration)**

**Figure 2.12:** Influence of the core stiffness on the seismic response of the dam (Kocaeli earthquake record)

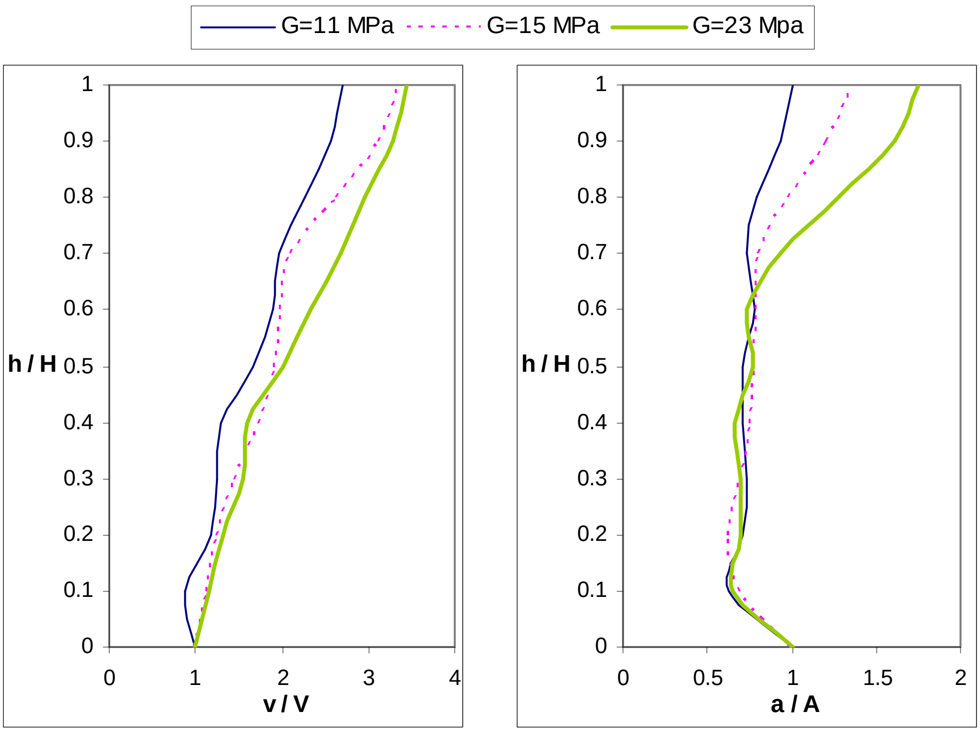


**(Velocity)** **(Acceleration)**

**Figure 2.13:** Influence of the shell stiffness on the seismic response of the dam

(Kocaeli earthquake record)

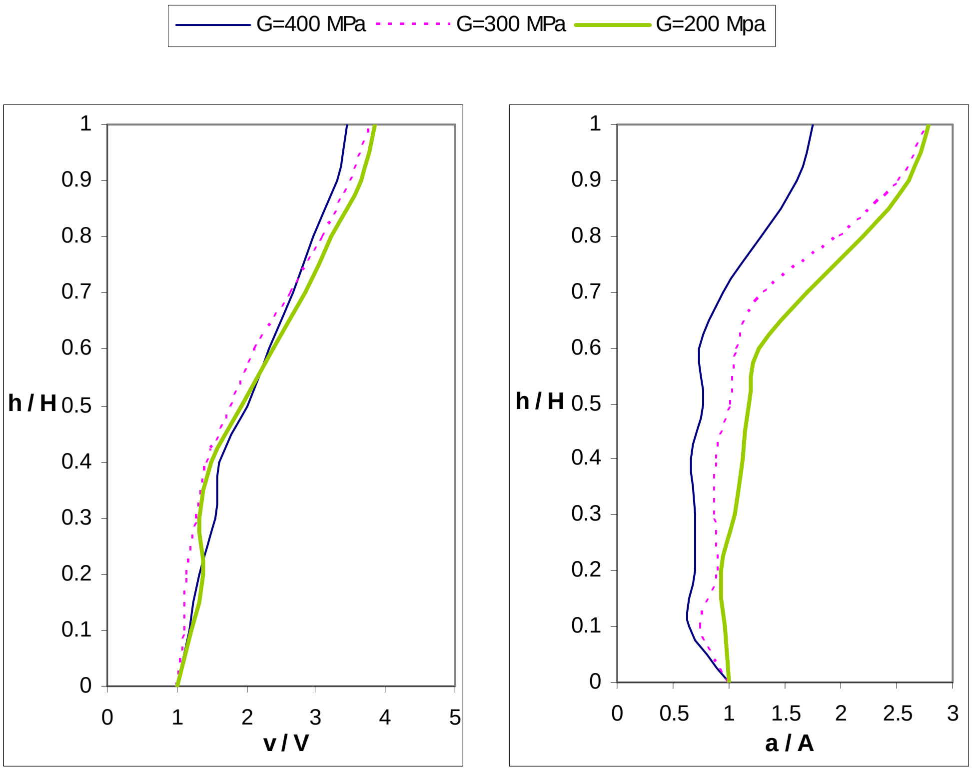


**(Velocity)** **(Acceleration)**

**Figure 2.14:** influence of the foundation stiffness on the seismic response of the dam (Kocaeli earthquake record)

## 2.4 Elastoplastic analysis

### 2.4.1 Presentation of the Mohr-Coulomb model

The Mohr-Coulomb plasticity model is used for materials that yield when subjected to shear loading. The yield criterion depends on the major and minor principal stresses. It is largely used in engineering studies. In addition the Mohr-Coulomb parameters are usually available for geomaterials.

The failure criterion used in the FLAC3D model is a composite Mohr-Coulomb criterion with tension cutoff (Figure 2.15). In labeling the three principal stresses so that:

$\sigma_1 \leq \sigma_2 \leq \sigma_3$ ………………………………………………………… (Eq.2.3)

The failure criterion is defined as:

$f = \sigma_1 - \sigma_3 N_\varphi + 2C(N_\varphi)^{0.5}$ …………………………………………… (Eq.2.4)

$N_\varphi = 1 + \sin(\varphi) / 1 - \sin(\varphi)$ …………………………………………… (Eq.2.5)

Where φ is the friction angle, C denotes the cohesion.

The plastic potential is given by :

$g = \sigma_1 - \sigma_3 N_\psi$ …………………………………………… (Eq.2.6)

$N_\psi = 1 + \sin(\psi) / 1 - \sin(\psi)$ …………………………………………… (Eq.2.7)

ψ denotes the dilatancy angle.

The tension failure criterion is given by:

$f_t = \sigma_3 - \sigma^t$ ………………………………………………………… (Eq.2.8)

$\sigma^t$ stands for the tensile strength.

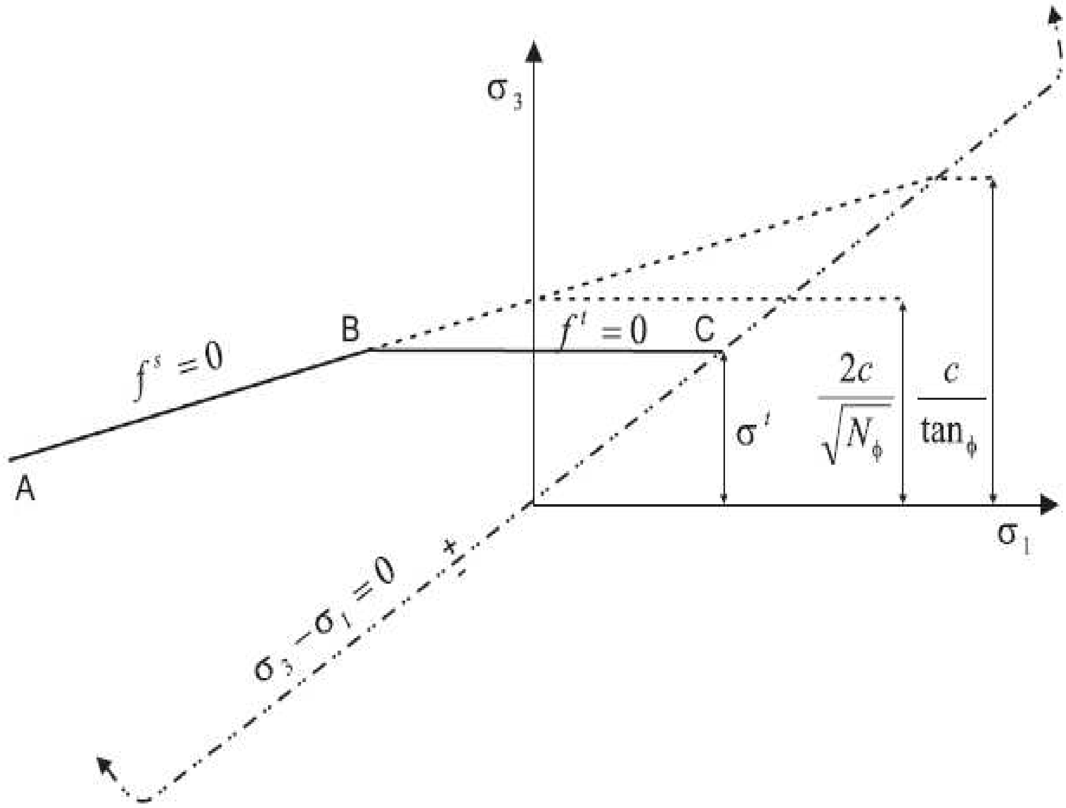


**Figure 2.15:** FLAC3D Mohr-Coulomb failure criterion

### 2.4.2 Reference example

**Presentation**

The reference example concerns the earth dam presented in figure 2.1. The parameters of the Mohr-Coulomb model are summarized in table 2.2. The foundation is assumed to be stiff with a Young's Modulus E = 1000 MPa. The Young's modulus of the core is equal to 40 MPa, while that of the shell is equal to 60 MPa. The Friction angle of the shell is equal to $\varphi = 35°$. The friction angle and cohesion of the core are equal to 15° and 100 kPa, respectively. The fundamental frequency of the dam is equal to $f_1 = 0.7$ Hz.

Analysis is conducted for the Kocaeli earthquake record with a peak velocity $V_m = 0.4$ m/s.

| Parameter | Units | Core | Shell |
|---|---|---|---|
| Friction Angle ($\varphi$) | (°) | 15 | 35 |
| Dilation angle ($\psi$) | (°) | 3 | 10 |
| Cohesion (c′) | (Pa) | 0.1 e6 | 100 |
| Young's modulus (E) | (MPa) | 40 | 60 |
| Poisson's ratio ($\nu$) | - | 0.3 | 0.3 |

**Table 2.2**: Reference example - properties for the earth dam

**Results**

Figure 2.16 shows the distribution of plasticity in the dam at the peak of excitation. It can be observed that plasticity is induced in a large part of the shell and in the lower part of the core. The upper part of the core remains in the elastic domain. Figure 2.17 shows the displacement pattern in the axis and the middle height of the dam at the maximum of seismic excitation. It can be observed that the displacement in the axis of the dam is close to the first mode of the dam; the variation of the displacement at the middle height shows a sharp increase at the extremities; which could indicate the imminence of soil instability in this area. The residual (permanent) displacement is presented in the figure 2.18. It shows the seismic loading induces residual displacement in the upper part of the dam and the extremities. The maximum of this displacement attains 0.80 m.

Figure 2.19 shows a comparison between the elastic and elastoplastic analyses at the maximum of velocity. It can be observed that the plastic deformation leads to a decrease in the velocity amplification, in particular in the upper part. This reduction attains about 50%. This result could be attributed to the energy dissipation by plastic deformation and to the influence of plasticity on the reduction of the fundamental frequencies of the dam as illustrated figure 2.20, which shows the influence of plasticity on the spectral response at the crest of the dam.

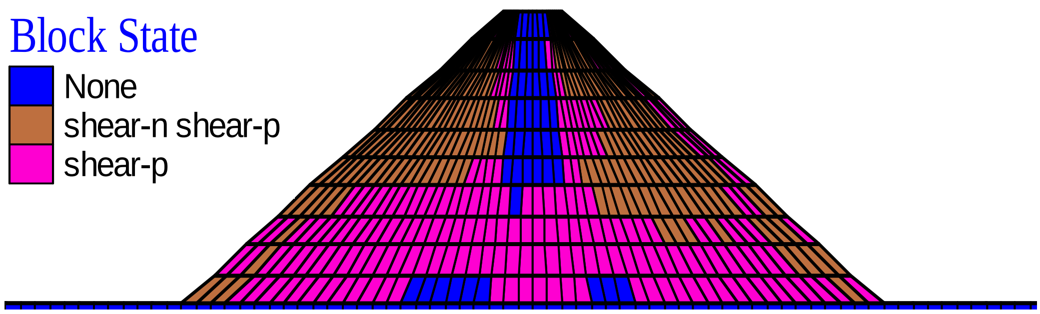


**Figure 2.16:** Reference example: Distribution of plasticity in the dam (Maximum excitation)

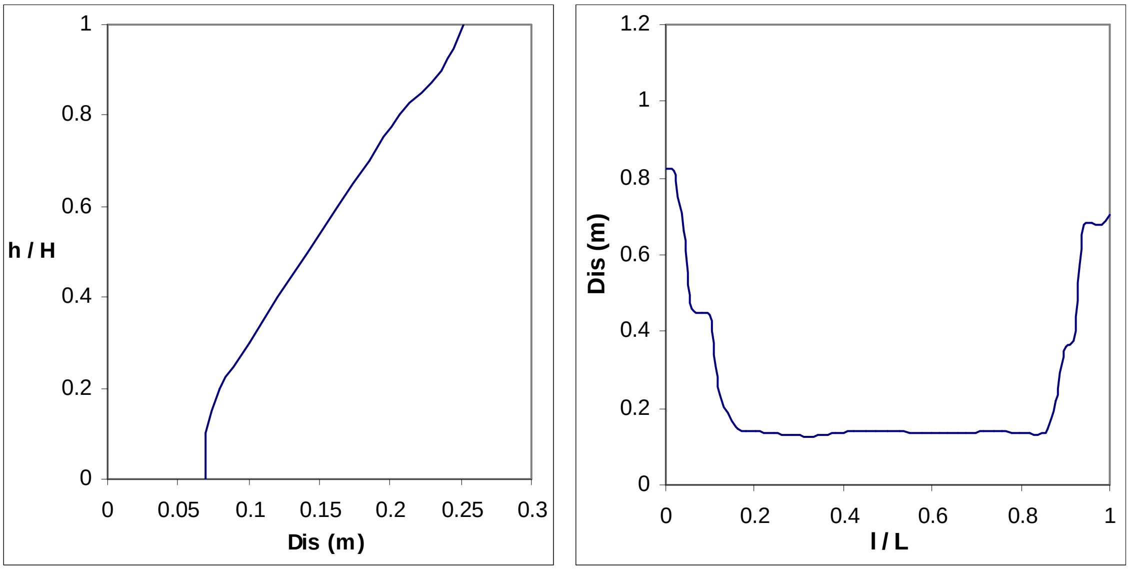


**(Vertical axis of the dam)** **(Middle height of the dam)**

**Figure 2.17:** Reference example: displacement pattern at maximum of seismic excitation

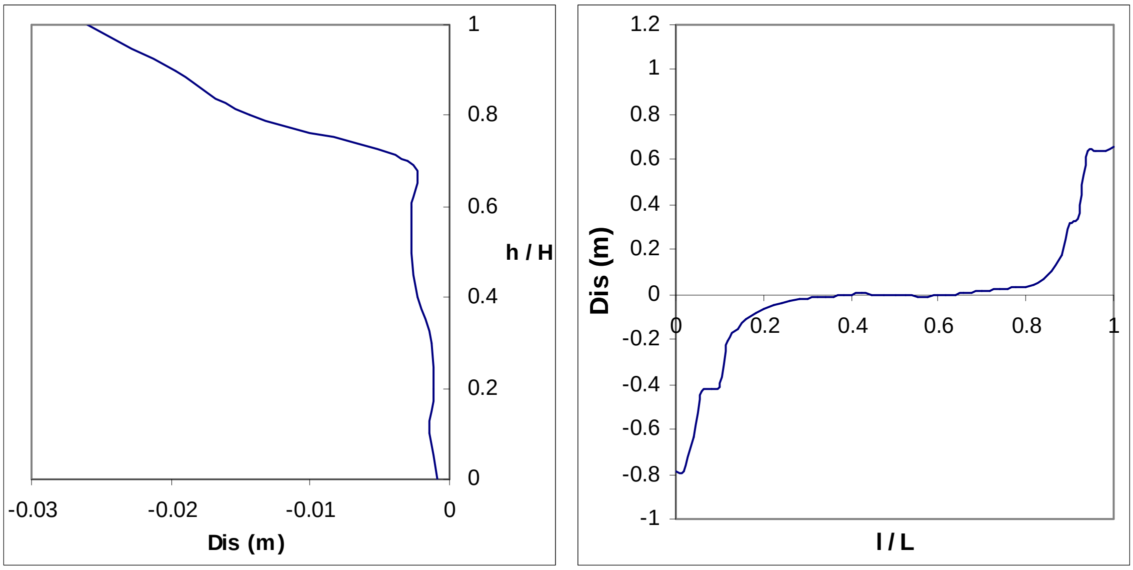


**(Vertical axis of the dam)** **(Middle height of the dam)**

**Figure 2.18:** Reference example: Residual displacement

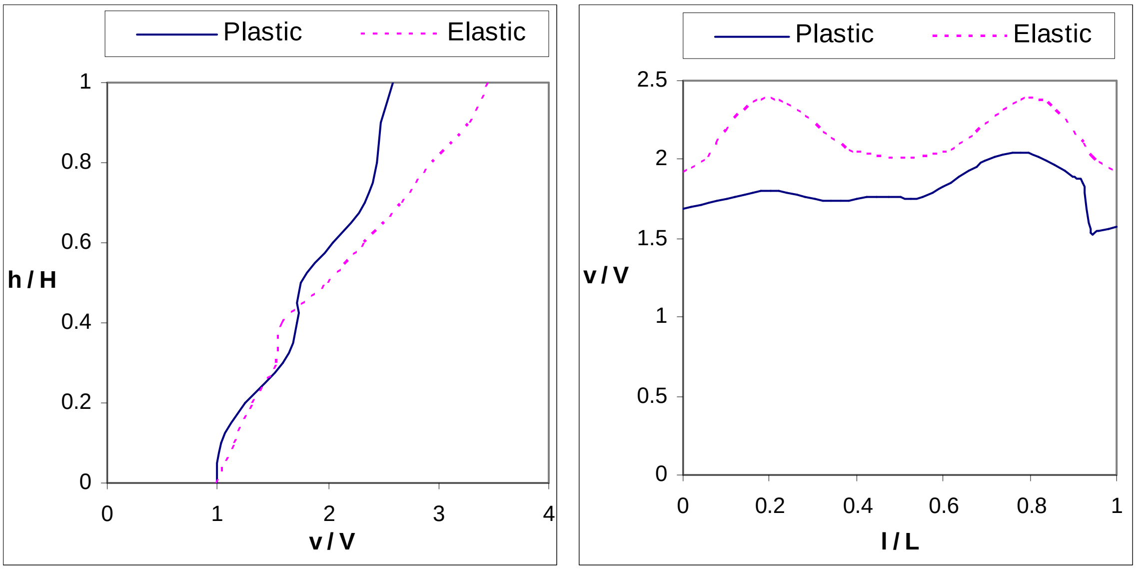


**(Vertical axis of the dam)** **(Middle height of the dam)**

**Figure 2.19:** Reference example: Influence of plasticity on the maximum of velocity

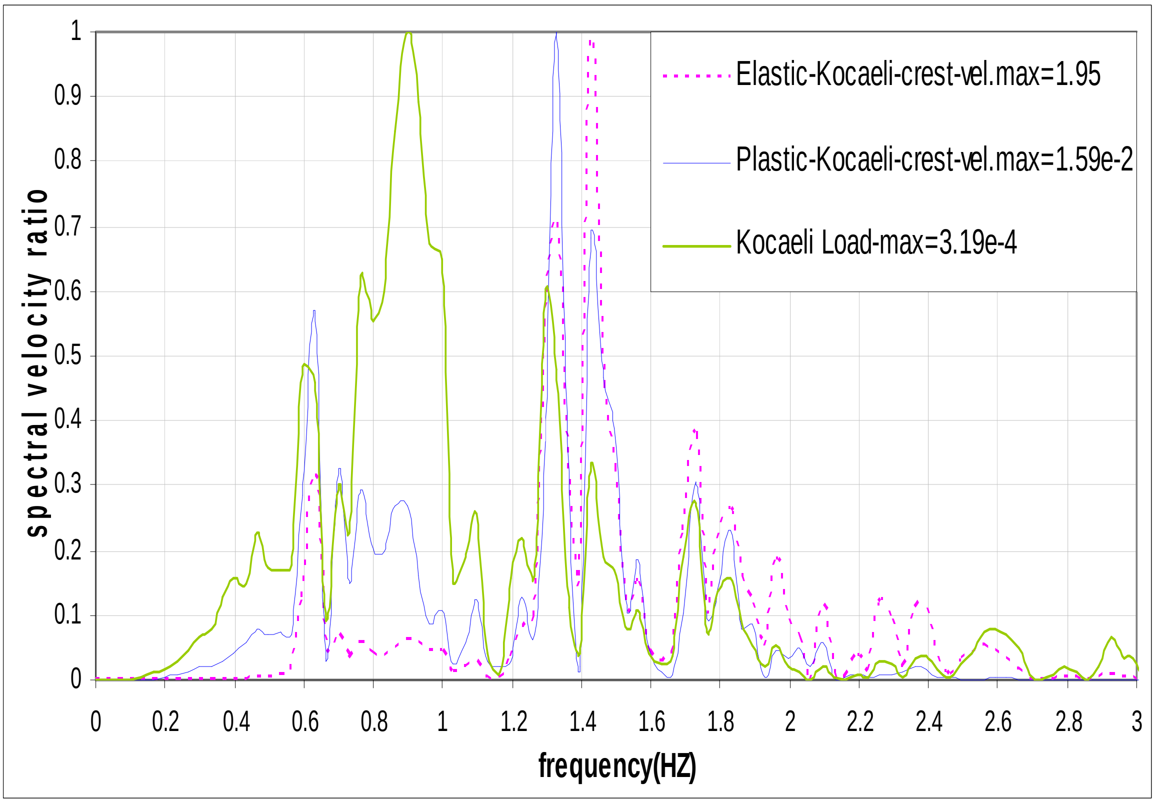


**Figure 2.20:** Reference example: Influence of plasticity on velocity spectra at the dam

### 2.4.3 Influence of the frequency content of the input motion

The response of the dam presented in the reference example was compared to that of the same dam subjected to the input motion recorded during the Tabas earthquake. The time history of this record is illustrated in figure 2.21. The magnitude of the input motion is equal to that used in the reference example ($V_a$ = 0.4 m/sec).

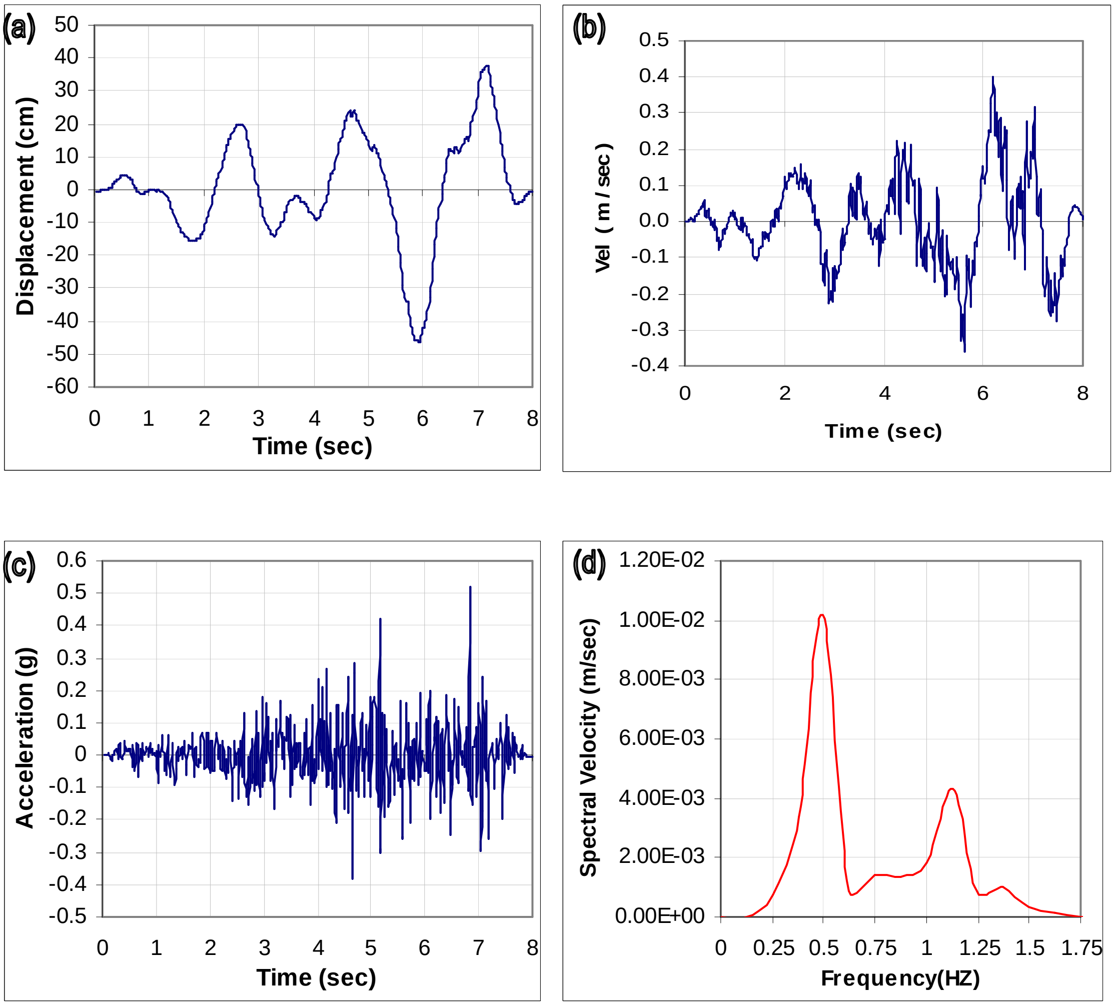


**Figure 2.21:** Tabas earthquake record:

a) Displacement, b) Velocity, c) Acceleration, d) Spectra

Figure 2.22 shows the distribution of plasticity in the dam at the maximum of velocity. It can be observed that plasticity is induced in a large part of the shell and in the lower part of he core. The upper part of the core remains in the elastic domain. This distribution is close to that obtained with the Kocaeli earthquake record (Figure 2.16). Figure 2.23 shows the displacement pattern in the axis and the middle height of the dam at the maximum of velocity. It can be observed that the displacement in the axis of the dam is close to the first mode of the dam; the variation of the displacement in the middle height shows a sharp increase at the extremities; which could indicate the imminence of instability in this area. The residual displacement is presented in figure 2.24. It shows that the seismic loading induces a residual displacement in the upper part of the dam and the extremities. The maximum of this displacement occurs at the extremities of the dam, it attains 0.80 m, which is close to that obtained with Koeali earthquake record. The permanent displacement at the crest is equal to 0.1 m, which is about 3 times higher than that obtained with the Kocaeli earthquake record.

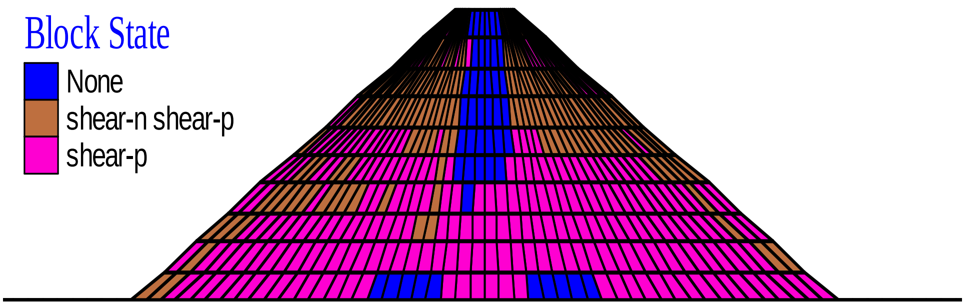


**Figure 2.22:** Distribution of plasticity in the dam (at maximum velocity), **(**Tabas earthquake record)

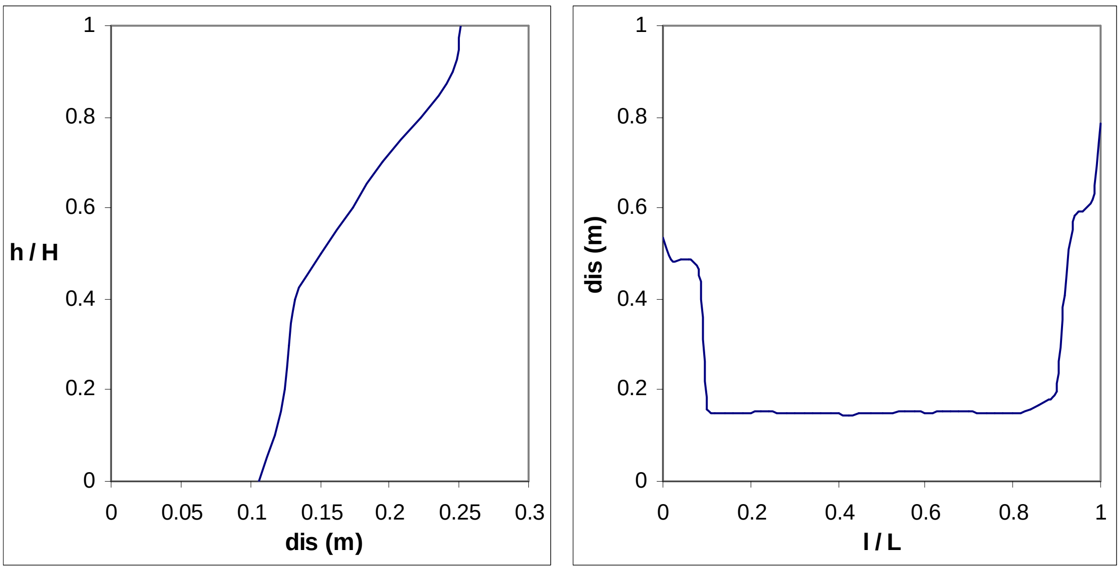


**(Vertical axis of the dam)** **(Middle height of the dam)**

**Figure 2.23**: Maximum of displacement induced by the Tabas Earthquake record

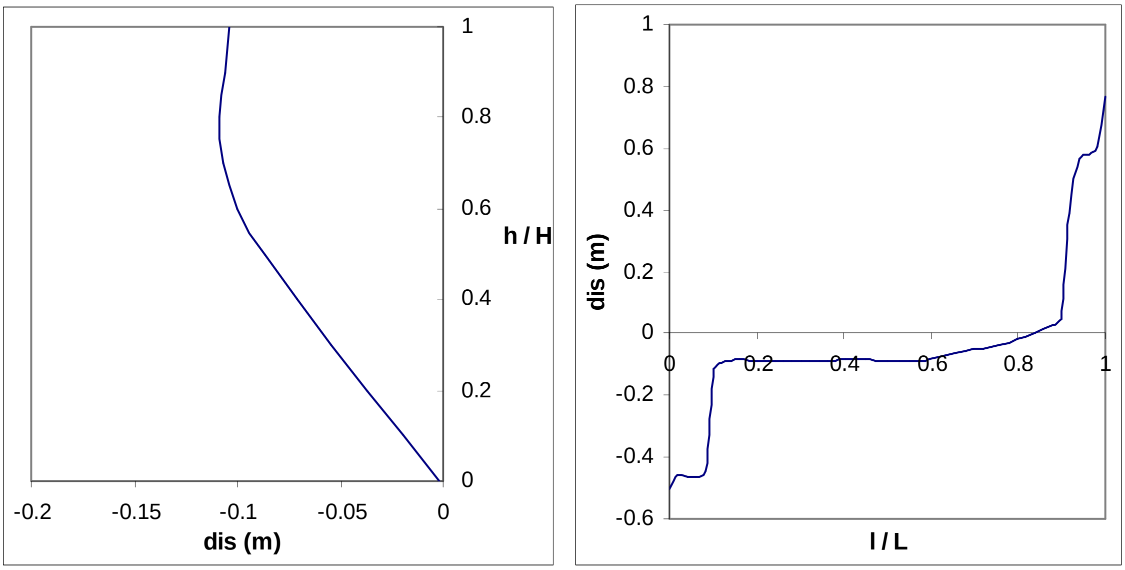


**(Vertical axis of the dam)** **(Middle height of the dam)**

**Figure 2.24:** Residual displacement induced by the Tabas Earthquake record

Figure 2.25 shows a comparison between the dynamic amplification profiles obtained with elastic analyses using the Kocaeli and Tabas earthquake records. We observe a good agreement between these profiles. The maximum velocity due to the Tabas earthquake record is equal to 3.26; this value is largely inferior to that obtained with the Kocaeli earthquake record (v/V=3.54). In order to analyse this result, we give in figure 2.26 the response spectra obtained with the Kocaeli and Tabs earthquake records together with the input motions. It can be observed that the peak of the response to Tabas earthquake record occurs at the frequency f = 0.75 Hz, which is largely inferior to the $1^{st}$ frequency of the dam ($f_1$ = 0.7 Hz).The peak of the response to Kocaeli record occurs at f = 1.45 Hz, which is close to the $2^{nd}$ frequency of the dam.

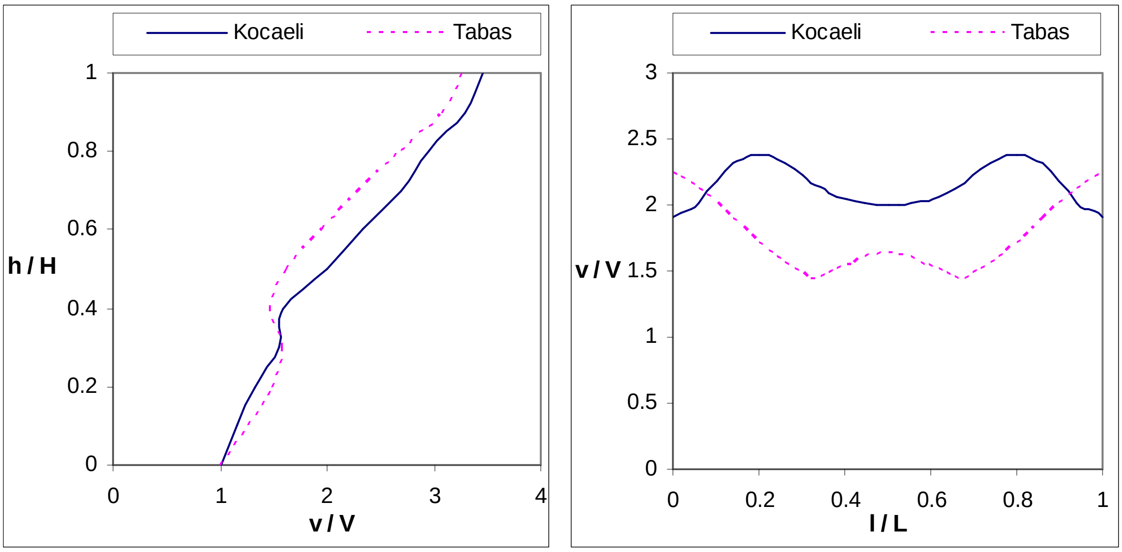


(Vertical axis of the dam) (Middle height of the dam)

**Figure 2.25:** Comparison of the elastic responses to the Kocaeli and Tabas earthquake records

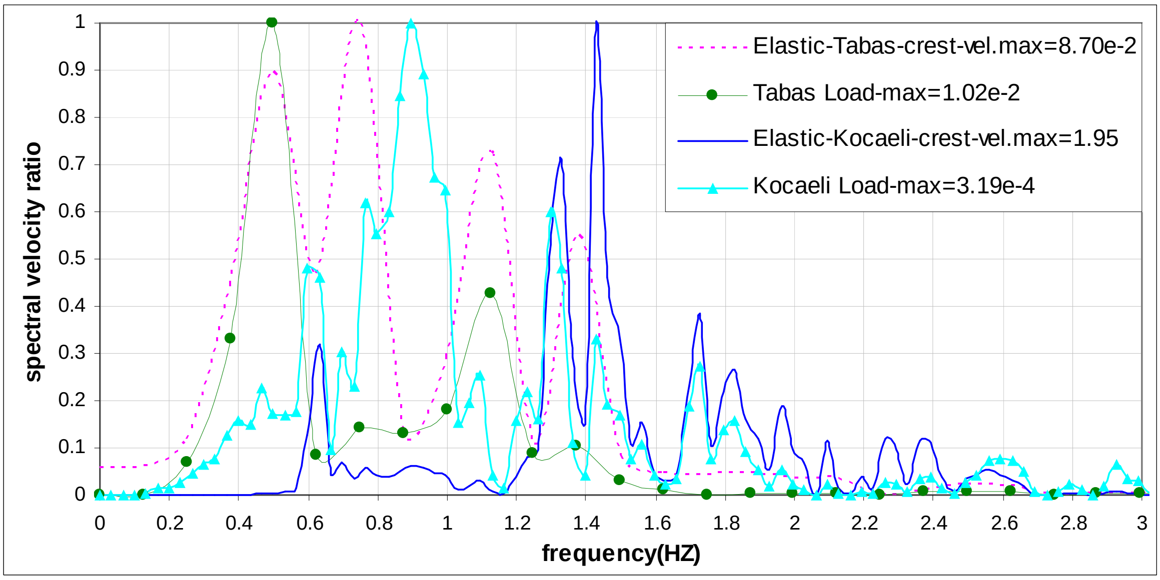


**Figure 2.26:** Comparison of the spectra of the elastic responses to the Kocaeli and Tabas earthquake records

Figure 2.27 shows a comparison between the dynamic amplification profiles obtained with the elastoplastic analyses of the dam subjected the Kocaeli and Tabs earthquake records. We observe a good agreement between these profiles. The maximum velocity due to the Tabas earthquake record is equal to 2.97; this value is higher than that obtained with the Kocaeli earthquake record (v/V=2.59). In order to analyse this result, we give in figure 2.28 the spectra obtained with the Kocaeli and Tabs earthquake records together with the input motions. It can be observed that the peak of the response to Tabas earthquake record occurs at the frequency f = 0.50 Hz, which is close to that obtained with the elastic response of the dam subjected to the Tabas earthquake record. This result indicates that the spectral response of the dam submitted to the Tabas earthquake record is not affected by the behaviour of the soil. This result can be attributed to the low dynamic amplification under this loading. The spectrum of the response to Kocaeli earthquake record indicates a shift of this response towards the low frequencies. This result is due to the plastic behaviour, which leads to a material softening and consequently to a reduction of the "dominant frequencies" of the dam.

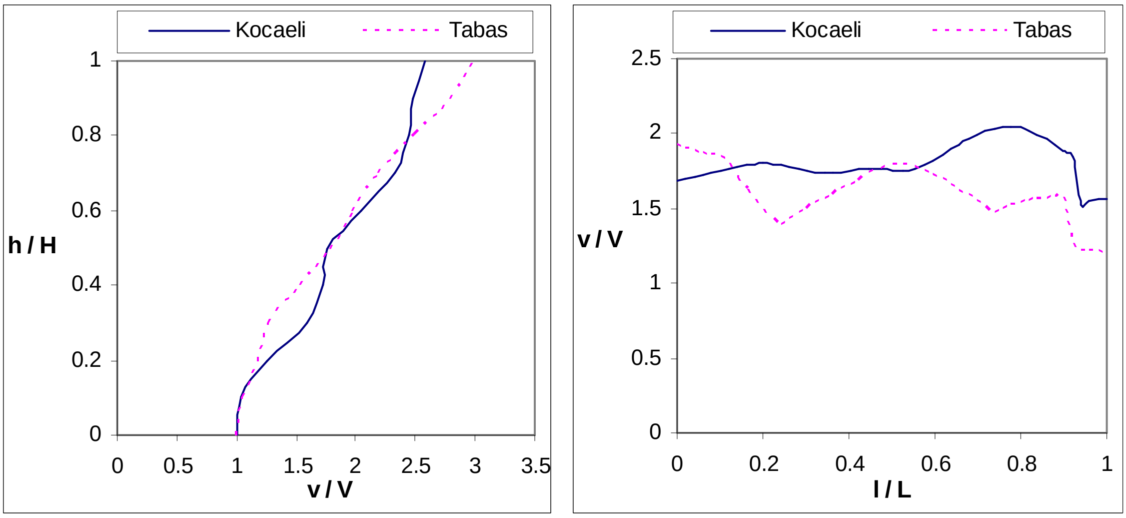


**(Vertical axis of the dam)** **(Middle height of the dam)**

**Figure 2.27:** Comparison of the elastoplastic responses to the Kocaeli and Tabas earthquake records

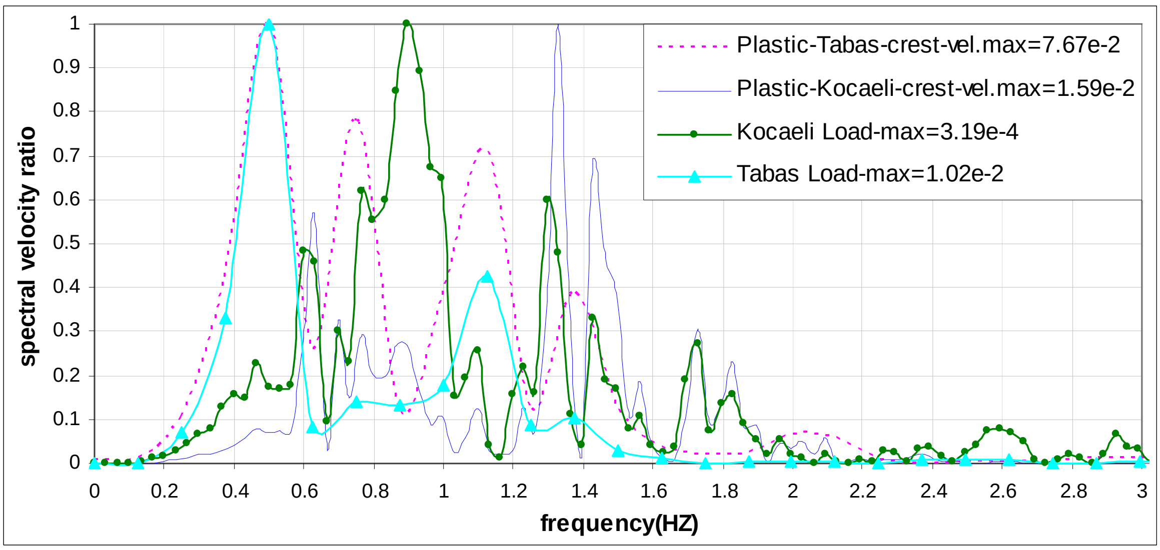


**Figure 2.28:** Comparison of the spectra of the elastoplastic responses to the Kocaeli and Tabas earthquake records

### 2.4.4 Influence of the loading amplitude

The influence of the loading amplitude on the dam response to the Kocaeli earthquake record was investigated through analyses conducted for three values of amplitude of the input motion ($V_a$ = 0.40, 1.60 and 3.60 m/s).

Figure 2.29 shows the influence of the input motion amplitude on the distribution of plasticity in the dam. It can be observed that the plasticity distribution increases with the loading amplitude. For both $V_a$ = 1.60 and 3.60 m/s, plasticity extends to the totality of the dam.

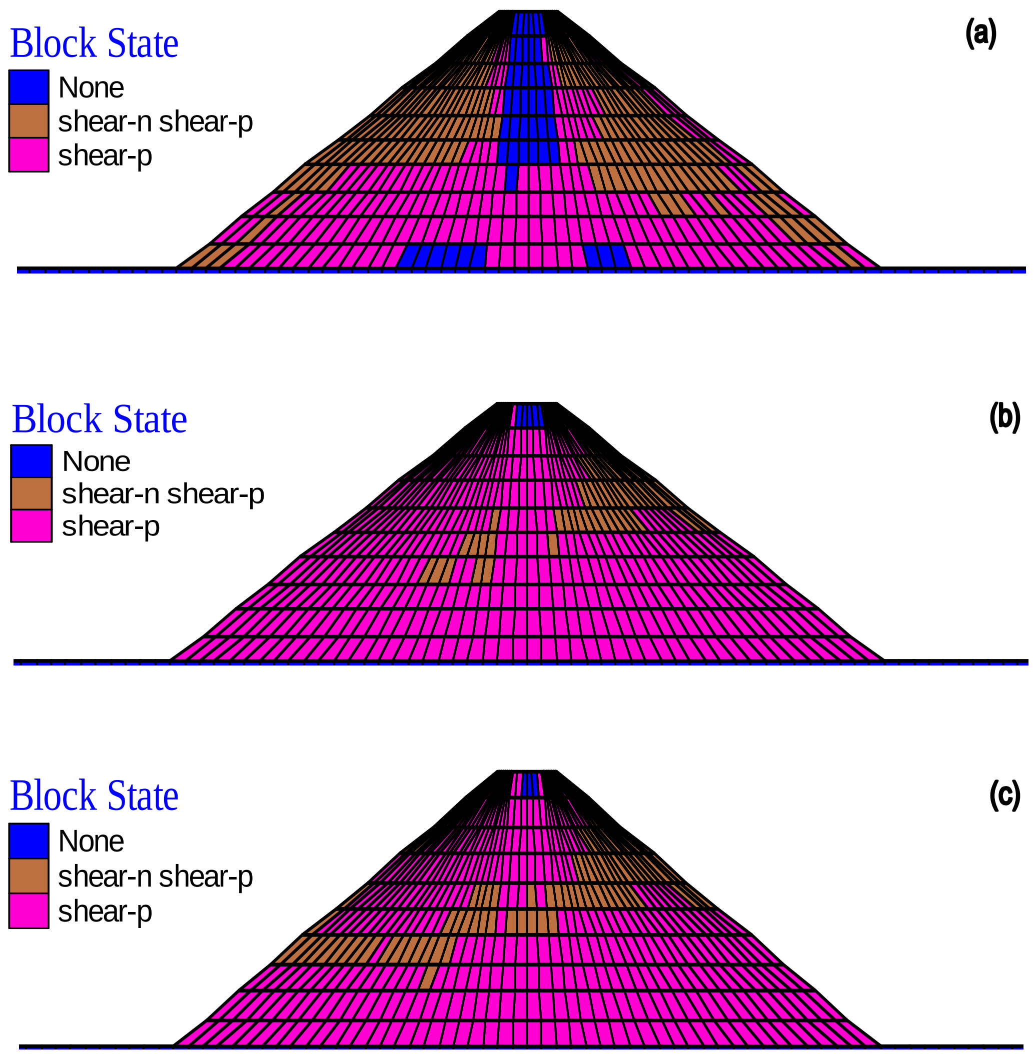


**Figure 2.29:** Influence of the loading amplitude on the distribution of plasticity (Kocaeli earthquake record)

a) $V_a$ = 0.40 m/s, b) $V_a$ = 1.60 m/s, c) $V_a$ = 3.6 m/s

Figure 2.30 shows the influence of the loading amplitude on the maximum of displacement in the vertical axis and at the middle height of the dam. It can be observed that the increase in the input motion amplitude leads to an important increase in this displacement, in particular near the lateral extremities of the dam, where the displacement attains 3.5 m for $V_a$ = 3.6 m/s. The variation of the displacement in the horizontal direction clearly indicates the presence of instability at high amplitude of the input motion.

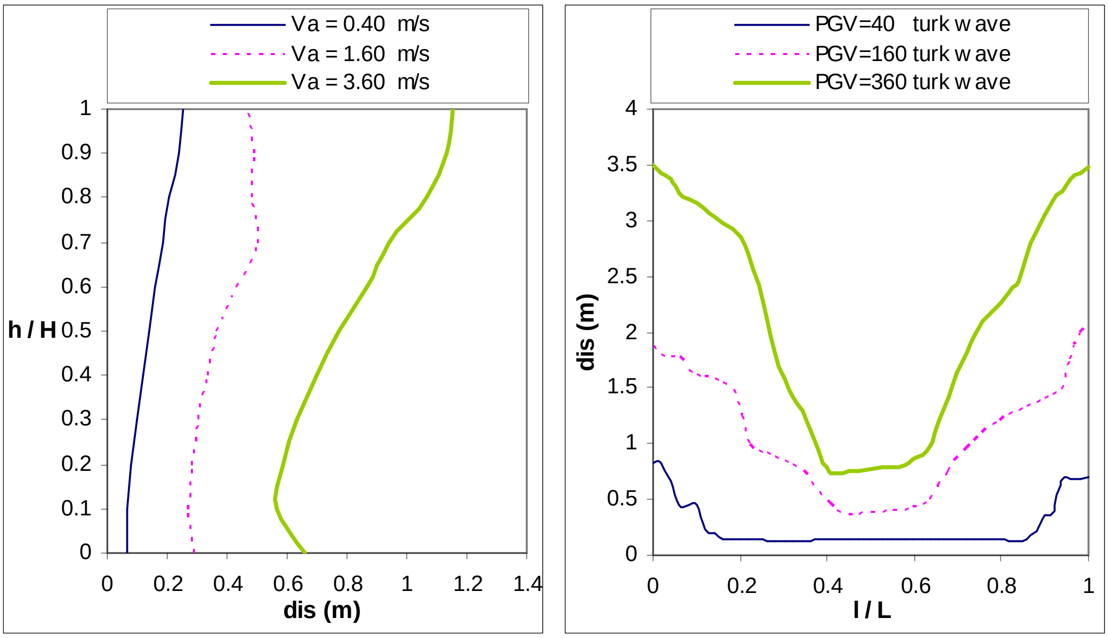


**(Vertical axis of the dam)** **(Middle height of the dam)**

**Figure 2.30:** Influence of the loading amplitude on the maximum of displacement in the dam (Kocaeli earthquake record)

### 2.4.5 Influence of the dam slope

Analyses were conducted for three values of the dam slope (S= 2.2, 2.4 and 2.6) with the Kocaeli earthquake record (Va = 40cm/sec). Figure 2.31 shows the influence of dam slope on the distribution of plasticity in the dam. It can be observed that this distribution is not affected by the variation of the dams slope between 2.2 and 2.6.

Figure 2.32 shows the influence of the slope of the dam on the maximum of displacement in the vertical axis and middle height of the dam. It can be observed that the variation of the slope between 2.2 and 2.6 has a low influence on the displacement induced in the dam. This low influence on the response of the dam is also confirmed by the dynamic amplification of the velocity as illustrated in figure 3.33.

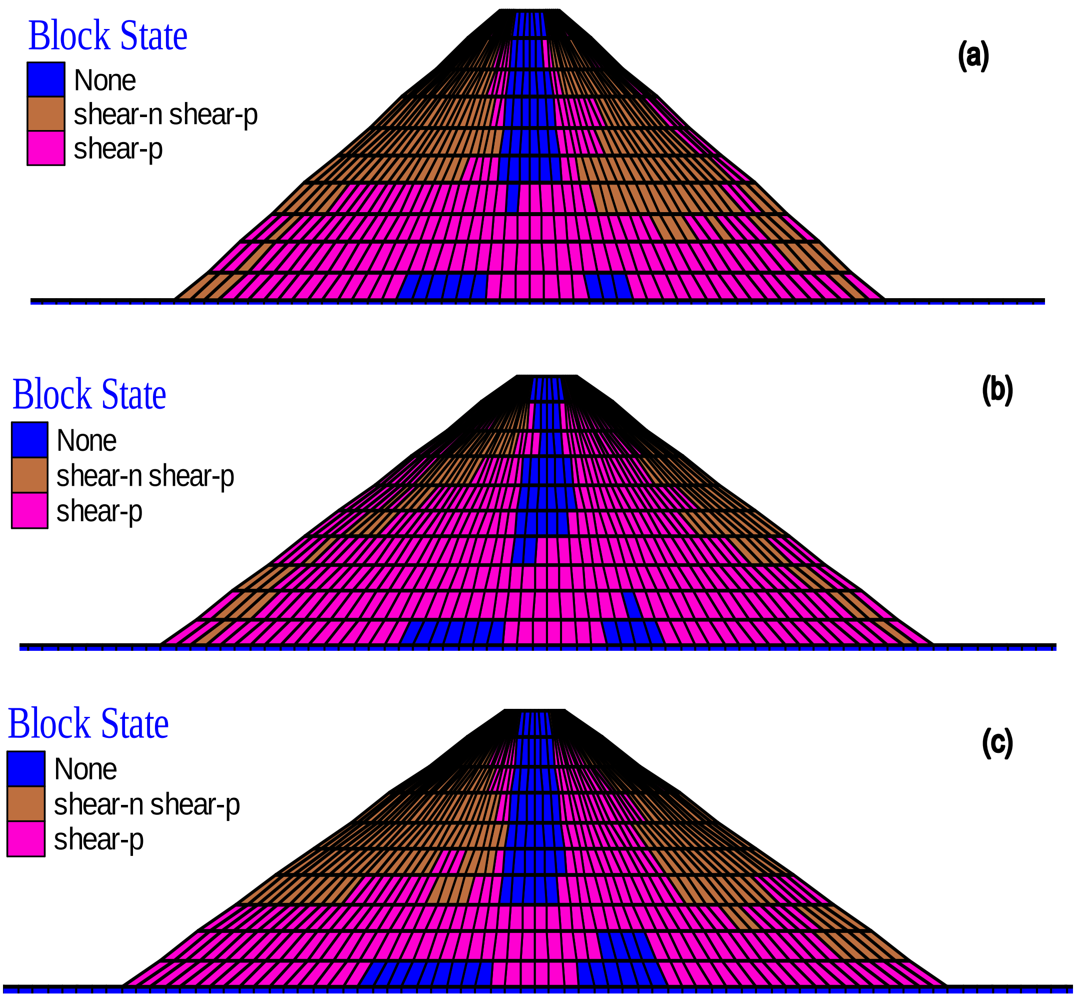


**Figure 2.31:** Influence of the slope of the dam on the distribution of plasticity

(Kocaeli earthquake record)

a) S = 2.2, b) S = 2.4, c) S = 2.6

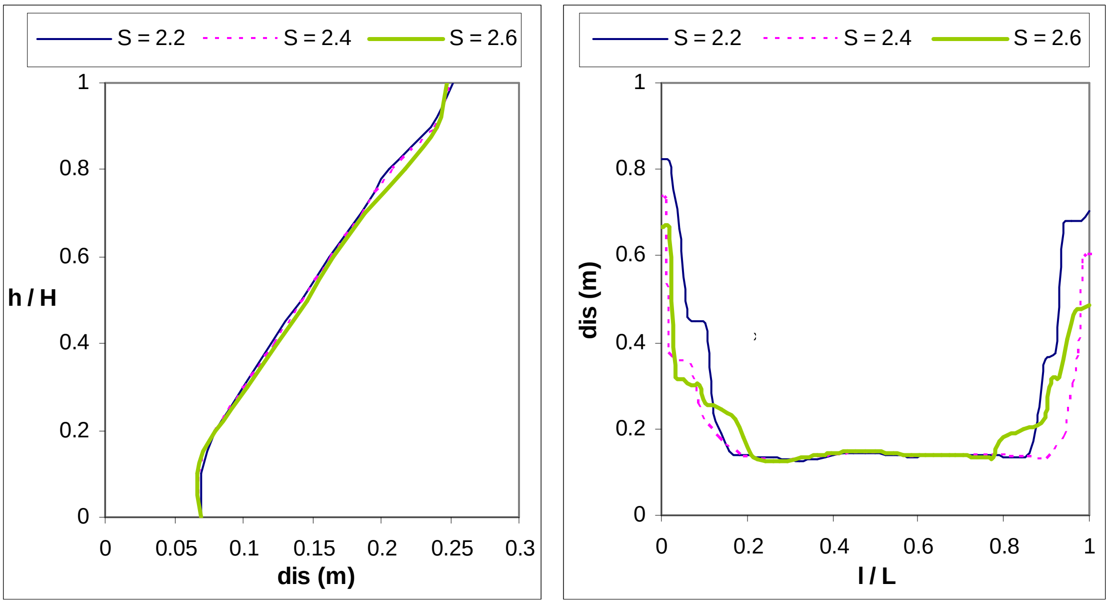


**(Vertical axis of the dam)** **(Middle height of the dam)**

**Figure 2.32:** Influence of the slope of the dam on the maximum of displacement induced by the (Kocaeli earthquake record)

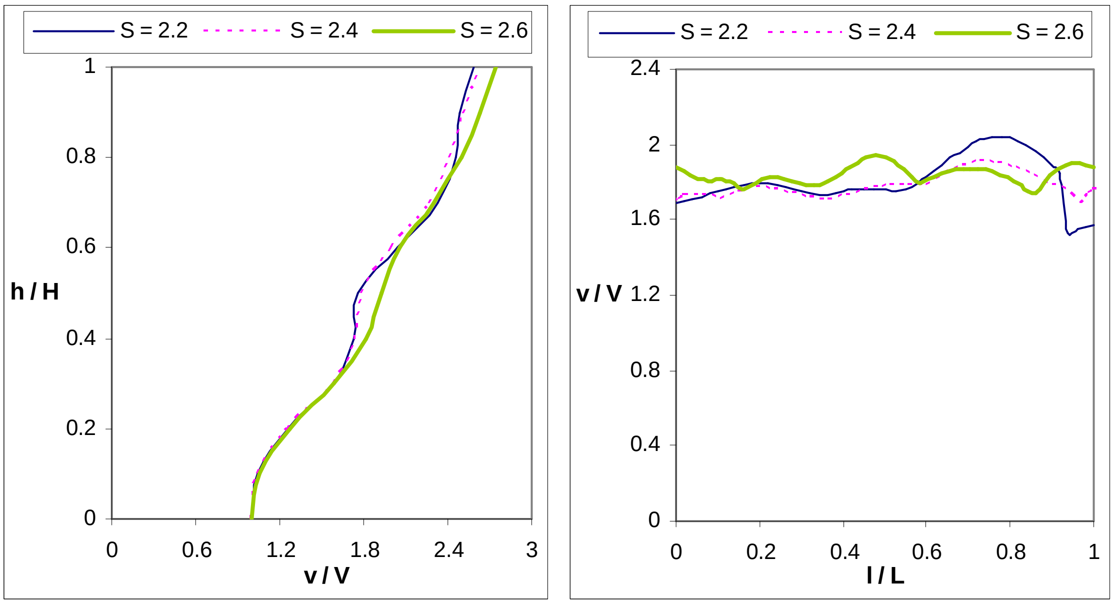


**(Vertical axis of the dam)** **(Middle height of the dam)**

**Figure 2.33:** Influence of the slope of the dam on the amplification of the velocity in the dam (Kocaeli earthquake record)

## 2.5 Conclusion

This chapter included analysis of the seismic behaviour of earth dams. The presence of the water phase was neglected. It corresponds to the response of the dam before water filling. Analyses were conducted for real earthquake records assuming a simple geometry for the dam. The behaviour of the earth material was assumed first elastic and then elastoplastic. In the latter, analyses were conducted using the simple and popular non associated Mohr-Coulomb criterion. The use of this model is justified by the difficulty to obtain constitutive parameters for more advanced constitutive relations including both isotropic and kinematic hardening.

Elastic analyses showed that the seismic loading induces mainly lateral displacement, which increases with the distance from the dam foundation. The maximum is observed near the dam crest. The mechanical properties of the core (shear stiffness and density) moderately affect the elastic response, while those of the shell affect significantly the response of the dam.

Elastoplastic analyses show that the seismic loading induces plasticity in a large part of the shell and in the lower part of the core. The variation of the displacement in the middle height shows a sharp increase at the extremities, which could indicate the imminence of instability in this area. The comparison between the elastic and elastoplastic responses shows that the plastic deformation leads to a decrease in the velocity in the dam, in particular in the upper part. This result could be attributed to the energy dissipation by plastic deformation and on the influence of plasticity on the reduction of the fundamental frequencies of the dam.

Analysis of the influence of the dam slope on its response shows that the variation of the slope between 2.2 and 2.6 has a moderate influence on the dam response to Kocaeli earthquake record input motion.

# CHAPTER III

## Seismic Response of the Earth Dams:

## Influence of the water-skeleton interaction

# CHAPTER III:

## Seismic Response of the Earth Dams:

## Influence of the water-skeleton interaction

### 3.1 Introduction

This chapter presents a numerical analysis of the influence of the water-skeleton interaction on the response of earth dams to seismic loading. Analysis is conducted first under undrained condition, which corresponds to a simplified analysis of the response of the dam. This analysis does not provide the variation of the pore water pressure; it constitutes a first stage of the analysis of the seismic response of the dam in total stresses.

Then, full coupled analysis is conducted in effective stresses using the non associated Mohr-Coulomb criterion. This analysis provides the variation of the pore water pressure. It allows investigating the influence of the water phase on the dam response to real earthquake input motion. This analysis will be first conducted for a reference case, which will be followed by a comparison of the undrained response of the dam to its full-coupled response.

### 3.2 Undrained analysis

Undrained analysis is conducted in total stresses. The shell material is assumed to be frictional, while that of the core is assumed to be purely cohesive; the undrained cohesion is assumed to increase with the initial effective vertical stress.

### 3.2.1 Reference example

The reference example concerns an earth dam with a clay core constructed on a homogeneous soil layer (Figure 3.1). Geotechnical properties of the dam are summarized in table 3.1. The foundation is assumed to be stiff with a Young's Modulus E = 1000 MPa. The Young's modulus of the core is equal to 40 MPa, while that of the shell is equal to 60 MPa. The friction angle of the shell is equal to 35°. The core is assumed to be purely cohesive; the cohesion is assumed to increase with the initial effective vertical stress ($\sigma'_v$) as follows:

$$C_u = \lambda_{cu} * \sigma'_v \qquad \text{(Eq.3.1)}$$

Analyses were conducted with $\lambda_{cu}$ =0.3.

Rayleigh damping is considered with a damping ratio $\beta$ = 0.05

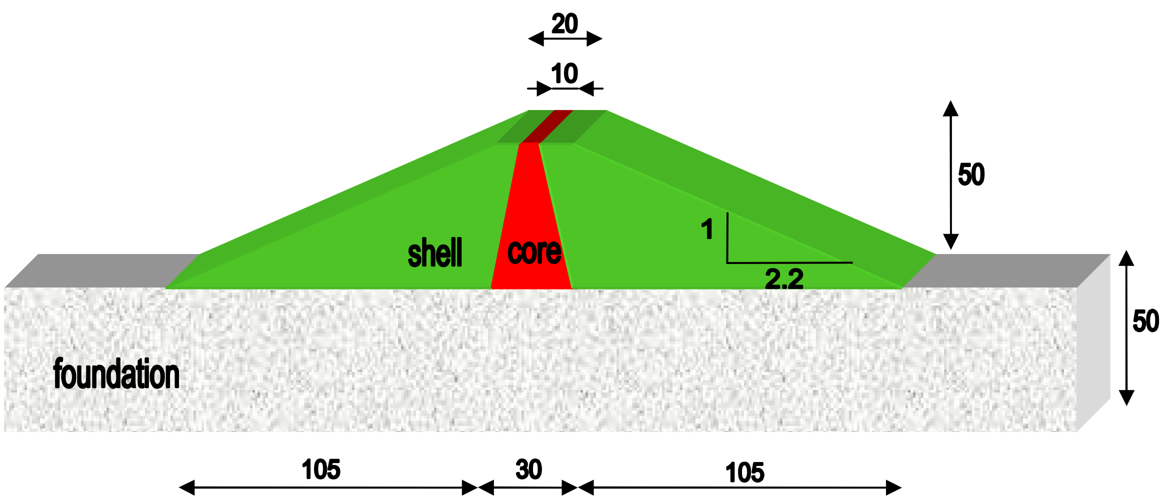


**Figure 3.1:** Reference example (Undrained analysis): Geometry of the dam

| Parameter | Units | Core | Shell | Foundation |
|---|---|---|---|---|
| Dry density (ρ) | ($kg/m^3$) | 1800 | 2000 | 2200 |
| Saturated density (ρ′) | ($kg/m^3$) | 2100 | 2500 | 2500 |
| Friction angle (φ) | (°) | 0 | 35 | 35 |
| Cohesion (c′) | (Pa) | $0.30*\sigma_v'$ | 100 | 0.2e6 |
| Young's modulus (E) | (MPa) | 40 | 60 | 1000 |
| Poisson's ratio (ν) | | 0.3 | 0.3 | 0.25 |
| Elastic shear modulus (G) | (MPa) | 15 | 23 | 400 |

**Table 3.1:** Undrained analysis: properties of the reference example

Figure 3.2 shows the spectral response of the dam under free condition. It provides the following frequencies for the dam: $f_1 = 0.7$ Hz; $f_2 = 1.4$ Hz.

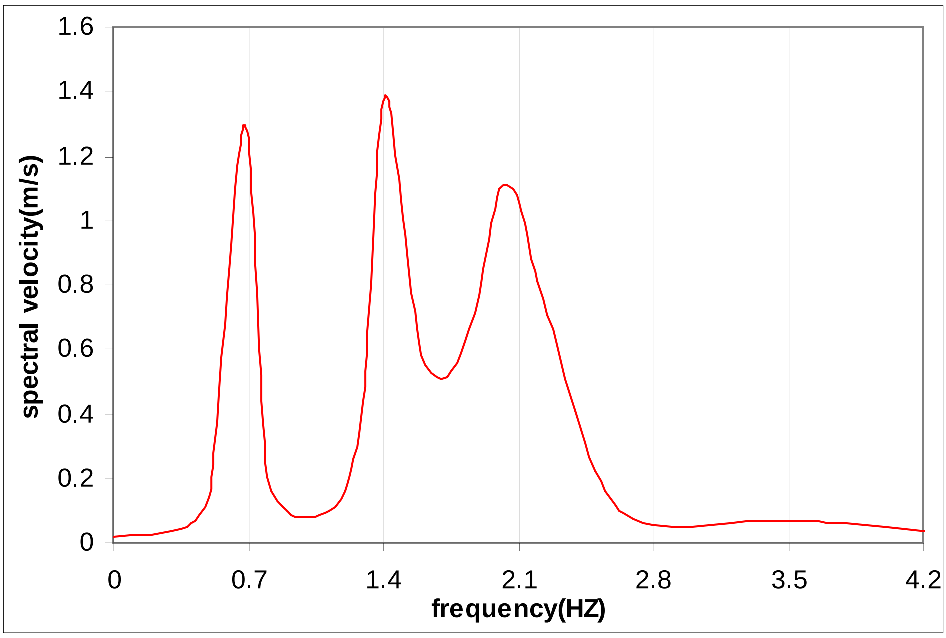


**Figure 3.2:** Reference example (Undrained analysis): Spectral response of the free motion.

Analysis is conducted for the Kocaeli earthquake record. The estimated peak velocity of this record is equal to 0.40 m/sec (peak acceleration 0.247g), and its duration is approximately equal 30 sec. The record for the base acceleration, velocity, and displacement of the input motion are shown in Figure 3.3. The frequency of the major peak is equal to 0.9 Hz.

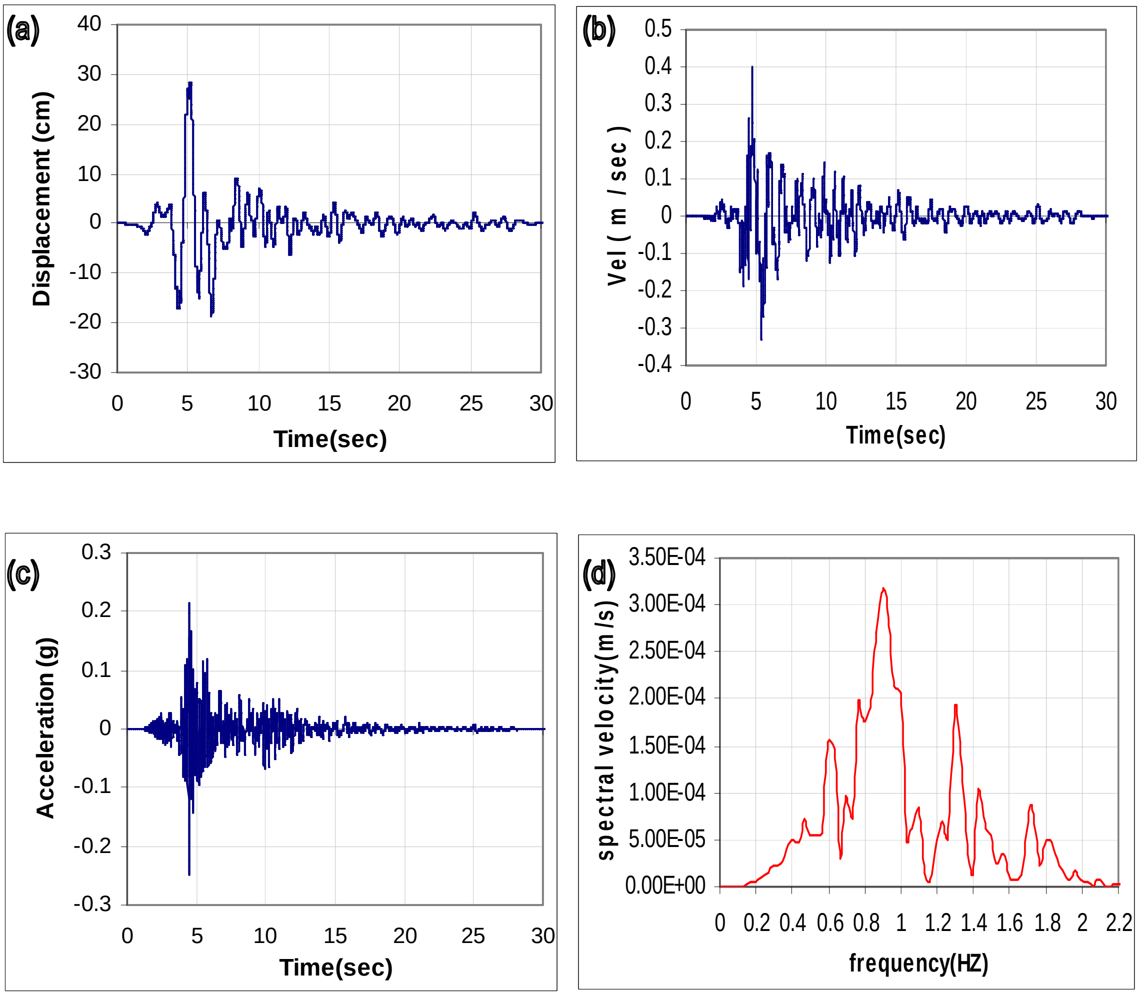


**Figure 3.3:** Kocaeli earthquake record (1999):

a) Displacement, b) Velocity, c) Acceleration, d) Spectra

## Results

Figure 3.4 shows the distribution of plasticity in the dam at the peak of excitation. It can be observed that plasticity is induced in the quasi totality of dam. The residual (permanent) displacement is presented in figure 3.5. It shows that the seismic loading induces a residual displacement in the upper part of the dam and the extremities. The maximum of this displacement attains 0.95 m.

Figure 3.6 shows the displacement pattern in the axis and the middle height of the dam at the maximum of seismic excitation. It can be observed that the displacement in the axis of the dam increases first with the distance from the base of the dam up to a peak and then decreases. This variation corresponds to a combination of the first and second modes of the dam. The variation of the displacement at the middle height shows a sharp increase at the extremities; which could indicate the imminence of soil instability in this area.

Figure 3.7 shows the seismic amplification of the velocity in the dam. It can be observed that the amplification increases first with the distance from the base of the dam up to a peak and then decreases. This variation corresponds to a combination of the first two modes of the dam. Figure 3.8 shows a comparison between the response spectra of the dam and the spectra of the input motion. It can be observed that the peak of the dam response occurs at the frequency f = 1.35 Hz which is close to the second frequency of the dam. A less pronounced peak appears at the frequency f =0.64 Hz.

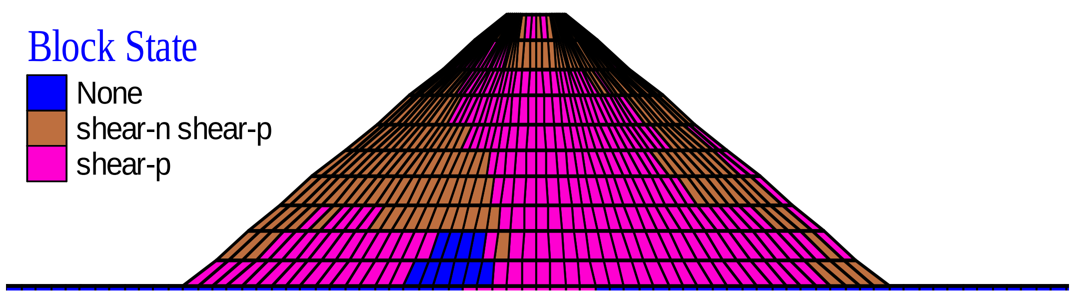


**Figure 3.4**: Undrained analysis, reference example: plasticity induced by the seismic loading

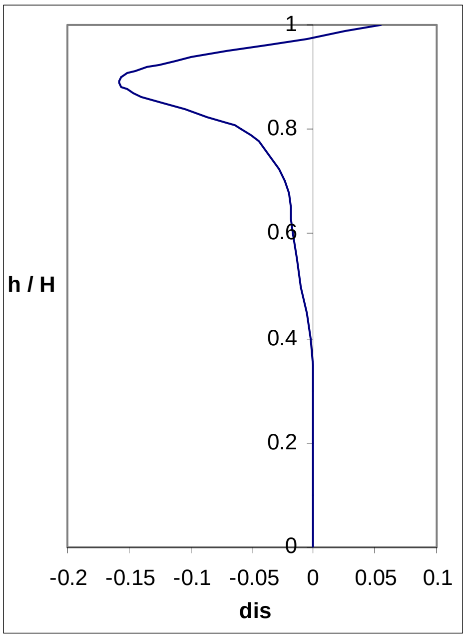


(Vertical axis of the dam)

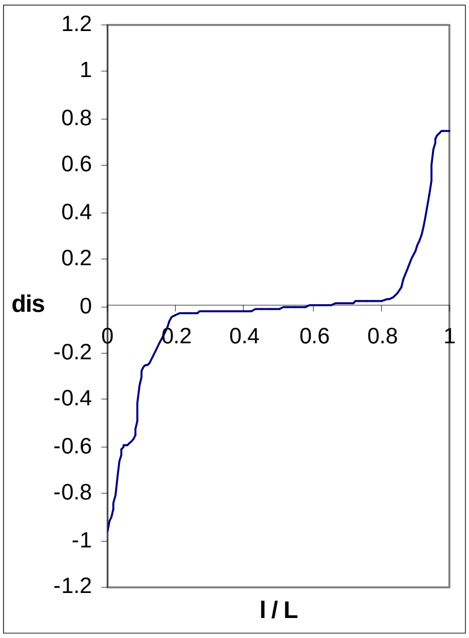


(Middle height of the dam)

**Figure 3.5**: Undrained analysis, reference example: Residual displacement

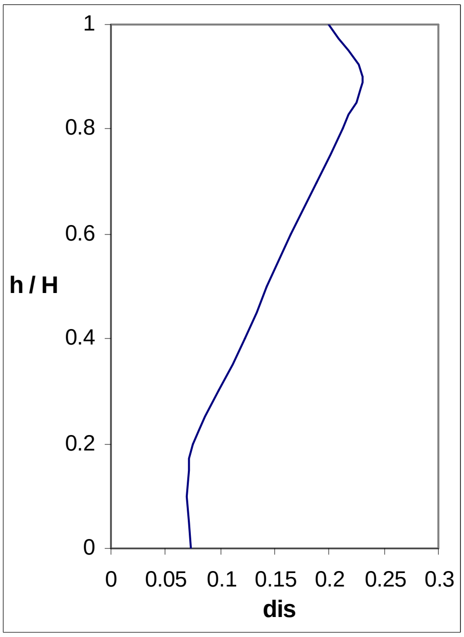


(Vertical axis of the dam)

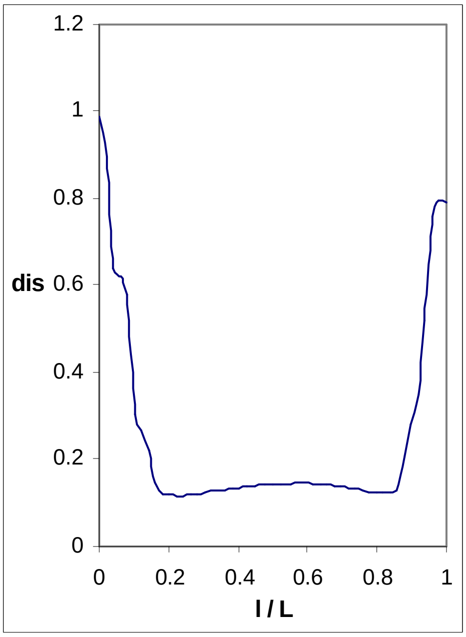


(Middle height of the dam)

**Figure 3.6**: Undrained analysis, reference example: displacement pattern at the maximum of the seismic excitation

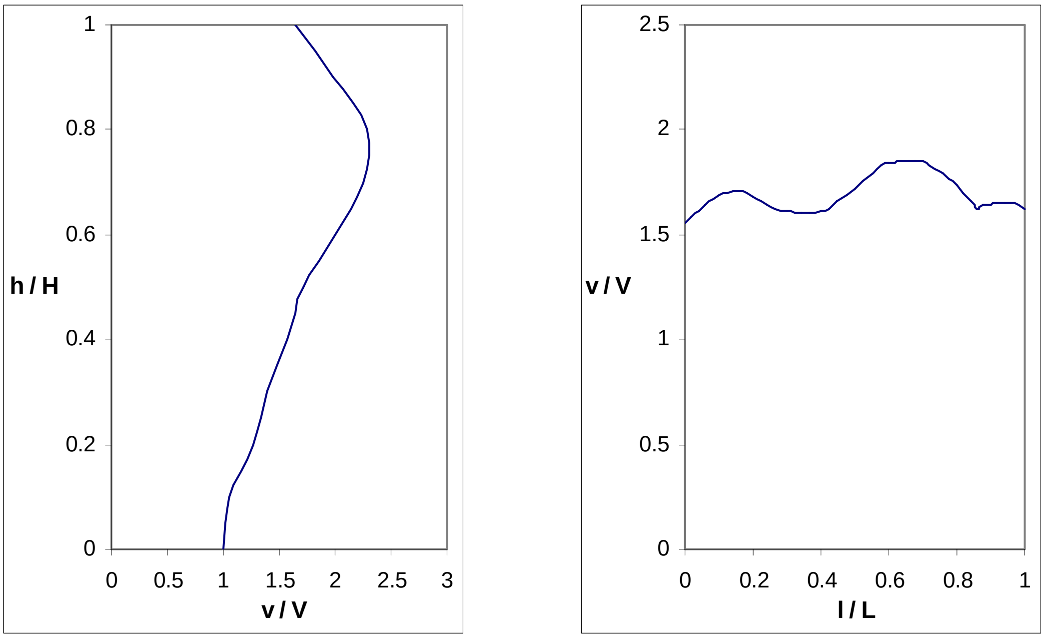


(Vertical axis of the dam) (Middle height of the dam)

**Figure 3.7**: Undrained analysis, reference example: seismic amplification of the velocity

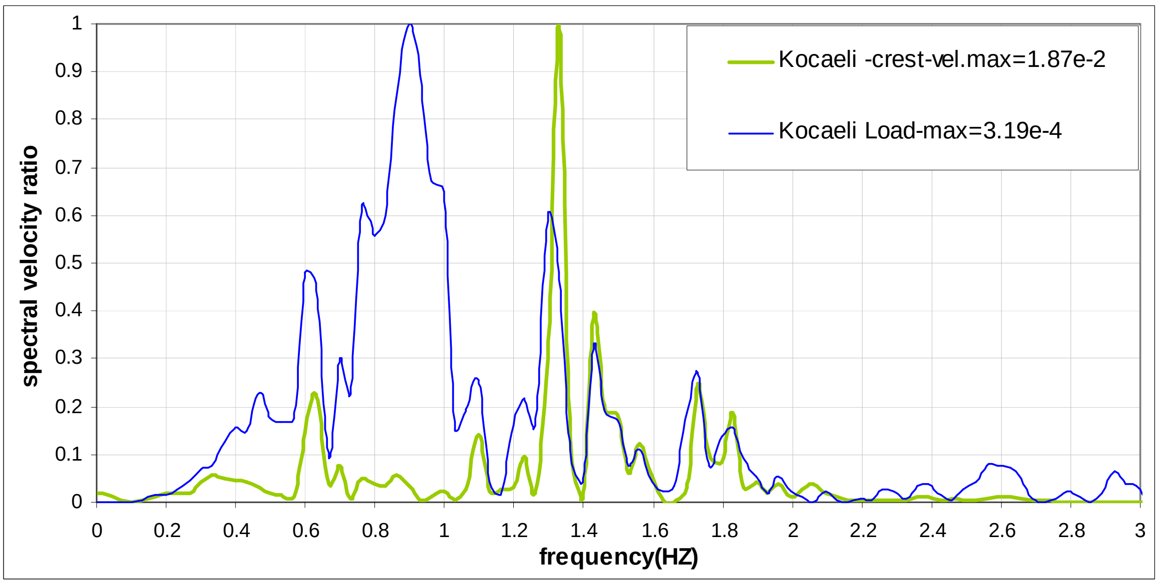


**Figure 3.8:** Undrained analysis, reference example; spectra of the dam response to Kocaeli earthquake record

## 3.2.2 Influence of the frequency content of the input motion

The response of the dam presented in the reference example was compared to that of the dam subjected to the input motion recorded during the Tabas earthquake. The time history of this record is illustrated in figure 3.9. The magnitude of the input motion is equal to that used in the reference example ($V_a$ = 0.4 m/sec). The major peak corresponds to the frzquency f =0.5 Hz, the second peak appears at the frequency f = 1.1 Hz.

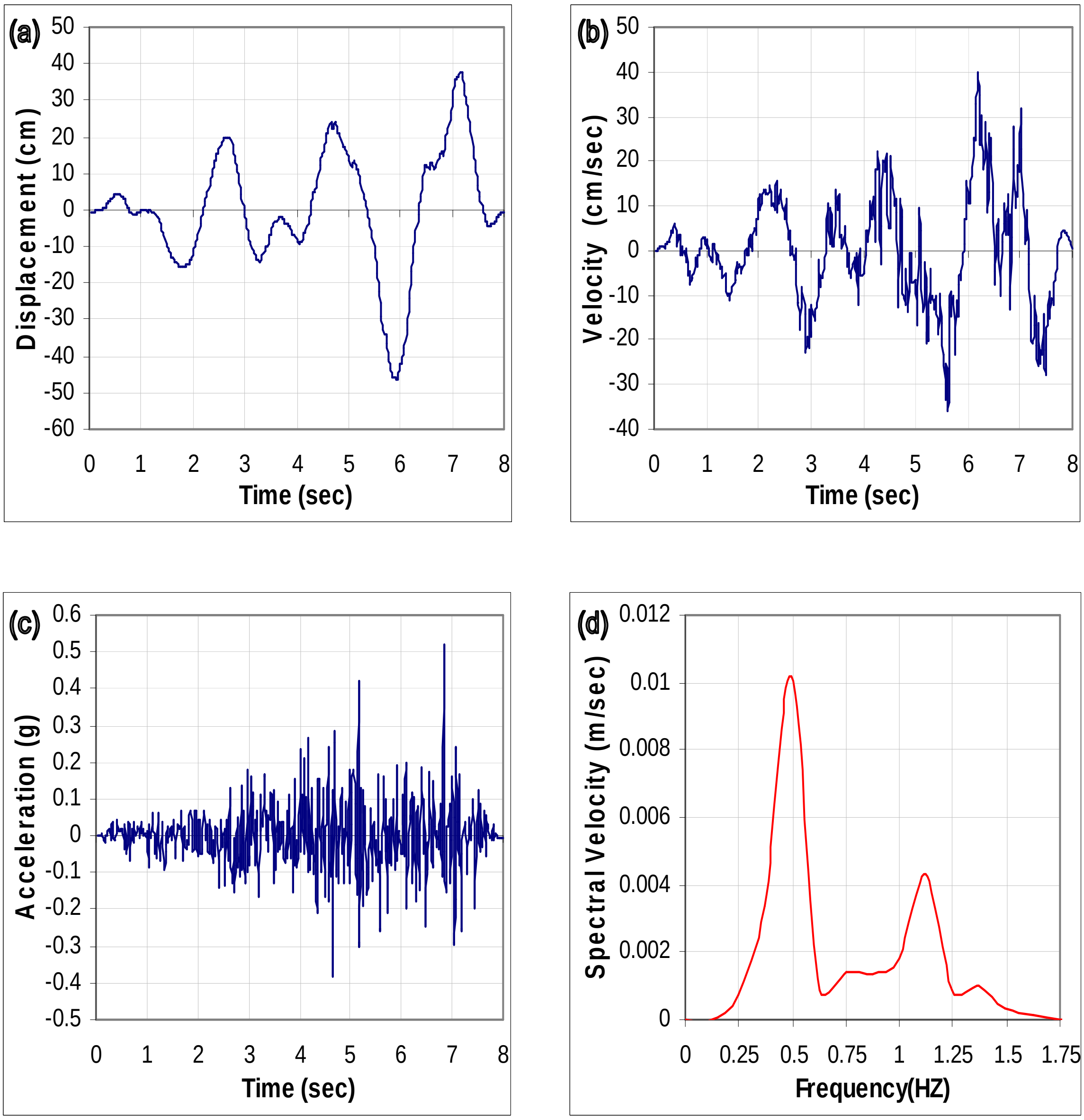


**Figure 3.9:** Tabas earthquake record:

a) Displacement, b) Velocity, c) Acceleration, d) Spectra

Figure 3.10 shows the distribution of plasticity in the dam at the maximum of velocity. It can be observed that plasticity is induced in the quasi totality of the dam. This distribution is close to that obtained with the Kocaeli earthquake record (Figure 3.4). Figure 3.11 shows the displacement pattern in the axis of the dam and at its middle height at the maximum of seismic excitation. It can be observed that the displacement increases with the distance from the base of the dam; the variation of the displacement in the middle height shows a sharp increase at the extremities; which could indicate the imminence of instability in this area.

The seismic amplification of the dam response to Tabas earthquake is compared to that due to the Kocaeli earthquake input motion (Figure 3.12). It can be observed that the amplification of the tow responses are very closes, except near the top of the dam, where the amplification of the response to Tabas input motion is higher than that due to Kocaeli earthquake record. The contribution of the second mode to the response to the Tabas input motion is less important than that to the response to Kocaeli input motion.

Figure 3.13 shows analysis of the response spectra of the dam to Kocaeli and Tabas earthquake records. It confirms that the peak of the response of the dam to Tabas earthquake input motion occurs at the frequency f = 0.5 Hz, which is inferior to that induced by the Kocaeli earthquake record input motion (f = 1.32 Hz).

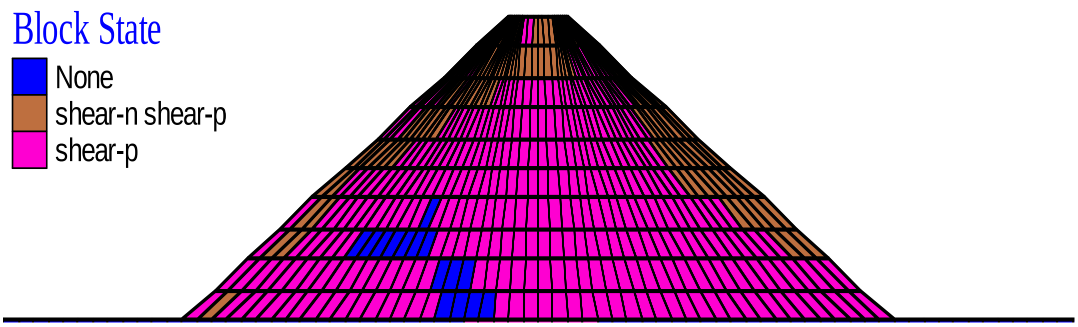


**Figure 3.10**: Undrained analysis: plasticity induced by the seismic loading (Tabas earthquake record)



 

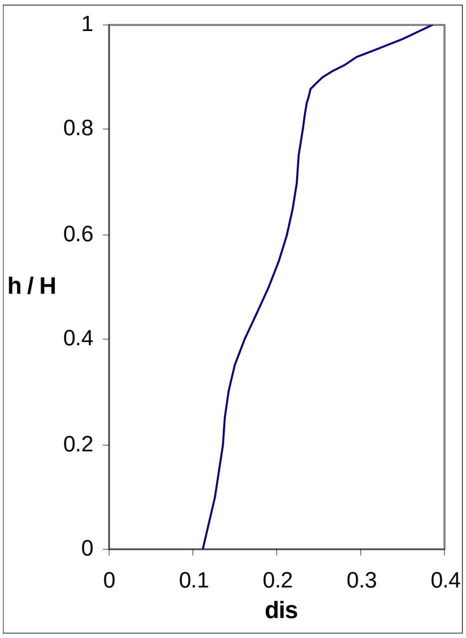


**(Vertical axis of the dam)**

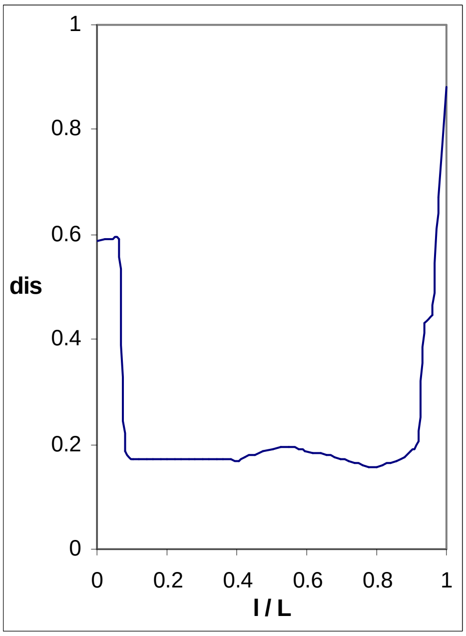


**(Middle height of the dam)**

**Figure 3.11:** Undrained analysis; displacement pattern at the maximum of seismic excitation (Tabas Earthquake record)

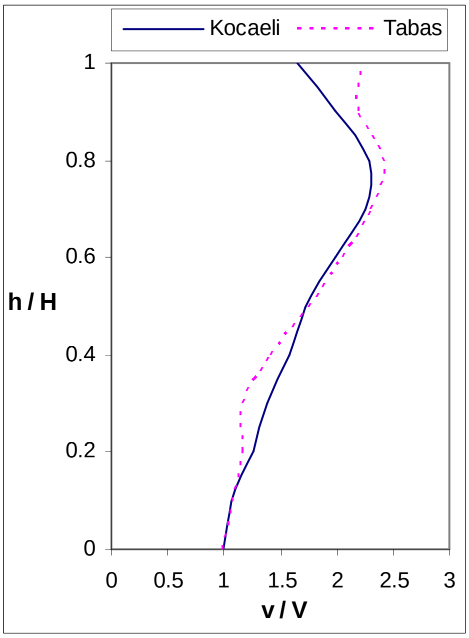


**(Vertical axis of the dam)**

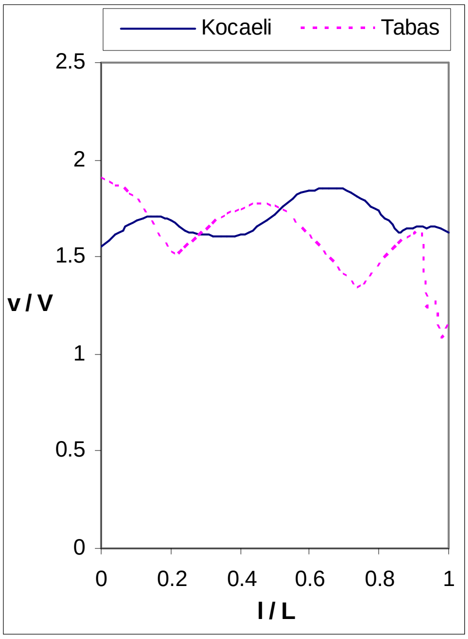


**(Middle height of the dam)**

**Figure 3.12:** Variations of velocities (v/V) for Kocaeli and Tabas earthquake wave

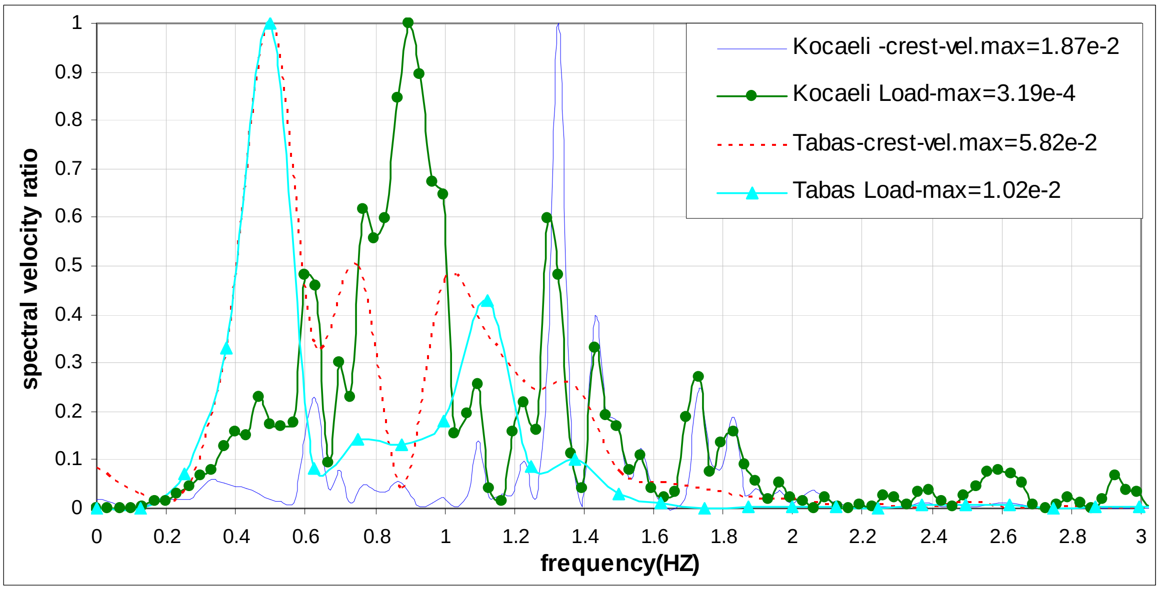


**Figure 3.13:** Undrained analysis spectra of the dam response to spectra of the dam to Kocaeli and Tabas earthquake records.

## 3.3 Full Coupled analysis

Full coupled analysis is conducted in effective stresses. This analysis takes into consideration the interaction between the fluid and solid phases. It takes into consideration the water flow in the dam. The non associated Mohr –Coulomb criterion is considered in the analysis. The first stage of the analysis concerns the initial state, that prior to the seismic excitation. It is carried considering the geometry and the boundary conditions under static loading.

In the following, we present first analysis of a reference example; it will be followed by a study of the influence of the frequency continent of the input motion.

The full coupled analysis will be compared to the undrained analysis.

### 3.3.1 Reference example

The reference example concerns the earth dam used in the undrained analysis (Figure 3.1). Geotechnical properties of the dam are summarized in table 3.2. The foundation is assumed to be stiff with a Young's Modulus E = 1000 MPa. The Young's modulus of the core is equal to 40 MPa, while that of the shell is equal to 60 MPa. The friction angle of the shell is equal to 35°. The core resistance is assumed to be purely cohesive; the cohesion of the core is equal to 100 kPa, the friction angle of the core is equal to 15. The permeability of the core is equal to $9.810^{-7}$ m/s.

Analysis concerns the response of the dam to the Kocaeli earthquake record.

| Parameter | Units | Core | Shell | Foundation |
|---|---|---|---|---|
| Dry density (ρ) | ($kg/m^3$) | 1800 | 2000 | 2200 |
| Saturated density (ρ′) | ($kg/m^3$) | 2100 | 2500 | 2500 |
| Friction Angle (φ) | (°) | 15 | 35 | 35 |
| Dilation | (°) | 3 | 10 | 3 |
| Cohesion (c′) | (Pa) | 0.1 e6 | 100 | 0.2e6 |
| Young's modulus (E) | (MPa) | 40 | 60 | 1000 |
| Poisson's ratio (ν) | | 0.3 | 0.3 | 0.25 |
| Elastic shear modulus (G) | (MPa) | 15 | 23 | 400 |
| Bulk modulus (K) | (MPa) | 33 | 50 | 666 |
| Porosity (n) | | 0.3 | 0.5 | 0.3 |
| Permeability | ($m^2$/(Pa sec)) | 1e-10 | 1e-8 | 3e-8 |
| Real permeability | (m/ sec) | 9.8e-7 | 9.8e-5 | 2.94e-4 |

**Table 3.2:** Full coupled analysis: properties of the reference example

## Results

Figure 3.14 shows the excess pore pressure ratio at three positions of the dam: the base the middle height and the top. This variation follows that of the input motion: an important increase/decrease in the pore pressure ratio up to peak which occurs at about 6 seconds followed by a decrease in the amplitude towards stabilization. At the top of the dam the excess pore pressure ratio increases up to 1.16, while at the middle height it attains 1.1; at the bottom of the dam the excess pore pressure ratio generally decreases and attains 0.9.

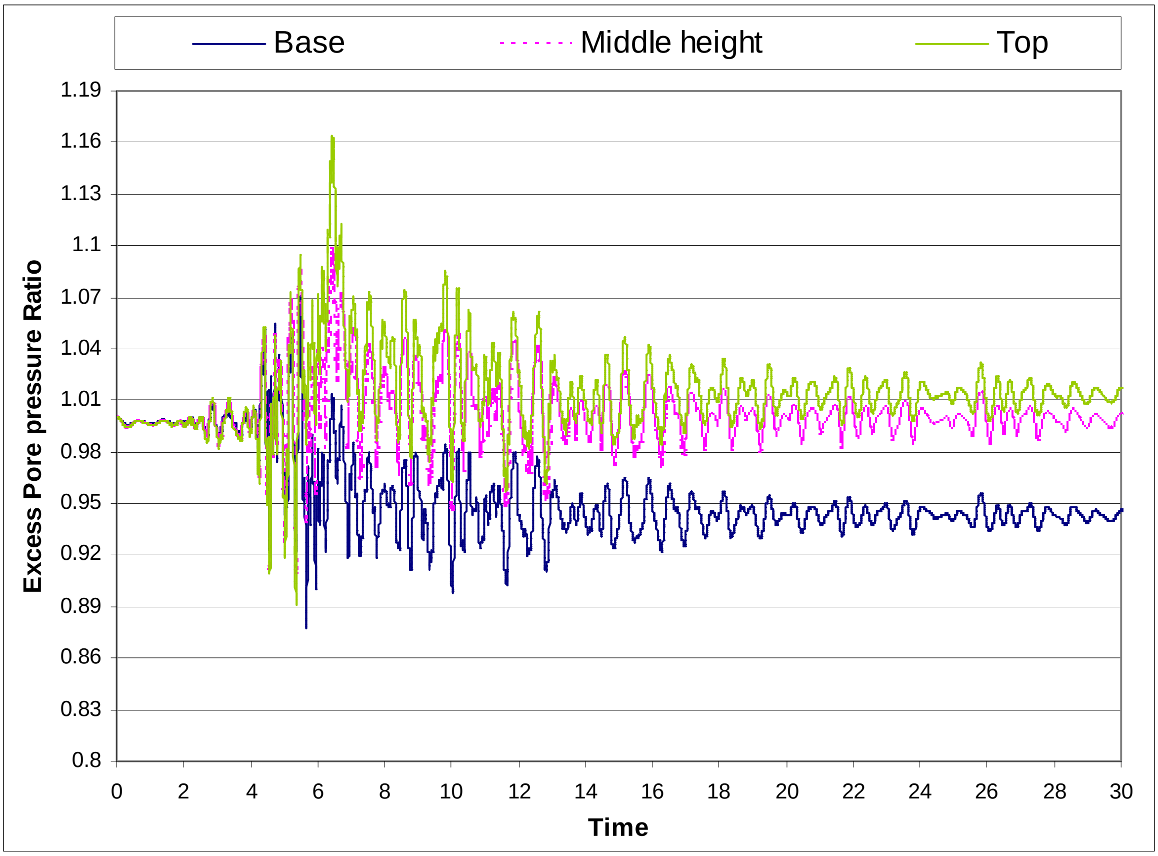


**Figure 3.14:** History of the excess pore pressure ratio at different points of earth dam (Kocaeli earthquake record)

Figure 3.15 shows the distribution of plasticity in the dam at the maximum of the seismic excitation. It can be observed that plasticity is induced in the quasi totality of the shell and in the lower part of the core. The upper part of the core remains in the elastic domain. It comparison to the undrained analysis (Figure 3.4), it can be noticed that the full coupled analysis predicts less extension of plasticity than the undrained analysis.

The residual (permanent) displacement is presented in figure 3.16. It shows that the seismic loading induces mainly a residual displacement at the dam extremities, which attains 0.70 m.

Figure 3.17 shows the displacement pattern in the axis and the middle height of the dam at the maximum of seismic excitation. It can be observed that the displacement in the axis of the dam increases with the distance from the base of the dam, with a quasi stabilization near the top of the dam. The variation of the displacement at the middle height shows a sharp increase at the extremities; which could indicate the imminence of a soil instability in this area.

Figure 3.18 shows the seismic amplification of the velocity in the dam. It can be observed that the amplification increases with the distance from the base of the dam with a quasi stabilization near the top of the dam. This variation corresponds to a combination of the first and second modes of the dam as can be observed on figure 3.19 which shows that the spectra of the velocity includes two peaks which occur at the frequencies f = 0.65 Hz and 1.3 Hz.

.

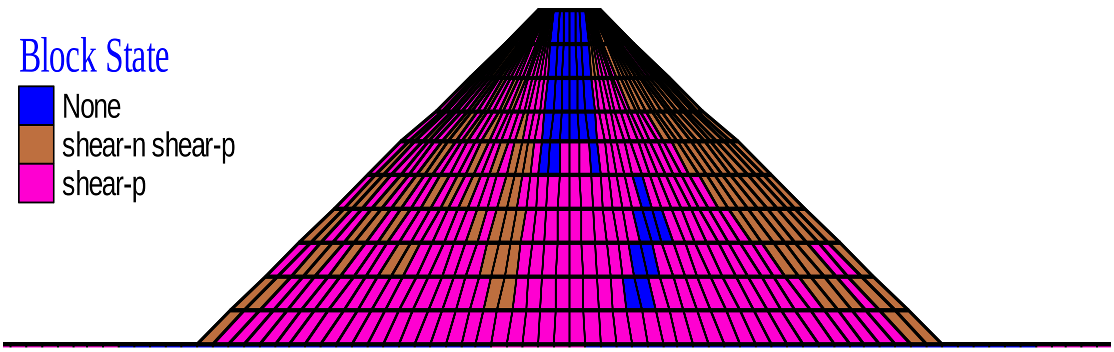


**Figure 3.15:** Full coupled analysis, reference example: plasticity induced by the seismic loading (Kocaeli earthquake record)

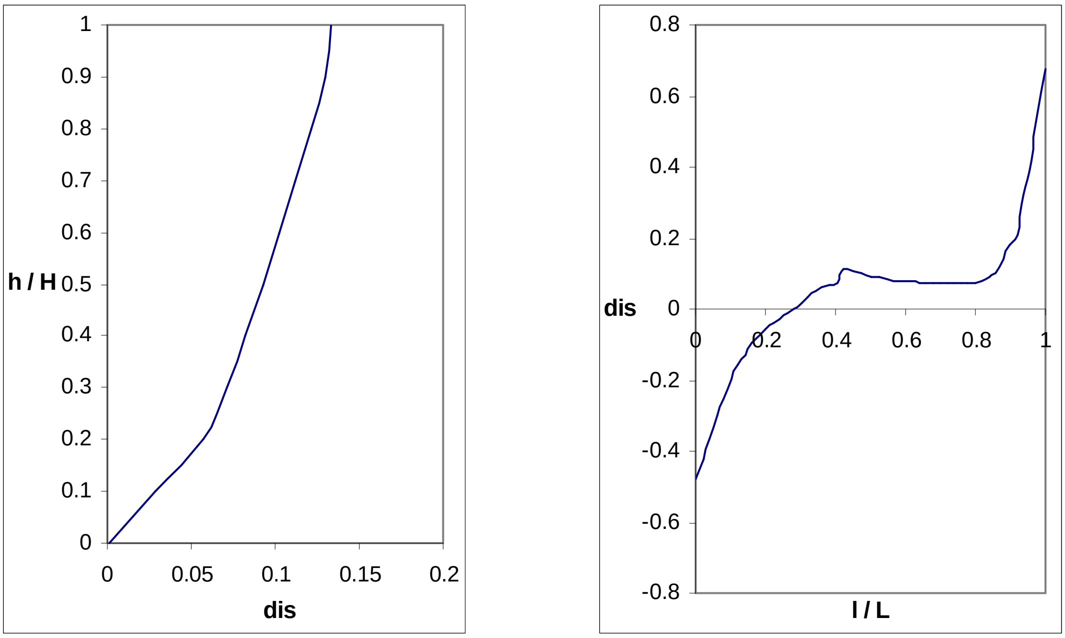


**(Vertical axis of the dam)** **(Middle height of the dam)**

**Figure 3.16**: Full coupled analysis, reference example: Residual displacement (Kocaeli earthquake record)

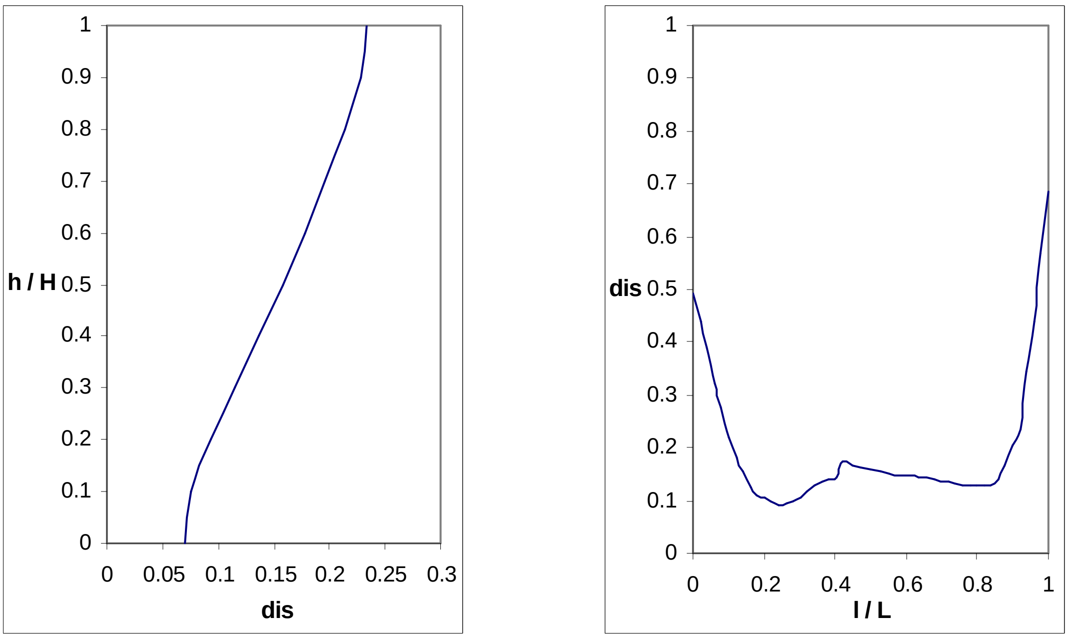


**(Vertical axis of the dam)** **(Middle height of the dam)**

**Figure 3.17**: Full coupled analysis, reference example: Displacement at the maximum of seismic excitation (Kocaeli earthquake record)

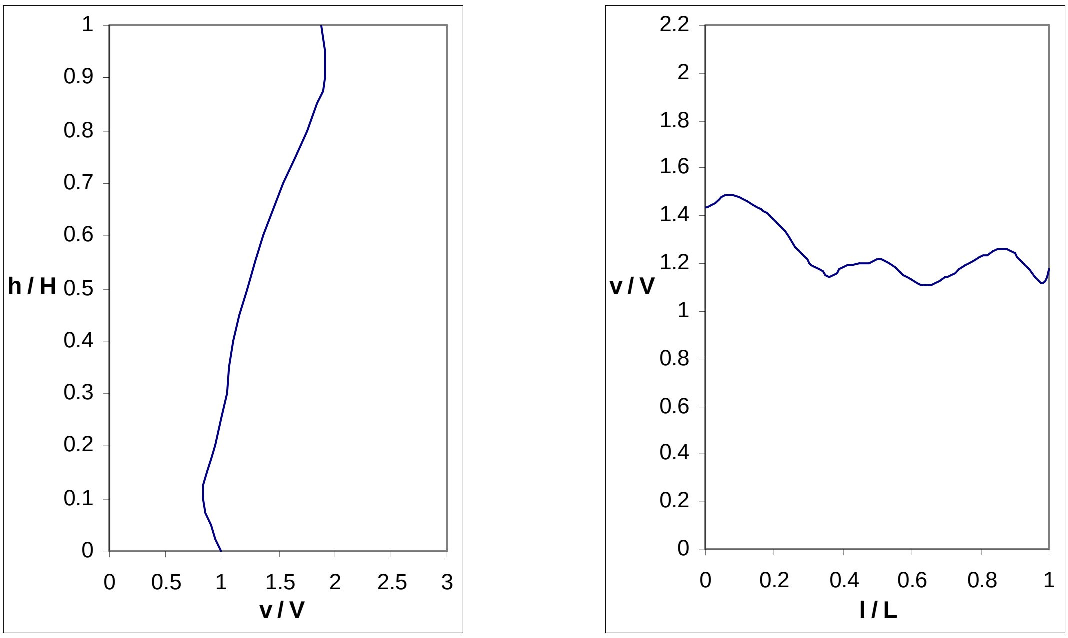


**(Vertical axis of the dam)** **(Middle height of the dam)**

**Figure 3.18**: Full coupled analysis, reference example: Velocity amplification at the maximum of the seismic excitation

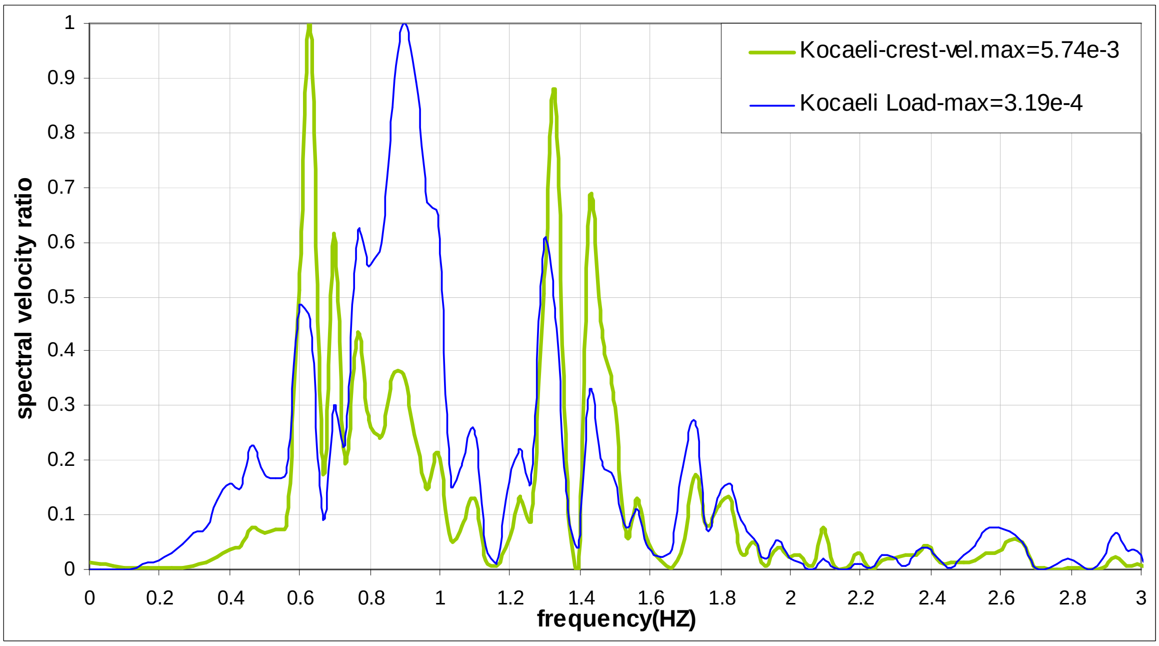


**Figure 3.19:** Full coupled analysis, reference example, Velocities spectra at the dam crest (Kocaeli earthquake record)

### 3.3.2 Influence of the frequency content of the input motion

The response of the dam presented in the reference example was compared to that of the dam subjected to the the Tabas earthquake record (Figure 3.9). The magnitude of the input motion is equal to that used in the reference example ($V_a$ = 0.4 m/sec).

Figure 3.20 shows the distribution of plasticity in the dam at the maximum of velocity. It can be observed that plasticity is induced in the quasi totality of the shell and in the lower part of the core. This distribution is close to that obtained with the Kocaeli earthquake record (Figure 3.15). The seismic amplification of the dam responses to Tabas earthquake record is compared to that due to the Kcaeli earthquake input motion in figure 3.21. It can be observed that the seismic amplification of the response to the Tabas Earthquake input motion is higher than that to the Kocaeli earthquake input motion. At the top of the dam, the difference attains about 50%.

Figure 3.22 shows analysis of the response spectra of the dam to Kocaeli and Tabas earthquake records. It shows that the response to Tabas earthquake record includes tow peaks which correspond to 0.50 and 0.75 Hz, while the peaks of the response to the Kocaeli earthquake correspond to 0.65 and 1.35 Hz. It can be noted that the contribution of high frequencies to the response of the dam to Kocaeli earthquake input motion is more important than their contribution to the response of the dam to Tabas input motion.

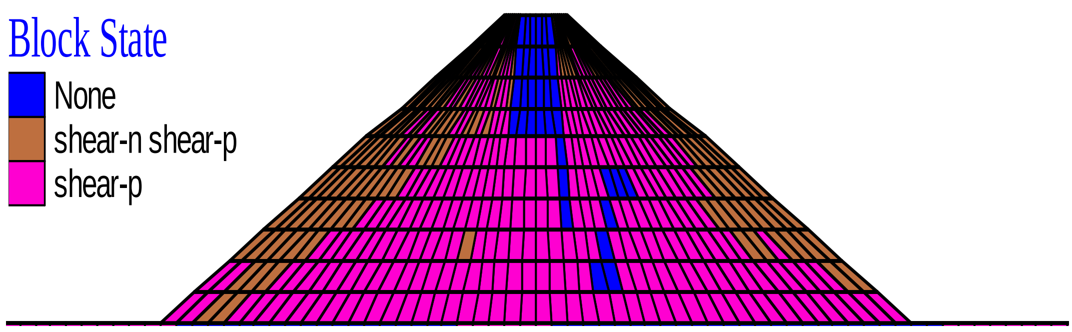


**Figure 3.20**: Plasticity induced by Tabas earthquake record at the maximum of the seismic excitation

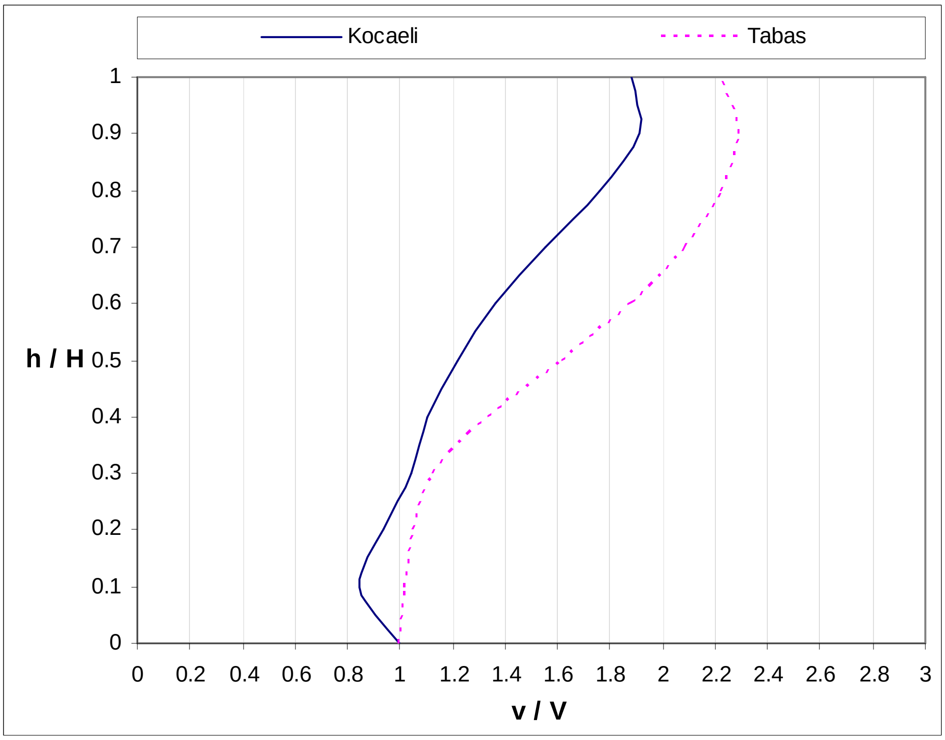


**Figure 3.21:** Full coupled analysis**:** Influence of the input motion on the velocity amplification

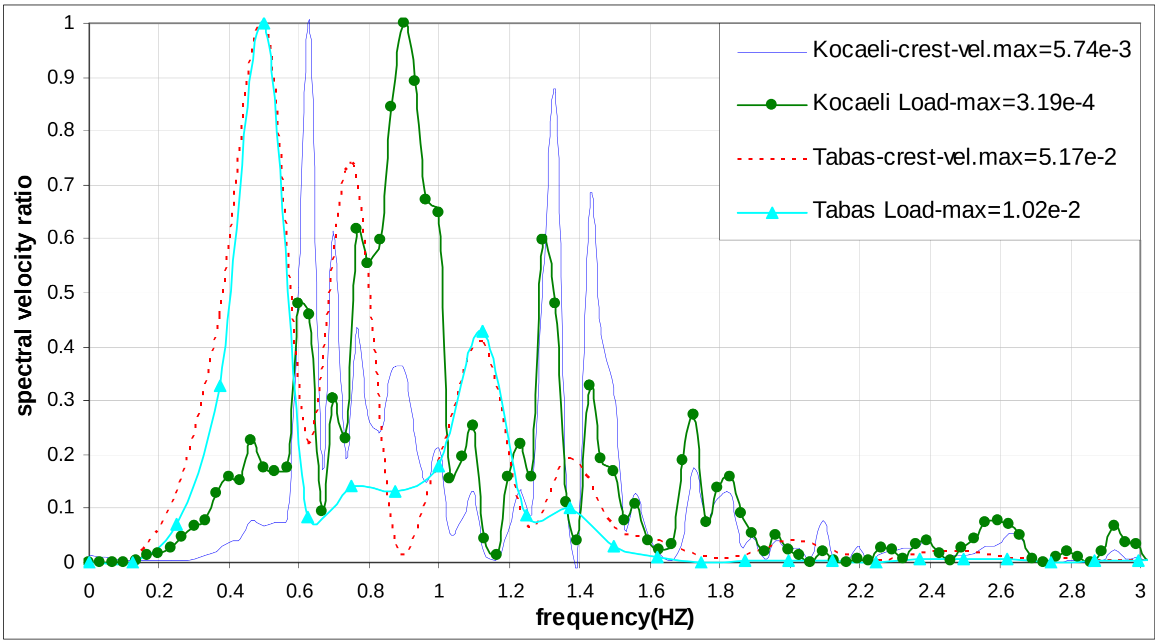


**Figure 3.22:** Full coupled analysis**:** Influence of the input motion on the velocity spectra

## 3.4 Comparison of undrained and full coupled analyses

Figure 3.23 shows a comparison of the velocity amplifications in the axis of the dam between the undrained and full coupled analyses of the dam subjected to Kocaeli earthquake record. It can be observed that the amplification of the undrained response is higher than that of the full coupled analysis. Both of the responses correspond to a combination of the first and second modes, but the contribution of the second mode seems to be more important in the case of the undrained response. Figure 3.24 confirms this observation. It shows that the full coupled response includes two peaks with equal values which correspond to the frequencies f = 0.65 Hz and 1.35 Hz, while the major peak of the undrained response occurs at the frequency f = 1.35 Hz. This result indicates that the undrained analysis could lead to an overestimation of the natural frequency of the dam, because of the overestimation of the dam stiffness.

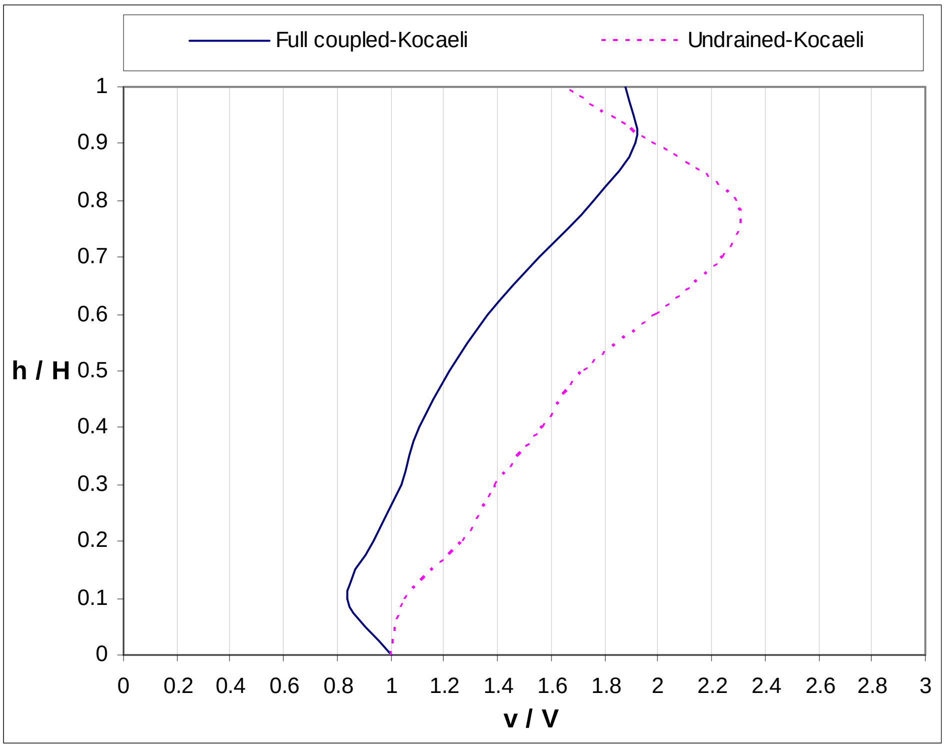


**Figure 3.23:** Comparison of the undrained and full coupled analyses Seismic amplification to the dam subjected to the Kocaeli earthquake record

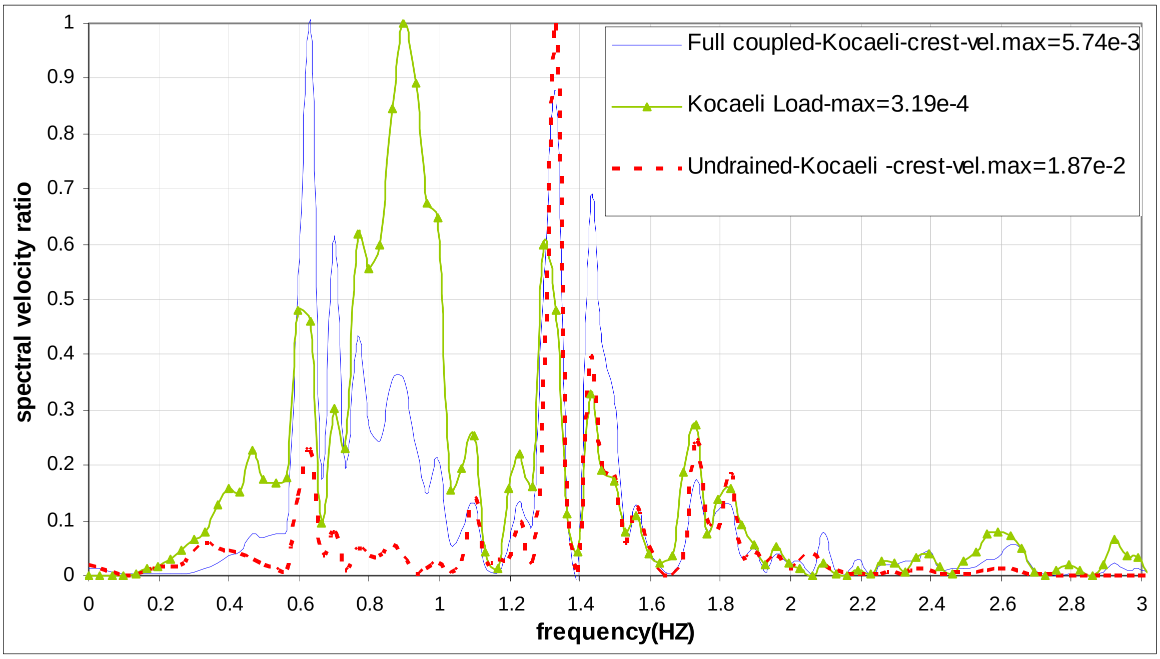


**Figure 3.24:** Comparison of the undrained and full coupled analyses Spectra of the seismic response at the top of the dam ( Kocaeli earthquake record)

Figure 3.25 shows a comparison of the velocity amplifications in the axis of the dam between the undrained and full coupled analyses of the dam subjected to Tabas earthquake record. We note trends similar to that observed on the dam response to Kocaeli earthquake record: (i) the amplification of the undrained response is moderately higher than that of the full coupled analysis, (ii) both of the responses correspond to a combination of the first and second modes, but the contribution of the second mode seems to be higher in the case of the undrained response. Figure 3.26 shows that the major peak of the undrained analysis corresponds to that of the full coupled analysis. It shows also that the undrained response includes higher frequencies than that of the full coupled analysis.

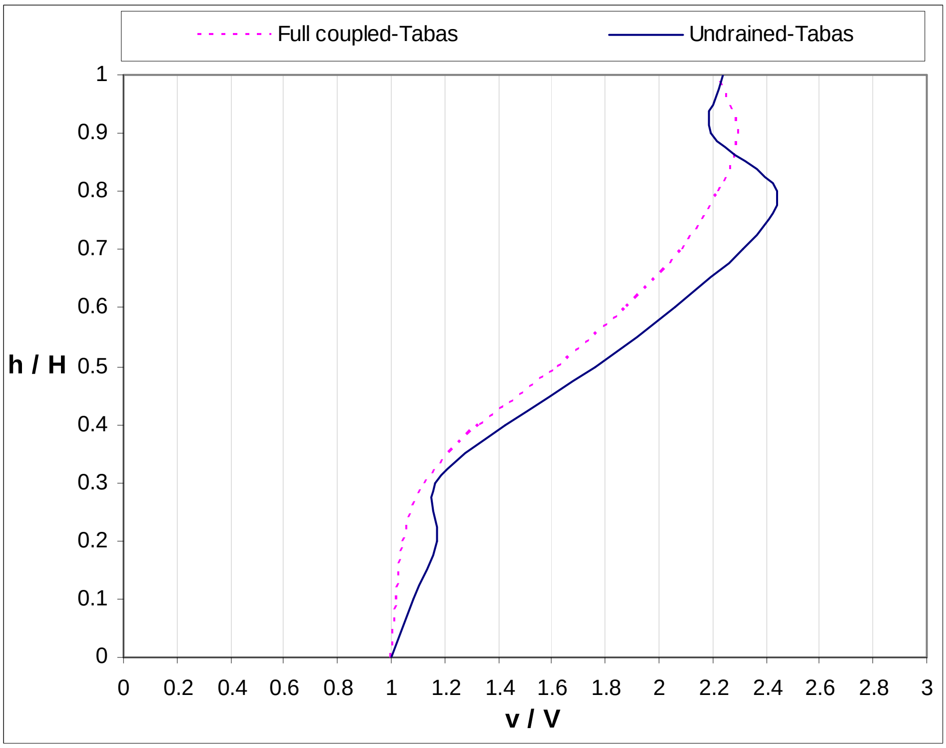


**Figure 3.25:** Comparison of the undrained and full coupled analyses Seismic amplification to the dam subjected to Tabas earthquake record

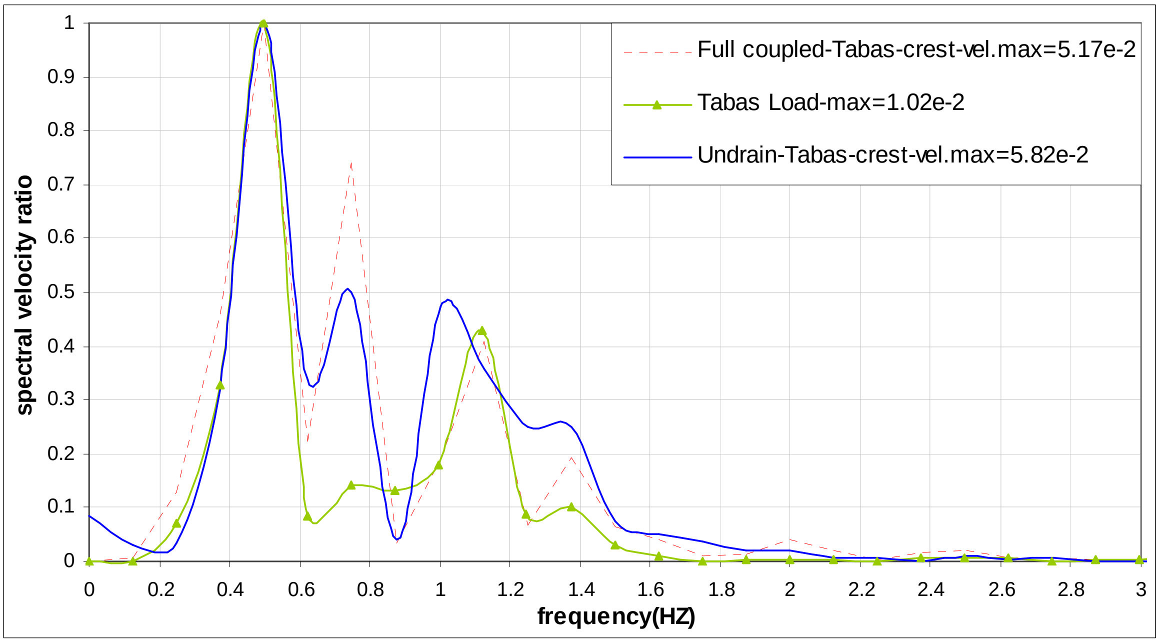


**Figure 3.26:** Comparison of the undrained and full coupled analyses Spectra of the seismic response at the top of the dam (Tabas eearthquake record)

## 3.5 Conclusion

This chapter included analysis of the seismic behaviour of earth dams in considering the presence of the water phase. It corresponds to a more realistic analysis than that presented in the second chapter. Analysis was first conducted under undrained condition. This response corresponds to the rapid response of the dam in neglecting the water flow in the core. This analysis is conducted in total stresses; it does not provide the pore pressure evolution. A full coupled analysis was also conducted in effective stresses. This analysis is more realistic than the undrained analysis. It accounts for the water flow and provides the variation of the pore pressure. The behaviour of the earth material was assumed to be governed by the non associated Mohr-Coulomb criterion.

Undrained analysis showed that both the Kocaeli and Tabas earthquake input motion induce plasticity in the quasi totality of the dam. They induce an important soil displacement and velocity near the lateral extremities of the dam, which could indicate the imminence of instability in this area. Analyses showed that the amplification of the response to the Tabas input motion is higher than that due to the Kocaeli earthquake input motion. The contribution of high frequencies to the Tabas input motion is less important than that to the response to the Kocaeli input motion.

Full coupled analysis showed that the seismic excitation induces an increase in the pore pressure in the upper part of the dam. This increase is not important and does not lead to soil liquefaction. Both the Kocaeli and Tabas earthquake input motion induce plasticity in the totality of the shell and in the lower part of the dam. They induce an important soil displacement and velocity near the lateral extremities of the dam, which could indicate the imminence of instability in this area. Analyses showed that the amplification of the response to the Tabas input motion is higher than that due to the Kocaeli earthquake input motion. The contribution of high frequencies to the Kocaeli input motion is more important than that to the response to the Tabas input motion.

Comparison of the undrained and full coupled analyses shows that the amplification of the undrained response is moderately higher than that of the full coupled analysis and the contribution of high modes to the undrained response is more important than their contribution to the full coupled response. This result indicates that the undrained analysis could lead to an overestimation of the natural frequency of the dam, because of the overestimation of the dam stiffness.

# GENERAL CONCLUSION

# General Conclusion

This thesis aimed to analyse using numerical modeling the seismic response of the dam. Analyses were conducted using the FLAC program which provides interesting facilities for geotechnical and earthquake studies.

The work concerned a simplified geometry of the dam, because it aimed to elaborate a methodology for the seismic analysis of earth dams under real earthquake records. The behaviour of the soil was described using the non associated Mohr-Coulomb criterion with tension cutoff. This criterion is largely used in engineering studies. It is realistic for the analysis of the dam response without the water phase, but not fully adequate for the full coupled analyses under high seismic excitation.

Elastic analyses showed that the seismic loading induces mainly lateral displacement, which increases with the distance from the dam foundation. The maximum is observed near the dam crest. The mechanical properties of the core (shear stiffness and density) moderately affect the elastic response, while those of the shell affect significantly the response of the dam.

Elastoplastic analyses show that the seismic loading induces plasticity in a large part of the shell and in the lower part of the core. The variation of the displacement in the middle height shows a sharp increase at the extremities, which could indicate the imminence of instability in this area. The comparison between the elastic and elastoplastic responses shows that the plastic deformation leads to a decrease in the velocity in the dam, in particular in the upper part. This result could be attributed to the energy dissipation by plastic deformation and on the influence of plasticity on the reduction of the fundamental frequencies of the dam.

Undrained analysis showed that both the Kocaeli and Tabas earthquake input motions induce plasticity in the quasi totality of the dam. They induce an important soil displacement and velocity near the lateral extremities of the dam, which could indicate the imminence of instability in this area. Analyses showed that the amplification of the response to the Tabas input motion is higher than that due to the Kocaeli earthquake input motion. The contribution of high frequencies to the Tabas input motion is less important than that to the response to the Kocaeli input motion.

Full coupled analysis showed that the seismic excitation induces an increase in the pore pressure in the upper part of the dam. This increase is not important and does not lead to soil liquefaction. Both the Kocaeli and Tabas earthquake input motion induce plasticity in the totality of the shell and in the lower part of the dam. They induce an important soil displacement and velocity near the lateral extremities of the dam, which could indicate the imminence of instability in this area. Analyses showed that the amplification of the response to the Tabas input motion is higher than that due to the Kocaeli earthquake input motion. The contribution of high frequencies to the Kocaeli input motion is more important than that to the response to the Tabas input motion.

Comparison of the undrained and full coupled analyses shows that the amplification of the undrained response is moderately higher than that of the full coupled analysis and the contribution of high modes to the undrained response is more important than their contribution to the full coupled response. This result indicates that the undrained analysis could lead to an overestimation of the natural frequency of the dam, because of the overestimation of the dam stiffness.

Full coupled analysis is recommended for the seismic analysis of the dam, because its takes into consideration the water flow in the dam and the interaction between the fluid- and soiled phases. Since the pore pressure variation depends on the volumes change of the skeleton, it is of major interest to use a constitutive relation which could properly describe the volumetric behaviour of the soil and the apparition of plasticity at low level of solicitation. This important feature constitutes an interesting continuation of this work. Analysis should also be conducted with more realistic geometries and soil properties.

# REFERENCES

# References


1. Abramento, M., Carvalho, CS. 1989 “Geotechnical parameters for the study of natural slopes instabilization at Sierra do Mar-Brazilian Southeast. ” Proceedings of the 12th international conference on soil mechanics and foundation engineering, Rio de Janeiro 1989;3:1599–602.
2. Asawa, GL.,2005 “Irrigation and Water Resources Engineering”, book, Indian Institute of Technology Rppykee, www.newagepublishers.com.
3. ASTM 2002 American Society for Testing and Materials, “Standard Test Method for Laboratory Compaction Characteristics of Soil Using Modified Effort”, ASTM D1557-02, ASTM International, P. O. Box C700, West Conshohocken, PA, 19428.
4. Aubry, D., Hujeux, J.C., Lassoudière, F., and Meimon, Y., Eds. 1982. “A Double Memory Model with Multiple Mechanisms for Cyclic Soil Behavior,” in International Symposium on Numerical Methods in Geomechanics , Zurich, A.A. Balkema, Rotterdam, pp 3–13.
5. Bathe, K.J. 1978. “ADINA/BM: A General Computer Program for Nonlinear Analysis of Mines Structures,” Final report to Office of Assistant-Director of Mining, U.S. Department of the Interior, Contract no. 30255008.
6. Beikae, M. 1996. “A Seismic Displacement Analysis Technique for Embankment Dams,” Proc. 16th Annual USCOLD Lecture Series, Los Angeles, July 22–26, pp. 91–109.
7. Bishop AW, 1959 “The principle of effective stress” Publication 32 Oslo: Norwegian Geotechnical Institute.
8. Bureau, G., Edwards, A., and Blümel, A.S. 1994. “Seismic Design of Stage IV Raising, Los Leones Dam, Chile,” Proc. 11th Association of State Dam Safety Officials (ASDSO) Conference, Boston, September, Suppl., pp 77–86.
9. Bureau, G., Inel, S., Davis, C.A., and Roth, W.H. 1996. “Seismic Response of Los Angeles Dam, During the 1994 Northridge Earthquake,” Proc. USCOLD Annual Meeting, Los Angeles, July 22–26, pp 281–295.
10. Bureau, G. 1997. “Evaluation Methods and Acceptability of Seismic Deformations in Embankment Dams,” 29th International Congress on Large Dams (ICOLD), Florence, Italy, May, Q. 73, R. 11, pp. 175–200.

11. Chen, Y., J.R. Miller, J.A. Francis, G.L. Russell, and F. Aires, 2003 "Observed and modeled relationships among Arctic climate variables". *J. Geophys. Res.*, 108, no. D24, 4799, doi:10.1029/2003JD003824.

12. Civil Systems, Inc. 1980. "SuperFLUSH," User's manual, Vols. I to III, report to Kozo Keikaku Engineering, Inc., Tokyo, October.

13. Coyne, Bellier, ECP/EDF-REAL 1991. "GEFDYN, a Computer Program for Geomechanics Finite Element Analysis: Two/Three-Dimensional Quasi-Static/Dynamic Coupled Mechanical-Hydraulics Software for Nonlinear Geomaterials Analysis, Paris, February.

14. Cundall, P.E. 1976. "Explicit Finite-Difference Methods in Geomechanics," 2nd International Conference on Numerical Methods in Geomechanics, Blacksburg, VA, June.

15. Davis, C.A, Sakado, M.M., 1994. "Response of the Van Norman Complex to the Northridge Earthquake", Association of Dam Safety Officials Conference Proceedings, Boston, MA, pp 241-255.

16. Dawson, E.M., Roth, W.H., Nesarajah, S., Bureau, G., and Davis, C.A. 2001. "A Practice-Oriented Pore-Pressure Generation Model," Proc. 2nd International FLAC Symposium, October, Lyon-Ecully, France, Itasca Consulting Group, Minneapolis, MN.

17. Duncan, J.M., Seed, R.B., Wong, K.S., and Ozawa, Y. 1984. "FEADAM84: A Computer Program for Finite Element Analysis of Dams," Geotechnical Engineering Research Report no. SU/GT/84–03, Department of Civil Engineering, Stanford University, Stanford, CA, November.

18. Elgamal, A. M., Scott, R. F., Succarish, M. F., and Yan, L., 1990. "La Villita Dam Response During Five Earthquakes Including Permanent Deformation", Journal of Geotechnical Engineering, American Society for Civil Engineers, Vol. 116, No. 10, pp 1443-1462.

19. Escario V, Sa´ ez J, 1986 "The shear strength of partly saturated soils". Ge´ otechnique 36:453–456.

20. Finn, W.D.L, Yogendrakumar, M. 1989. "TARA 3-FL: Program for Analysis of Liquefaction-Induced Flow Liquefaction," University of British Columbia, Vancouver, Canada.

21. Finn, W.D.L. 1991. "Estimating How Embankment Dams Behave during Earthquakes," Water Power and Dam Construction , London, April, pp. 17–22.

22. Finn, W.D.L., Gillon, M.D., Yogendrakumar, M., and Newton, C.J. 1992. "Simulating the Seismic Response of a Rockfill Dam," Proc. NUMOG-4, A.A. Balkema, Rotterdam, pp. 379–391.
23. Finn, W. D. L., Ledbetter, R. H., and Marcuson III, W. F.,January 12-16, 1994. "Seismic Deformations in Embankments and Slopes," Proceedings, Symposium on Developments in Geotechnical Engineering (From Harvard to New Delhi, 1936-1994), ed. by A.S. Balasubramaniam, S.W. Hong, N. Phien-Wej, and P. Nutslaya, , Bangkok, Thailand, pp 233-264.
24. Fok, K.L., Hall, J.F., Chopra, A.K. 1986. "EACD-3D User's Manual," Department of Civil Engineering, University of California, Berkeley; "Hydrodynamic and Foundation Flexibility Effects in Earthquake Response of Arch Dams," ASCE J. Struct. Eng., 112 (no. 8), 1810–1828.
25. Fredlund D.G., Xing Anqing, Fredlund M.D., arbour S.L.B, 1995 "The relationships of the unsaturated soil shear strength to the soil-water characteristic curve" Can. Geotech.J.32: 440-448.
26. Fredlund DG, Morgenstern NR, Widger RA, 1978 "The shear strength of unsaturated soils" Can Geotech J 15:313–321.
27. Gan JKM, Fredlund DG, Rahardjo H, 1988 "Determination of the shear strength parameters of an unsaturated soil using the direct shear test" Can Geotech J 25:500–510.
28. Harris, D.W. 1986. "Dynamic Effective Stress Finite Element Analysis of Dams Subjected to Liquefaction," Report REC–ERC–86–4, Embankment Dams Branch, Division of Dam and Waterway Design, Engineering and Research Center, U.S. Department of the Interior, Bureau of Reclamation, Denver, CO, December.
29. Hudson, M., Idriss, I.M., and Beikae, M. 1994. "QUAD4M: A Computer Program to Evaluate the Seismic Response of Soil Structures Using Finite Element Procedures and Incorporating a Compliant Base," May, Department of Civil and Environmental Engineering, University of California, Davis.
30. ICOLD (Bulletin 72), 1989 "Selecting Seismic Parameters for Large Dams", Guidelines, prepared by Committee on Seismic Aspects of Dam Design, International Commission on Large Dams, Paris.
31. ICOLD (International Committee on Large Dams). 1992. "Third Benchmark Workshop on Numerical Analysis of Dams," Bergamo, Italy, International Committee on Large Dams and Italian Committee on Large Dams.

32. ICOLD (International Committee on Large Dams). 1994. “Fourth Benchmark Workshop on Numerical Analysis of Dams,” Paris, France, International Committee on Large Dams and French Committee on Large Dams.
33. ICOLD (International Committee on Large Dams). 1999. “Fifth Benchmark Workshop on Numerical Analysis of Dams,” June 2–5, Denver, CO, International Committee on Large Dams, Bureau of Reclamation and U.S. Committee on Large Dams.
34. Idriss, I.M, Sun, J.I. 1992. “User’s Manual for SHAKE91,” November, Department of Civil and Environmental Engineering, University of California, Davis.
35. Inel, S., Roth, W.H., De Rubertis, C. 1993. “Nonlinear Dynamic Effective-Stress Analysis of Two Case Histories,” Session on Geotechnical Aspects of Recent Earthquakes, Proc. 3rd International Conference on Case Histories in Geotechnical Engineering, St. Louis, MO, June 1–6.
36. Itasca Consulting Group. 1992. “FLAC: Fast Lagrangian Analysis of Continua. vol. I. User's Manual; vol. II.Verification Problems and Example Applications”, Itasca Consulting Group, Minneapolis, MN.
37. Itasca Consulting Group.2005. “FLAC: Fast Lagrangian Analysis of Continua. vol. I. User's Manual; vol. II.Verification Problems and Example Applications”, Second Edition (FLAC3D Version 3.0), Minneapolis, Minnesota 55401 USA.
38. Janbu, N., 1963 “Soil Compressibility as Determined by Oedometer and Triaxial Tests,” Proc. European Conference on Soil Mechanics and Foundation Engineering, Wiesbaden, Germany, vol. 1, pp. 19–26.
39. Jansen, R.B., 1987. “The Concrete Face Rockfill Dam. Performance of Cogoti Dam under Seismic Loading,” Discussion of a paper presented at ASCE Symposium on Concrete Face Rockfill Dams, ASCE J. Geotech. Eng. Div., 113 (no. 10), 1135–1136.
40. Khalili N, Khabbaz MH (1998) “A unique relationship for $\chi$ for the determination of the shear strength of unsaturated soils” Géotechnique 48:681–687.
41. Kuhlmeyer, R. L., and J. Lysmer, 1973 “Finite Element Method Accuracy for Wave Propagation Problems,” J. Soil Mech. & Foundations Div., ASCE, 99(SM5), 421-427.
42. Lamborn, M.J, 1986 “A micromechanical approach to modeling partly saturated soils” M.Sc.thesis, Texas A & M University, College Station, Tex.
43. Lee S.J., Lee S.R., Kim Y.S, 2003 “An approach to estimate unsaturated shear strength using artificial neural network and hyperbolic formulation” Computers and Geotechnics 30 (2003) 489–503.

44. Lokmer, I., Herak, M., Panza, G.F. and Vaccari, F., 2002 “Amplification of strong ground motion in the city of Zagreb”, Croatia, estimated by computation of synthetic seismograms. Soil Dynamics and Earthquake Engineering; (22), 105-113.
45. Lysmer, J., Udaka, T., Tsai, C.-F., Seed, H.B. 1975. “FLUSH: A Computer Program for Approximate 3-D Analysis of Soil-Structure Interaction Problems,” Report no. EERC 75–30, November, Earthquake Engineering Research Center, University of California, Berkeley.
46. Makdisi, F, Seed, H.B. 1977. “A Simplified Procedure for Estimating Earthquake-Induced Deformations in Dams and Embankments,” EERC Report no. UCB/EERC–77/19, Earthquake Engineering Research Center, University of California, Berkeley.
47. Martin, G. R., Finn W. D. L, Seed H. B, 1975, Fundamentals of Liquefaction Under Cyclic Loading, J. Geotech., Div. ASCE, 101(GT5), 423-438.
48. Martin, P.P. and Niznik, J.A, 1993. “Prediction of Static and Dynamic Deformation Response of Blue Ridge Dam, Georgia, U.S.A.,” Proc. International Workshop on Dam Safety Evaluation, April 26–28, Grindelwald, Switzerland, vol. 2, pp. 133–147.
49. Mejia, L.H, Seed, H.B, 1983. “Comparison of 2-D and 3-D Dynamic Analysis of Earth Dams,” ASCE J. Geotech. Eng., 109 (no. GT11), 1383–1398.
50. Miao L, Liu S, Lai Y, 2002 “Research of soil–water characteristics and shear strength features of Nanyang expansive soil”. Eng Geol 65:261–267.
51. Ming HY, Li XS, 2003 “Fully coupled analysis of failure and remediation of lower San Fernando dam”. Journal of Geotechnical and Geoenvironmental Engineering, ASCE; 129(4):336–49.
52. Newmark, N.M, 1965. “Effects of Earthquakes on Dams and Embankments, Rankine Lecture,” Géotechnique 15 (2), 139–160.
53. Öberg, AL., Sällfors, G. 1997 “Determination of shear strength parameters of unsaturated silts and sand based on the water retention curve. ” Geotech Test J 20:40–48.
54. Paolucci, R., 2002. “Amplification of earthquake ground motion by steep topographic irregularities”, Earthquake Engineering and Structural dynamics, 2002; 31:1831-1853 pp.
55. Rassam DW, Williams DJ. 1999 “A relationship describing the shear strength of unsaturated soils” Canadian Geotechnical Journal 1999; 36(2):363–8.
56. Romo, M.P., Resendiz, D. 1981. “Computed and Observed Deformations of Two Embankment Dams under Earthquake Loading,” in Dams and Earthquakes,

Proceedings, Paper 30, Institute of Civil Engineers, London, Thomas Telford, London, pp. 267–274.

57. Roth, W.H., Scott, R.F., Cundall, P.A. 1986. "Nonlinear Dynamic Analysis of a Centrifuge Model Embankment," 3rd U.S. National Conference on Earthquake Engineering, August 24–28, Charleston, SC, vol. I, Earthquake Engineering Research Institute, Oakland, CA, pp 506–516.
58. Roth, W.H., Bureau, G., Brodt, G. 1991. "Pleasant Valley Dam: An Approach to Quantifying the Effect of Foundation Liquefaction," Proc. 17th International Congress on Large Dams, Vienna, June, pp 1199–1223.
59. Seed, H.B., et Idriss, I.M. 1970. Soil moduli and damping factors for dynamic response analysis. Earthquake Engineering Research Center, University of Califormia, Berkeley, Calif. Rapport no EERC 70-10.
60. Seed, H.B., Idriss, I.M. 1970b. "A Simplified Procedure for Evaluating Soil Liquefaction Potential," Report no. EERC 70–9, Earthquake Engineering Research Center, University of California, Berkeley.
61. Seed, H. B., Makdisi, F. I., and De Alba, P., July 1978. "Performance of Earth Dams During Earthquakes," Journal of Geotechnical Engineering, American Society of Civil Engineers, Vol, 104, No. GT7, pp. 967-994.
62. Seed, H. B, Sept. 1979. "Considerations in the Earthquake-Resistant Design of Earth and Rockfill Dams", 19th Rankine Lecture of the British Geotechnical Society, Geotechnique, Vol XXIX, No. 3, pp. 215-263.
63. Seed, H.B., 1983. "Earthquake-Resistant Design of Earth Dams," Proc. ASCE Symposium on Seismic Design of Embankments and Caverns, ASCE National Convention, Philadelphia, May 16–20, pp. 41–64, American Society of Civil Engineers, New York.
64. Seed, H. B., Idriss, I. M., Arango, I. 1983. "Evaluation of Liquefaction Potential Using Field Performance Data." Journal of Geotechnical Engineering, American Society of Civil Engineers, Vol. 109, No. 3, pp 458-482.
65. Seed, H. Bolton, Seed, Raymond B., Lai, S.S., Khamenehpour B., 1985. "Seismic Design of Concrete Faced Rockfill Dams," Concrete Face Rockfill Dams-Design, Construction and Performance Symposium Proceedings, ASCE, October 1985, pp 459-478.

66. Serff, N., Seed, H.B., Makdisi, F.I., and Chang, C.K. 1976. "Earthquake-Induced Deformations of Earth Dams," EERC Report no. EERC/76–4, Earthquake Engineering Research Center, University of California, Berkeley.
67. Sharam, R K., Sharam, T K., S., 2007 "Irrigation engineering", book, Chand, S. and company LTD, An iso 9001,Ram nagar, new delhi-110 055.
68. Siegel, R.A. 1975. "Computer Analysis of General Slope Stability Problems; STABL User's Manual," Joint Highway Research Project, Report No. JHRP-75-8, Project No. C-36-36K, File No. 6-14-11, Purdue University, Lafayette, IN, June.
69. Terzaghi,K., 1936 "The shear resistance of saturated soils" Proceeding, 1st International Conference on Soil Mechanics and Foundation Engineering, Cambridge, Vol. l., pp. 54-56.
70. USCOLD (U.S. Committee on Large Dams). 1984. "Bibliography on Performance of Dams during Earthquakes," compiled by Philip Gregory, University of California, Berkeley.
71. USCOLD (United States Committee on Large Dams), 1992. "Observed Performance of Dams during Earthquakes", USCOLD Committee on Earthquakes.
72. USCOLD (U.S. Committee on Large Dams), 1992a. "Directory of Computer Programs in Use for Dam Engineering in the United States," Committee on Methods of Numerical Analysis of Dams, March, Denver, CO.
73. USCOLD (U.S. Committee on Large Dams), 1992b. "Observed Performance of Dams during Earthquakes," Committee on Earthquakes, July, Denver, CO.
74. USCOLD (U.S. Committee on Large Dams), 2000. "Observed Performance of Dams during Earthquakes," vol. II, Committee on Earthquakes, October, Denver, CO.
75. Vanapalli, SK, Fredlund DG, Pufahl DE, Clifton AW, 1996 "Model for the prediction of shear strength with respect to soil suction. " Can Geotech J 33:379–392.
76. Von Thun, L., Harris, C.W., 1981. "Estimation of Displacements of Rockfill Dams Due to Seismic Shaking," Proc. International Conference on Recent Advances in Geotechnical Engineering and Soil Dynamics, St. Louis, MO, April 26–May 3, vol. I, pp 417–423.
77. Vrymoed, J.L., 1996. "Seismic Safety Evaluation of Two Earth Dams," in Earthquake Engineering for Dams, Proc. Western Regional Technical Seminar, Association of State Dam Safety Officials, April 11–12, Sacramento, Association of State Dam Safety Officials, Lexington, KY, pp. 215–234.

78. Wilson, R. C., Keefer, D. K., 1985 "Predicting areal limits of earthquake-induced landsliding, evaluating earthquake hazards in the Los Angeles Region", USGS Professional Paper, Ziony, J. I., Editor, pp. 317-493.
79. Wright, S.G., 1992. "UTEXAS3 Version 1.2, a Computer Program for Slope Stability Calculations," Shinoak Software, Austin, TX.